BEARING CAPACITY OF VERTICALLY LOADED FRP AND PVC SINGLE PILES

Omer Muhammad EDAN

MSc THESIS

Civil Engineering

Supervisor: Assoc. Prof. Dr. H. Suha AKSOY

APRIL-2019

T.C.

FIRAT ÜNİVERSİTESİ

FEN BİLİMLERİ ENSTİTÜSÜ

BEARING CAPACITY OF VERTICALLY LOADED FRP AND PVC SINGLE PILES

Yüksek Lisans Tezi

Omer Muhammad EDAN

162115107

Tezin Enstitüye Verildiği Tarih : 06.03.2019

Tezin Savunulduğu Tarih: 12.04.2019

Anabilim Dalı: İnşaat Mühendisliği

Programı: Geoteknik

Danışman: Doç.Dr.H.Suha AKSOY

Doç.Dr.Muhammet KARATON

Dr.Öğr.Üyesi Abdulhakim ZEYBEK

NİSAN-2019

ACKNOWLEDGMENTS

First of all, in the name of Allah, the Most Gracious, the Most Merciful. All praises and thanks be to Allah, we seek His help and mercy, the Almighty, who has created the heavens and the earth, and brought into being deep darkness as well as light. On whom we definitely depend for sustenance, guidance and help.

This research study conducted in partial fulfillment of the requirements for the master degree of Applied Science in Civil Engineering at Firat University, and financially supported by BAP of Firat University, project number MF.18.42. However, I put a lot of my efforts into this thesis. But it is clear that no one can finish his/her thesis without any support from the others such as supervisor, colleagues, friends, and classmates. Therefore, I would like to express and give many thanks to my supervisor Assoc. Prof. Dr. H. Suha AKSOY and Res. Assist. Mesut GÖR, as well as Res. Assist. Aykut ÖZPOLAT, and all my friends, colleagues and classmates. In addition, I would like to express my feelings to my deceased parents who made me this person to reach this brilliant destination I always thank them for their efforts that have raised me up. I have also special thanks to my family members for their continued motivation to achieve my goals with a positive result.

Omer Muhammad EDAN

APRIL - 2019

DECLARATION

No portion of the work referred to in the thesis has been submitted in support of an application for another degree or qualification of this or any other university or other institutes of learning.

Omer Muhammad Edan

APRIL - 2019

TABLE OF CONTENTS

SUMMARY

Bearing Capacity of Vertically Loaded FRP and PVC Single Piles

Heavy structures, high-rise buildings, and marine structures increase the tendency to use pile foundations. Since conventional pile foundations are mainly made of timber, steel, and concrete. These piles have a limited life cycle and high maintenance costs, especially where they are used in marine applications, industrial environments and corrosive soils. In order to extend the service life of these piles and reduce the impact of deterioration on the pile bearing capacity a larger pile cross section is often recommended, as well as some chemical treatments are also applied, while both of these options have led to spending an extra budget to build a required pile foundation. Despite the fact that chemical treatments have a negative impact on environmental pollution and the health of those people who do it.

Recently, because of their high corrosion resistance, Fiber Reinforced Polymer (FRP) and recycled plastic piles have been developed for use as an alternative to these piles in the aforementioned environments. Since piles carry and transfer axial loads through the pile point capacity and/or the skin friction resistance (i.e., pile shaft capacity or pile shaft friction resistance), and despite the uncertainties associated with the pile behavior, the mechanical, physical and structural behavior of conventional piles were well documented. Nevertheless, due to the novelty of composite piles, the database of these piles still does not contain sufficient data. One of the concerns in composite piles and although it is not yet quite clear in the conventional piles is the pile shaft behavior (i.e., the pile-soil interface resistance). The friction force at the soil-pile interface is estimated primarily using the interface shear box test. Some uncertainties regarding this test method, especially for sandy soils, leads to the measurement of high values of the interface parameters (i.e., c and δ) in relatively low-to-high relative density.

Because of the uncertainties associated with the pile axial behavior and in particular the pile shaft behavior, the designers often use the approximation values to estimate the interface friction angle (δ) during their design. For example, Terzaghi and Peck (1948) reported that many designers take into account that the interface friction angle (δ) is equal to two of three (2/3) of the measured value of the internal friction angle (φ), Coyle and Castello (1981) considered 0.8φ, and according to various studies, the δ seems to be in the

range between 0.5 to 0.8φ (Das, 2015). These approximations in the evaluation of shear interface parameters prevent making economical designs and sometimes lead to stability problems. However, the actual bearing capacity of the pile is measured by performing field load tests, but it is impossible to determine the independent contribution of the pile shaft capacity to the ultimate pile bearing capacity.

Therefore, in this study, the ultimate bearing capacity and pile base resistance of two composite piles (i.e., concrete-filled FRP and PVC pipe piles), as well as the independent contribution of pile shaft capacity were determined by carrying out a number of load-displacement model experiments at different relative densities (i.e., D_r = 10%, 40%, 65% and 90%) of model sand.

The experimental results demonstrated the fact that the interface friction angle increases with increasing relative density considerably whereas this behavior was not observed in the interface shear box test, and that the interface friction angle at low relative density (i.e., D_r = 10%) can be ignored while in the interface shear box test, this relative density has high interface friction angle and cannot be easily ignored in the calculation of piles bearing capacity. In addition to model experiments, piles were modeled in the finite element environment to calculate the ultimate pile bearing capacity, as well as compare them to theoretical and experimental results. Finite element analysis has provided roughly the same settlement values at failures as that model experiments have. However, in particular, for high relative densities (i.e., D_r = 40%, 65%, and 90%), finite element analysis has not yielded a good agreement in terms of load-displacement behavior (p-y behavior) under certain conditions of this study. In model experiments, p-y behavior is a nonlinear relationship in all relative densities, whereas in finite element analysis it has become a nonlinear relationship where D_r = 10 and has become a linear relation where D_r=40 %, 65%, and 90%. In fact, this behavior is far from being expected, because, at high relative densities, the pile shaft capacity must be increased; and therefore, the degree of curvature of the p-y behavior must also be increased (i.e., it should be a non-linear relationship).

Keywords: FRP pile, PVC pile, Pile point capacity, Pile shaft capacity, Direct shear test, Interface shear angle, Finite element analysis.

ÖZET

FRP ve PVC Tekil Kazıkların Düşey Yükler Etkisi Altında Taşıma Güçlerinin Belirlenmesi

Yüksek binalarda ve liman yapılarında gittikçe artan oranlarda kazıklı temeller tercih edilmektedir. Bu tür yapılarda tercih edilen geleneksek kazık malzemeleri olan ahşap, çelik ve beton özellikle liman yapılarında ve aşındırıcı çevresel şartlarda kullanıldıklarında sınırlı ömre sahip ve tamir maliyetleri yüksek malzemelerdir. Hizmet ömürlerini uzatmak için bu tür zeminlerde kazıkların kesit alanlarının artırılması veya kimyasal koruma önlemleri tavsiye edilmektedir. Bu işlemler ise maliyetlerin büyük oranda artmasına neden olmaktadır. Ayrıca kimyasal koruma önlemlerinin olumsuz çevresel etkileri olduğu bilinmektedir. Son yıllarda uzun servis ömürleri ve olumsuz çevresel koşullardan etkilenmemeleri nedeniyle cam elyaf takviyeli plastik (fiber reinforced plastic, FRP) ve geri dönüştürülmüş plastik kazıklar, geleneksel kazık malzemelerine bir alternatif olarak kullanılmaya başlanmıştır.

Kazıklar, yapısal yükleri uç direnci ve yüzey sürtünmesi yoluyla taşırlar. Geleneksel kazık malzemelerinin mekanik, fiziksel ve yapısal davranışları ile ilgili pek çok kaynak mevcuttur. Ancak kompozit kazıkların son zamanlarda kullanılmaya başlaması nedeniyle literatürde yeterli kaynak mevcut değildir. Kompozit kazıklar ile ilgili en tartışmalı ve bilinmeyen konu bu malzemeler ile zeminlerin sürtünme davranışıdır. Yapılan ilk araştırmalarda zemin-kazık malzemesi arasındaki sürtünme kuvvetleri, kesme kutusu deneyleriyle belirlenmiştir. Özellikle sıkı kumlarda, bu test yöntemi ile düşük sürtünme parametreleri (c,δ) ölçülebilmektedir.

Kazık eksenel yükleme davranışlarındaki bu belirsizlikler, yaklaşık değerlerin kabul edilerek tasarım yapılmasına neden olmaktadır. Terzaghi ve Peck (1948), yüzey sürtünme açısının (δ), zeminin içsel sürtünme açısının (φ) 2/3'üne eşit olduğunu kabul etmişlerdir. Coyle ve Castello (1981) ise yüzey sürtünme açısının 0.8φ alınabileceğini belirtmişlerdir. Pek çok araştırmada δ değerinin 0.5 ile 0.8φ arasında alınması gerektiği belirtilmiştir (Das, 2015). Bu kabuller zaman zaman ekonomik olmayan tasarımlar yapılmasına sebep olurken zaman zaman ise stabilite kayıpları yaşanmasına neden olmaktadır. Kazıkların gerçek taşıma güçleri sadece arazide yapılan kazık yükleme deneyleri ile belirlenebilmektedir.

Ancak yine de bu kazıkların taşıdıkları toplam yükün ne kadarını uç direnciyle, ne kadarını yüzey sürtünmesiyle taşıdıkları bilinmemektedir.

Bu çalışmada, iki kompozit (beton dolgulu FRP ve beton dolgulu PVC) kazığın nihai taşıma güçleri, uç dirençleri ve yüzey sürtünme değerlerinin kazık yükleme deneyleri yardımıyla belirlenmesi amaçlanmıştır. Deneylerde 4 farklı sıkılıkta (D_r = %10, %40, %65 ve %90) kum zeminler kullanılmıştır.

Deneyler sonucunda, kesme kutusu deney aletiyle yapılan yüzey sürtünme açısı ölçümlerinin aksine, yüzey sürtünme açısının artan sıkılıkla sürekli arttığı görülmüştür. Elde edilen yüzey sürtünme açısı değerlerinin özellikle düşük rölatif sıkılık değerlerinde, kesme kutusu deney aletiyle elde edilen değerlerden çok düşük olduğu görülmüştür. Ayrıca yapılan model kazık yükleme deneyleri sonlu elemanlar yöntemiyle sayısal olarak modellenmiş ve elde edilen sonuçlar model deneylerinin sonuçları ile karşılaştırılmıştır. Yapılan sonlu elemanlar analizleri sonucunda, deneylerden elde edilen oturma değerleri ile sonlu eleman analizleri neticesinde elde edilen oturma değerlerinin birbiri ile uyumlu olduğu gözlemlenmiştir. Ancak özellikle orta sıkı ve sıkı (D_r = %40, %65, and %90) zeminlerde sonlu eleman analizlerinden elde edilen yük deformasyon eğrilerinin (p-y eğrileri) deneysel sonuçlarla benzeşmediği görülmüştür. Sonlu eleman analizlerinden elde edilen p-y eğrilerinin doğrusal olduğu belirlenmiştir. Oysa deneylerden elde edilen p-y eğrileri non-lineerdir. Gerçekte kazık yüzeyi ile zemin arasındaki sürtünme arttıkça p-y eğrisinin eğriliğinin artacağı ve non-lineer olacağı bilinmektedir.

Anahtar Kelimeler: FRP kazık, PVC kazık, Kazık uç direnci, Kazık yüzey sürtünmesi, Kesme kutusu deneyi, Yüzey sürtünme açısı, Sonlu elemanlar analizi.

LIST OF FIGURES

Page No

LIST OF TABLES

Page No

LIST OF SYMBOLS

pH : Degree of acidity or alkalinity

FRP : Fiber Reinforced Polymer

SRP : Structurally Reinforced Plastic

δ : Pile-soil Interface Friction Angle

φ : Internal Friction Angle

FHWA : Federal Highway Administration

HDPE : High-Density Polyethylene

PVC : Polyvinyl Chloride

C : Cohesion

MDPE : Medium-Density Polyethylene

D_{50} : Soil Particle Mean Size

GFRP : Glass Fiber Reinforced Polymer

UV : Ultraviolet

SPT : Standard Penetration Test

CPT : Cone Penetration Test

RPP_S : Recycled Plastic Piles

SED : Strain Energy Density

UPVC : Unplasticized Polyvinyl Chloride

p-y : Load-Displacement

D_r : Relative Density

Q_u : Ultimate Bearing Capacity of Pile

Q_p : Pile Point or End-Bearing Capacity of Pile

Q_f : Shaft Capacity, Shaft Friction Resistance, or Skin Friction Resistance of Pile

A_p : Pile Point Area

q : Mean Overburden Pressure at the Pile Toe

N_q : Bearing Capacity Factor

γ : Soil Unit Weight

B : Least or Short Dimension of Pile (Pile Diameter)

N_γ : Bearing Capacity Factor

s_γ : Shape Factor

$K_{p\gamma}$: Terzaghi's Coefficient of Passive Earth Pressure

d_c : Depth Factor

N_c : Bearing Capacity Factor

s_q : Shape Factor

d_q : Depth Factor

d_γ : Depth Factor

L_b : Embedment Depth of Pile

D' : Pile Diameter

L : Pile Length

K_p : Coefficient of Passive Earth Pressure

D" : Embedment Depth of Pile

B" : Short Dimension of Pile

L" : Long Dimension of Pile

N_q^* : Bearing Capacity Factor

Pa : Atmospheric Pressure (100 kN/m2)

η : Surface Angle in Radian at Pile Toe

$\sigma_0^{-\prime}$: Mean Effective Soil stress at the Pile Toe

N_σ^* : Vesic's Bearing Capacity Factor

K_o : Coefficient of Lateral Earth Pressure at Rest

B' : Least Dimension of Pile (Pile Diameter)

N_q' : Bearing Capacity Factor

f : Unit Skin Friction Resistance

K : Coefficient of Lateral Earth Pressure

σ_0' : Mean Effective Vertical Pressure at the Desired Depth

p : Pile Circumference or Pile Perimeter

L' : Critical Pile Embedment Length $\leq$ 15D

D : Pile Diameter

D_{tank} : Diameter or Short Dimension of Model Tank

D_{pile} : Diameter of Pile

LVDT : Linear Variable Displacement Transducer

γ_d : Dry Unit Weight

e : Void Ratio

ASTM : American Society for Testing and Materials

DSB : Direct Shear Box

G_s : Specific Gravity

$\gamma_{d\ min}$: Minimum Dry Unit Weight

$\gamma_{d\ max}$: Maximum Dry Unit Weight

e_{min} : Minimum Void Ratio

e_{max} : Maximum Void Ratio

D_{max} : Maximum Grain Size

D_{min} : Minimum Grain Size

D_{10} : 10% of the Sand Particles are Finer than this Size.

D_{30} : 30% of the Sand Particles are Finer than this Size.

D_{60} : 60% of the Sand Particles are Finer than this Size.

Cu : Uniformity Coefficient

Cc : Coefficient of Curvature

1. INTRODUCTION

1.1. Statement of the Problem

Heavy structures, high-rise buildings, and marine applications have always increased the use of pile foundations with higher bearing capacity and installed at a deeper depth. Each year, a number of pile foundations have reached its design lifespan and to keep these piles in service or to replace them with other piles, a billion dollars is spent. In addition, timber, steel, and concrete are the most common materials that are used in the construction of conventional pile foundations. Chemical agents (i.e., salts, and freezing and thawing), fungi and marine borer are the main agents that deteriorate conventional pile foundations. Applications of these piles in the harsh environment, organic soil conditions and naval environments associated with well-known problems such as deterioration from marine borer attack and fungi, corrosion and degradation of timber, steel, and concrete piles, respectively. Aforementioned problems in the harsh environmental applications make conventional piles to have a limited life cycle and high repair cost.

Nowadays, some industrial foundations have tried to reduce the rate of steel corrosion to the lowest value. For example, the corrosion rate of steel in industrial environments has been estimated at up to 0.2 mm/year by the British Steel Corporation (Shaia, 2013). However, in the harsh soil environment, 0.03 mm/year is the maximum corrosion rate was recorded for an extracted steel pile after 25 years of service (Han et al., 2003). Concrete degradation happens at low levels of pH with the high concentration of sulfate and chloride salt compositions in ground soils (Fleming et al., 2008). The annual repair cost for replacement or maintenance of deteriorated piles in waterfront structures is approximately $1 billion in the United States (Lampo et al., 1998). Figure 1.1. shows the corrosion of conventional piles.

Developments in the modern industrial revolution increase the tendency for the necessary use of the composite piling, especially in harsh environments such as industrial environments, marine applications and aggressive soils. However, the initial costs of composite piles 2-3 times higher than the traditional piles, and the manufacturer's assessment of the service life of the composite piles is about 50-75 years, so long-term durability makes them economically feasible (Pando et al., 2002b).

Plastic and fiber reinforced polymer (FRP) composite piling is an industrial attempt to propose another technique as an attractive option to the conventional piling system. The

most commonly accepted characteristics of composite piles are light-weight, high specific strength, durability and speed of application. However, composite piling provides emerging technology and it is expected to have a prestigious future because in various geotechnical and structural applications FRP and plastic shells serve as structural elements in the deep foundation systems (Shaia, 2013).

a) Deteriorated timber pile b) Degraded concrete pile c) Corroded steel pile

Figure 1.1. Deterioration of conventional piles (b and c adopted from Shaia, 2013).

Composite piling is still not widely accepted as geotechnical issues, this is due to limited guidelines and insufficient knowledge on the history of composite piling. For example, the FRP composite piles reinforced with steel pipe core are usually used under the conditions, which exposed to water; in this case, it seems that FRP shell only works to protect steel pipes from corrosion. Most of the use of Structurally Reinforced Plastic (SRP) Piles in marine environments are used in the applications of fender piling, while it is considered to have the capacity to load carrying applications (Guades et al., 2012).

To ascertain the validity of any new materials entering civil applications, a large study must be conducted before they are being accepted, especially in foundation applications. Mechanical and physical properties, structural behavior, construction costs, durability, and drivability are the most important things to be clearly defined. Iskander (2002) reported that despite their high durability and environmental benefits, further fieldwork is necessary to determine the mechanical and physical properties of composite materials more clearly than they currently exist. Design guidelines and experiment

recommendations are also highlighted. In addition, verification of theoretical and experimental studies through long-term monitoring is essential.

The use of composite piling in geotechnical applications began a few years ago and there is still some uncertainty involves these piles compared to the traditional piling system. This is primarily due to the relatively higher initial cost compared to traditional piling, lack of the database of the previous works and absence of sufficient knowledge, especially for their applications in the harsh environments (Shaia, 2013). For these reasons, the axial capacities (i.e., total or ultimate bearing capacity, base capacity or base resistance, and shaft capacity or shaft friction resistance) of axially loaded single-model composite piles, in particular, shaft capacity of single-model composite piles, are an attempt of this study to fill a gap in knowledge and to show the capacities of these single-model composite piles in terms of load-displacement behavior.

The shaft friction resistance is one of the concepts of the structural behavior of the pile against the applied axial loads. The friction-resistant behavior is one of the concerns in composite pile foundations, and even it is still not quite clear in conventional pile foundations. Many designers consider the interface friction angle (δ), two of three (2/3) of the measured value of the internal friction angle (φ) of the surrounding soil in their designs **(**Terzaghi and Peck, 1948), Coyle and Castello (1981) considered the (δ) equal to 0.8φ and is generally estimated between 0.5 to 0.8φ (Das, 2015)**.** However, it is clear that (δ) changes for a certain soil with different materials. Despite many studies on the behavior of pile shaft friction resistance, but still, the (δ) between soil-pile interface is not exactly known and designs are made with the use of approximate values. This approximate assessment of the interface friction angle has an effect in determining the number and dimension parameters in the design of single pile in the pile group system. In addition, the low value (δ) prevents designers from making an economic design that significantly increases project time and costs, while a high (δ) value leads to structural stability problems, especially in low relative densities (Aksoy et al., 2016).

1.2. General Description of Pile Foundations

Piles are long structural members mainly made of timber, steel, and concrete. They are deep and high cost foundations compared to shallow foundations. However, pile foundations require more cost and time than the shallow foundation, but in such cases, when the expected settlement exceeds the allowable limit in the case of the application of

the shallow foundation or when the soil layers near the ground have the low bearing capacity and cannot provide sufficient support for the applied loads, application of the piles is being necessary to provide appropriate structural safety.

Piles carry and transfer applied loads from the superstructure, to the ground soil layers gradually, or through compressible soils or water onto stiffer or bedrock strata. Pile foundations are used in many cases, it can be used to support high-rise structures to resist wind uplift forces, it also necessary in naval applications to support lateral forces from the impact of ships and sea waves. Vertical and horizontal forces may act on piles at the same time when they are used in such cases, such as bridge piers and abutments, retaining walls and machine foundation. Piles carry axial loads in two ways, point or tip bearing, and/or shaft friction resistance (i.e., pile shaft capacity or pile skin friction resistance). However, the significance of pile base resistance on the total pile capacity is neglected in case of loose sand and/or small piles in diameter, and in particular, in the case of compressible soils (i.e., no bed-rocks or hard stiff soil layers under the pile toe), in such a case, pile capacity is fully taken from the shaft friction resistance (i.e., pile shaft capacity or pile skin friction resistance).

Piles are mostly made of conventional materials such as timber, steel or concrete. Timber piles have been used in the early days but the use of steel and concrete piles started in the 19th and 20th century, respectively. Conventional piles have a low life cycle and high repair costs, especially in corrosive soils, industrial applications, and marine environments. Applications of conventional piles in the previous-mentioned environments associated with expected environmental problems such as timber deterioration due to marine borer attack and fungi, steel corrosion, and concrete degradation. Annual repair costs required to treat pile foundations that are affected by marine problems resulting from concrete deterioration and steel erosion is more than $2 billion in the United States of America (Iskander et al., 2001). Therefore, in recent years plastic-based materials; Fiber-Reinforced Polymers (FRPs) and recycled plastic materials are in progress to be an attractive option for traditional piles in harsh environments.

1.3. Deterioration of Traditional Piles

1.3.1. Timber Piles

There was no considerable deterioration in the timber piles affected by the fungi and marine borer attack until a considerable effort was made to prevent water pollution in the harbors and waterfronts. One of the concessions to access these environmentally friendly activities is the significant growth of marine attackers on the waterfront, resulting in significant damage to the marine timber infrastructure (Iskander, 2002).

The most famous marine borer attackers are Teredo, Bankia, and Limnoria. Teredo and Bankia are two types of shipworms. At the beginning of their lives, the larvae of these borers go into the timber section and follow the timber grains. Digging deeper tunnels is their function besides their growth. Figure (1.2.a.) shows a Swiss-cheese shaped hole in the interior of the timber resulting in numerous tunnels into the timber piles (Iskander, 2002).

The Limnoria's activities are concentrated at the timber surface. They nibbled the timber surface and lose the timber in diameters up to 25.4mm yearly (Figure 1.2.b.). So far, many techniques have been used to extend the pile's service life and prevent the impact of degradation, corrosion, and deterioration on the pile serviceability, but still unstoppable. Creosote and arsenate are the most effective pressure-treatment techniques that are used to reduce or minimize the impact of marine borer attack (Iskander, 2002). However, these pressure-treatment techniques lead to environmental pollution and don't stop marine borer from attacking the timber piles absolutely. Even treated timber piles are exposed to fungal attack in the central part because it is not possible to penetrate the preservative treatment all the way to the timber section (Lopez-Anido et al., 2004).

1.3.2. Steel Piles

Application of steel elements in the industrial zone and marine applications associated with corrosion, which causes to deterioration in the steel section and loses its thickness (Figure 1.3.a.). The rate of steel corrosion is about 0.03 mm and 1.2 mm per year in the regular soil conditions and splash zone, respectively (Iskander, 2002). Steel corrosion can be assessed by applying special coating layers of heavy metal composition, but these treatments have a negative impact on the environmental pollution (Iskander, 2002).

(a) (b)

Figure 1.2. (a) Teredo and Bankia tunneling in a timber pile, and (b) Limnoria worms attacking timber piles (adopted from Iskander, 2002).

1.3.3. Concrete Piles

Sodium and calcium chlorides compositions in the water are the most effective and destructive chemical agents that have severe effects on the concrete degradation. Electrical currents are produced when these salt compositions cross the concrete and reach the steel bars through the cracks in the concrete cover and corrode the steel bars. The steel bars lose their thickness in diameters that cause to lose their bond with the surrounding concrete and the reduction in member cross section is happened, thereby the concrete is expanded and high tensile stress in the concrete is induced, resulting spalling and concrete cracking (Figure 1.3.b.). Despite the chemical agents the climate changes, freezing, and thawing lead to further concrete degradation (Iskander, 2002).

1.4. Composite Piles

The composite piling (i.e., plastic based-materials composite piling) refers to the latest revolution in the foundation industry to offers composite products as a substitution of conventional piling and to overcome the deteriorate problems associated with these piles in harsh environments. Recent industrial developments progressed to use FRPs and recycled plastic materials for the purposes of replacement and/or protection of conventional timber, steel, and concrete piles, with the aim to produce composite piles that have a potential to

support structures safely in the naval applications and corrosive soils or other corrosive environments with lower repairs cost and long cycle life than traditional piles.

(a) (b)

Figure 1.3. (a) A steel pile lost its section almost 100%, and (b) a concrete pile lost its section about 75% (adopted from Iskander, 2002).

Composite materials (recycled plastics and reinforced fibers) show good compatibility compared to traditional pile materials. This is due to their specific characteristics such as lightweight, high strength-to-weight ratio, corrosion resistance, chemical, and environmental resistance and low maintenance cost (Sakr et al., 2005). Recent industrial developments have advanced the use of recycled plastic materials to produce composite piles for two purposes. First, using recycled plastic materials in the production of composite piles has economic and environmental benefits to landfill them. Second, the applications of plastic piles in the harsh environment have the advantages of service life and maintenance costs over traditional piles (Tetra Tech, 1999).

A typical installation of the composite piles in literary works was recorded in water-front barriers, fender piles and as bearing piles for low weight structures (Iskandar and Hassan, 1998). Fiberglass or high-density polyethylene reinforced with fiberglass with other additives are used in the manufacture of composite piling products to enhance their mechanical properties, durability, and ultraviolet (UV) resistance (Iskandar, 2002).

The composite piles are still limited to use in some offshore facilities and a number of harbors. The composite piles are mostly used for fender piles application and

replacement of steel shells with the exception of a few applications to support piers. Tiffany Street Pier in New York City is one application of recycled plastic piles (Iskander, 2002). Also, slope stability can be achieved with recycled plastic pins (Loehr et al., 2000). The FRP and plastic composite piling require adequate design recommendations and appropriate installation techniques to overcome their application barriers and challenge over traditional pile foundation systems (Iskandar, 2002). First, it should have the potential to gain economic satisfaction in their own manufacturing process and cost challenges based on life cycle (Iskander and Hassan, 1998). Second, their mechanical and physical characteristics must be clarified, and confirmation of long-term durability in various field conditions is required (Frost and Han, 1999). Third, additional efforts are required to further understanding of piles drivability behavior and load carrying capacity (Ashford and Jakrapiyanun, 2001). Fourth, further development in design guidelines and standard recommendations is also significant (Lampo, 1999). And fifth, a number of composite piles must be installed in the field, and then large-scale field load tests, as well as long-term vertical monitoring, are necessary (Iskander, 2002).

Research outcomes revealed that the FRP composite concrete-filled pile is the best type among all other FRP piles to carry axial loads. The Federal Highway Administration (FHWA) in the United States of America has recommended that the FRP composite piling have a significant capacity as axial-bearing piles and have the potential to be an interesting option for conventional piling foundations, especially in naval applications and harsh soils environments (Juran and Komornik, 2006). However, the lack of sufficient databases has led to the use of composite piles in some applications without considering their structural capacity, for example in those applications that are exposed to water FRP shells are used to protect steel piles, in such cases, the structural capacity of FRP shell is ignored. Another example is the use of structurally reinforced plastic piles for fender applications while these piles appear to have the ability to load-bearing applications (Guades et al., 2012).

1.4.1. Application History of Composite Piles

The replacement of timber fender piles by the composite piles at the Port of Los Angeles is the first applications of composite piles as a fender replacement piles (Heinz, 1993). The first driven process of the recycled plastic composite pile (recycled plastic shell-steel pipe core pile) as a segmented prototype pile was recorded in history at the port of Los Angeles in April 1987 (Horeczko, 1995). The dimensions of the prototype pile are

18 m and 0.33 m in length and diameter, respectively. The prototype pile is structurally strengthened with a steel pipe core 0.125 m in diameter. The pile segments were connected at every 6 m joints via a threaded coupling. These piles suffered from delamination between plastic shell and steel pipe core during the driving process. However, composite piles are currently produced with a guarantee against delamination (Iskander and Stachula, 2002). Over the next few years, a number of vendors or company have offered various composite pile products that are made of virgin, recycled, and hybrid composites (Iskander, 2002). Since the first driven process of the composite piles was recorded in 1987, it has been used in the construction of a number of other projects (Pando et al., 2006). Common applications of composite piling are naval fender piles, load-bearing piles for lightly-loaded structures and experimental studies (Iskander and Hassan,1998).

1.4.2. Composite Piles Products

In the early 21st century, several manufacturers began to show their products in the marketing places. The available products are mostly produced for the purpose of timber piling replacement, most of them are made of fiberglass or high-density polyethylene (HDPE) with fiberglass or steel reinforcement. However, a number of manufacturers declare that their products have a potential to field applications as a bearing pile and structural applications, but still the application of their products are limited in fender piling (Iskander, 2002).

Composite piles are commercially available in the market with diameters ranging from 20.32 to 60.96 cm, in structurally reinforced composite piles, typically 6 to 24 FRP or steel bars are used and bar diameters ranging from 1.91 to 3.58 cm (Plastic Pilings, 2001; Seaward International, 2001). The composite piling products, including field driving performance and availability in the market (Figure 1.4.(a-h)), are (a) Steel Pipe Core Piles, (b) Structurally Reinforced Plastic (SRP) Piles, (c) Concrete-filled FRP Pipe Piles, (d) Fiberglass Pultruded Piles, (e) Fiberglass Reinforced Plastic Piles, (f) Hollow FRP Pipe Piles, (g) FRP sheet Piles and (h) plastic lumber piles (Pando, 2003; Guades et al., 2012; Zyka and Mohajerani, 2016).

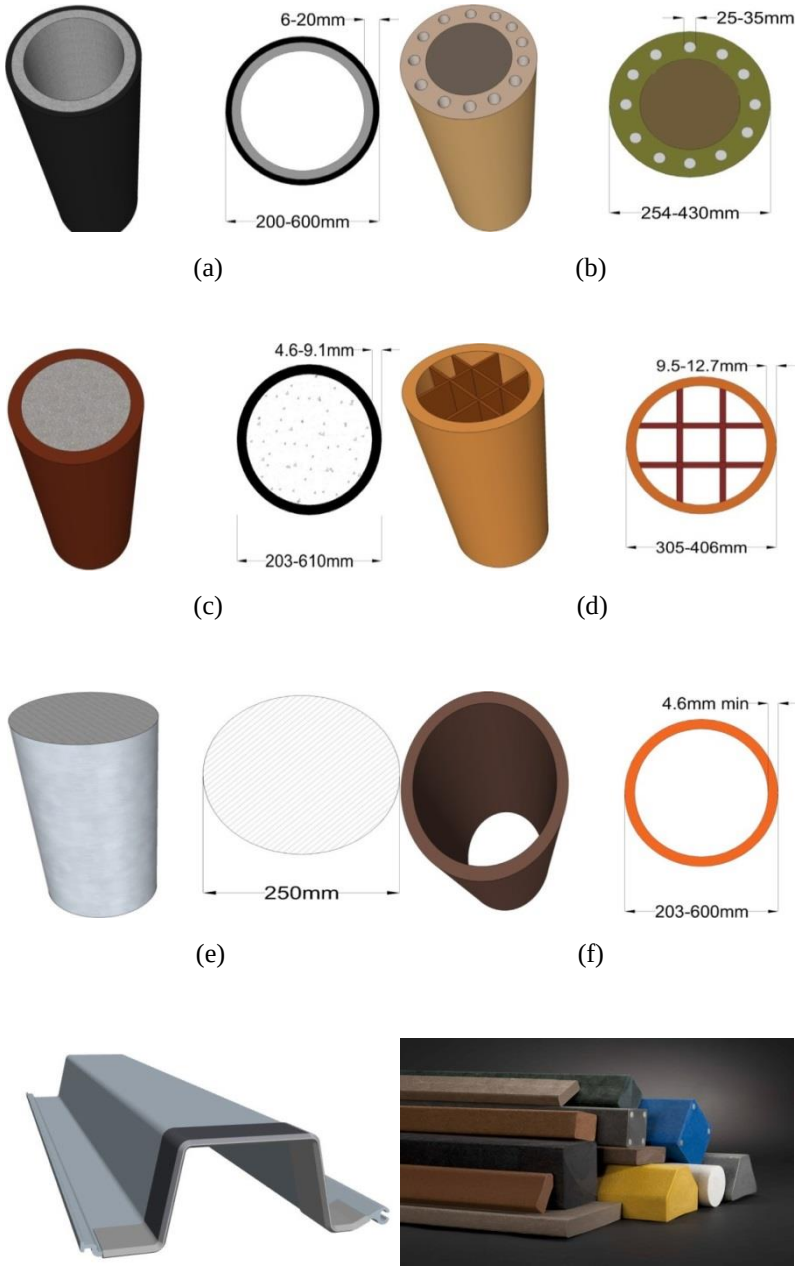

Figure 1.4. (a-h). Common types of composite piles (Pando, 2003; Guades et al., 2012; Zyka and Mohajerani, 2016).

1.5. Literature Review

1.5.1. Direct Shear Test

The interface friction force that is mobilized with a relative displacement between soils and building materials is an important component in the design of many geotechnical engineering applications. The interface friction parameters (i.e., cohesion and interface

friction angle) are mostly used in the design of pile foundations. The interface parameters of the pile-soil structure are mainly estimated using the following methods (Rinne, 1989):

1. Back analysis of failures of full-scale structures.
2. Instrumented field experiments; and
3. Laboratory testing using conventional techniques modified for interface studies.

Laboratory tests are mostly conducted using the interface shear box test to measure interface parameters. However, the relationship between horizontal displacement and soil shear strength is always increased in the interface shear box test. While field load tests have shown that the friction force between the soil-pile interface increases with the increase in pile embedment length to a limit where the embedment length of pile to its diameter ($(L_b/D)_{cr}$) reaches its critical state and then decreases with the displacement of the pile (Das, 2015). In addition, the interface shear box test provides conservative values particularly for high relative densities compared with low relative densities. The interface friction angle (δ) values proposed in the literature are generally contradictory, for example, Terzaghi and Peck (1948) depends on the results of many researchers, Coyle and Castello (1981), suggested 0.67φ and 0.80φ, respectively, while other researchers proposed 0.5 to 0.8φ (Das, 2015). These differences in the evaluation of the interface friction angle can be summarized in two points; First, the factors that have an effect on the interface friction angle are not well predicted. Second, the working mechanism of the direct shear box is in conflict with the load transfer mechanism of the pile. However, considerable studies have been conducted, and several researchers have explained how the properties of the interface components can affect the observed values of the interface friction angle (δ), as well as, the plastic deformation of the structural surface due to interface shearing resistance has been sufficiently studied. Any evaluation of (δ) values should represent the characteristics of the contact surfaces and associate them with the behavior of the material during the relative movement. Several literary works of the sand-pile interface are briefly presented below:

Potyondy (1961) conducted direct shear tests to investigate interface behavior between four types of soil (sand, clay, cohesive granular soil and Silt (rock flour)) and three different materials (wood, steel, and concrete). Test results showed that the materials surface roughness, moisture content, soil composition, and intensity of the normal stress were the four main factors governing the interface friction angle. The researcher suggested that the value of adhesion can be neglected for a cohesive granular soil with clay content

less than 15 %, as well, a clay soil with sand content less than 8% can be considered as a pure cohesive clay.

O'Rourke et al., (1990) conducted extensive direct shear box tests to measure the interface friction angle between four different sands and different polymers like HDPE lining, HDPE pipe, MDPE pipe, PVC pipe, and PVC lining. The test results indicated that an increase in the interface friction angle was achieved with increasing sand density, whereas it decreased as the surface hardness of the polymers increased. In addition, the sand type was another factor that has had an effect on the interface friction angle, but the normal stress levels were not. They stated that the interface friction angle of polymeric materials can be easily estimated from a simple correlation (δ/φ) ranging from 0.55-0.65, especially for HDPE and MDPE, respectively.

Frost and Han (1999) performed direct shear test to investigate the interface behavior between the FRP-composite material and sand, as well as to compare the interface characteristics of FRP-sand and steel-sand. The test results revealed that the shear behavior of FRP-sand interface was governed by relative roughness (i.e., surface roughness of the material/soil particle mean size (D_{50})), the levels of normal load, the density of the soil mass at the beginning of the test, and the granular shapes (angular or round). However, how the sample was prepared, the shearing rate and the height of the soil specimen had the ignorable effect on the quantitative coefficient of the interface friction.

Pando et al., (2002a) conducted a series of direct shear tests to predict interface shear behaviors of two different sandy soils on a pre-stressed concrete pile and two different FRP composite piles. The test results revealed that the relative roughness (i.e., surface roughness of the material/soil particle mean size (D_{50})), surface hardness, and particle shape dominated the interface friction angle (δ) behavior. The sandy soil, which had a sub-rounded to rounded particle shape, showed the lower value of (δ) on a hard surface of FRP composite material compared to a softer one. The first was due to sliding soil grains and the second due to penetration of sand grains along the FRP surface. However, sandy soil, which had sub-angular to angular particle shape, showed similarly the same value of (δ) on each of the FRP composite materials, due to sand grains plowing on the FRP surface. Because of its surface roughness properties, the pre-stressed concrete pile provided proper interlocking of soil grains with the piles surface, thus developing the highest value of (δ) on each sandy soil.

Sakr et al., (2005) conducted an experimental study to compare interface shear behavior between steel/dense-sand and FRP/dense-sand. Test results revealed that the relative roughness of FRP materials and round sand grains governed the interface friction angle. The FRP materials showed relatively the same or slightly higher angle than the steel, thus the use of composite piles has added benefits over traditional piles due to degradation or corrosion resistance in addition to shaft friction resistance (i.e., pile shaft capacity).

Al-Mhaidib (2006) conducted a direct shear test and pile model uplift capacity test to investigate the behavior of steel-sand interface. The test results showed that the internal friction angle (φ) increased with increasing shear rate, as well, interface friction angle (δ) was also increased at different surface roughness. While, for a certain test method, the amount of (δ/φ) remained relatively constant for the different steel surface roughness when the shear rate was increased. The soil specimens were sheared at the rate of (0.0048, 0.048, 0.08, 0.4 and 0.9 mm/min) and measured values of (φ) were (38.7°, 40.1°, 42.5°, 44.6°, and 46.5°), respectively. In the pile-model uplift capacity tests the values of (δ) of smooth surface steel were (18.6°, 22.4°, 24°, 26.3°, and 28.5°) and rough surface steel were (56.7°, 59.7°, 60.3°, 62.3°, and 63.9°), respectively. But in direct shear tests the values of (δ) of smooth surface steel were (16°, 18.8°, 19.5°, 21.5°, and 23.2°) and rough surface steel were (37°, 38.1°, 40°, 42.3°, and 44.5°), respectively. In the interface shear box test, the (δ/φ) ratio of both smooth and rough steel surfaces were (0.41, 0.47, 0.46, 0.48 and 0.5) and (0,96, 0.95, 0.94, 0.95 and 0.96), respectively.

Aksoy et al., (2016) performed a number of direct shear tests to estimate the interface friction angle (δ) between FRP-clayey sandy soil, steel-clayey sandy soil, and wood-clayey sandy soil. Five clayey sandy soils (S_1, S_2, S_3, S_4, and S_5) were prepared at different amounts of clay content (0%, 20%, 30%, 40%, and 45%), respectively. The internal friction angle (φ) of clayey sandy soils (S_1, S_2, S_3, S_4, and S_5) were (φ_1=43°, φ_2=39.5°, φ_3=41.5°, φ_4=35°, and φ_5=28°), respectively. The interface friction angle (δ) of FRP-clayey sandy soils were (δ_1=34.5°, δ_2=37°, δ_3=36°, δ_4=32°, and δ_5=22.7°) , steel-clayey sandy soils were (δ_1=26.5°, δ_2=31.5°, δ_3=29.2°, δ_4=27°, and δ_5=18°) and wood-clayey sandy soils were (δ_1=37.6°, δ_2=40°, δ_3=39°, δ_4=34°, and δ_5=24.3°), respectively. The (δ/φ) ratio of FRP-clayey sandy soils were (δ_1/φ_1=0.80, δ_2/φ_2=0.93, δ_3/φ_3=0.86, δ_4/φ_4=0.91, and δ_5/φ_5=0.81), the steel-clayey sandy soils were (δ_1/φ_1=0.61, δ_2/φ_2=0.79, δ_3/φ_3=0.70, δ_4/φ_4=0.77, and δ_5/φ_5=0.64) and wood-clayey sandy soils were (δ_1/φ_1=0.87, δ_2/φ_2=1.01, δ_3/φ_3=0.93, δ_4/φ_4=0.97, and δ_5/φ_5=0.86). The test results emphasized that FRP piles can

challenge conventional steel piles in shaft friction resistance (i.e., pile shaft capacity), as well as high durability, low life-cycle and repair costs. However, the bearing capacity of FRP and wood piles that had the same dimensions were too close.

Almallah et al., (2018) conducted several direct shear tests between three different sandy soils (dense sand (φ_1=44.05°), dense silty sand (φ_2=42.72°), and sandy lean clay (φ_3=22.5°)) and two different surfaces (smooth and rough) glass FRP (GFRP) materials. The interface friction angle (δ) between the above three soils and smooth GFRP material were (δ_1=32.37°, δ_2=35.96, and δ_3=12.41°), and rough GFRP material were (δ_1=36.81°, δ_2=37.11°, and δ_3=15.74°), respectively. The (δ/φ) ratio of smooth GFRP were (δ_1/φ_1=0.73, δ_2/φ_2=0.83, and δ_3/φ_3=0.55) and rough GFRP were (δ_1/φ_1=0.83, δ_2/φ_2=0.86, and δ_3/φ_3=0.70), respectively. The test results indicated that the value of (δ) was changed with the surface roughness characteristics of the material, the amount and rounds of coarse-grained particles and soil dense states.

1.5.2. Pile Drivability

Piles are often driven into foundation soils using driving machines such as a hammer or vibrator machine. In addition, under certain conditions, piles are also installed by means of jetting or partial augering. The machines which are used for piles driving are (a) the drop hammer, (b) the single-acting air or steam hammer, (c) the double-acting and differential air or steam hammer, and (d) the diesel hammer. In pile driving techniques, the cap is put on the head of the pile to keep it away from any damage caused by the driving effect, and a cushion is also suggested to optionally be placed on the cap. The function of the cushion is to reduce the damaging effect and distribute driving force on the pile over a longer period of time. Bored piles are usually installed by means of drilling shaft machines (i.e., continuous flight auger) (Das, 2015).

Due to the manufacture of composite piles, driving techniques are used to install FRP and plastic piles. For this reason, a successful driving process is one of the main obstacles that challenge the composite piles. Performing proper driving installation of thin-walled pipe shell is difficult in the dense sand and the hard-driving process may challenges the pile installation safely. This is absolutely true when the driving process is concerning with low stiffness materials such as thin-wall FRP shell compared to conventional pile materials (Sakr et al., 2004). The conventional machines that are used to drive piles, they strike a hammer on the head of the pile and significant damages can be observed at the head and/or

at the bottom of the pile, where rocks or stiff soils are faced. Toe driving is an innovative and more efficient pile installation technique recently developed and tested in Canada. In this technique, the impact force is applied inside the FRP shell or steel thin-walled shell at its toe using an impact hammer (Sakr et al., 2004). Two of the literary works on composite pile driving are briefly presented below:

Ashford and Jakrapiyanun (2001) conducted analytical studies to make a drivability comparison between the FRP composite piles to traditional concrete and steel piles. The test results indicated that FRP composite piles had the capability to provide relatively the same design capacity as the traditional piles above with the medium-size driving hammer. However, due to low impedance, FRP composite piles reached their maximum capacity (at refusal) to only 65-75% of the traditional piles. They recommended that further research is necessary to study the behavior of FRP composite piles under the driving impact.

Mirmiran et al., (2002) relying on the results of full-scale field experiments, reported that concrete-filled FRP piles having the same strength and dimension parameters as concrete piles can be driven safely without any significant damages at the pile head either in the concrete core or in the FRP shell. No special pile tip was needed and no separation has been observed in the hybrid system. The FRP piles also had the ability to drive under a higher blow counts, allowing a concrete pile to meet current specifications. Even FRP-filled concrete pile can be driven deeper than concrete piles, with a larger driving hammer used to drive conventional concrete piles.

1.5.3. Long-Term Durability

Insufficient data is highlighted in the database of long-term performance and durability of composite piles (Lampo, et al., 1998; Iskander and Hassan, 1998; Iskander, et al., 2001). Composite piles are deteriorated by a chemical agent, UV radiation and are mainly by freeze-thaw cycles due to water absorption. However, nowadays, the effect of UV radiation has reduced to a lesser extent through the application of special protective coats and the addition of additives in the manufacture of composite piles (Pando et al., 2006). Several researchers have shown that water absorption can considerably damage FRP composite piles by means of service life reduction (Garcia, et al., 1998), degradation in modulus of elasticity, strength capacity, and strain to failure (Springer, et al., 1980). An example of resistance to deterioration of composite elements was recorded in 1999 for steel-reinforced plastic piles that were installed at Pier Bravo in NAS North Island, San

Diego, CA. The piles were inspected at 3.5 years after installation and no significant corrosion was observed (Pando et al., 2006). Two of the literary works related to the long-term durability of composite piles are summarized below:

Iskander and Hassan (2001) conducted comprehensive unconfined compression tests to estimate the degradation of plastic composite materials. They found that high-density polyethylene (HDPE) materials were exposed to the maximum degradation rate at pH = 2 companies with the highest temperature of experiments (25 ° C). However, test results indicated that surface erosion did not take place, if any, was caused by its chain breakage only. They thought that real HDPE piles may show higher degradation resistance than specimens, this due to larger in diameters and enhanced material characteristics at the surface.

Pando et al., (2002b) conducted an experimental program of laboratory studies to predict long-term axial and flexural capacity of the concrete-filled FRP pile exposed to water in the marine environments. The FRP test specimens were submerged in water at a different temperature and then the effect of moisture absorption on the FRP strength was studied as a function of immersion time. Based on the test results, it can be estimated that the long-term axial and flexural capacity has been reduced by 5 to 24 percent compared to the short-term axial and flexural capacity, respectively.

1.5.4. Structural Behavior of Composite Piles Under Axial Loading

A great effort has been made to investigate the structural behavior of concrete-filled FRP pipe piles (Lampo et al., 1998; Samaan et al., 1998; Mirmiran et al., 1999; Fam, 2000; Fam and Rizkalla, 2001a, b; Mirmiran et al., 2001; Moran and Pantelides, 2002; Becque et al., 2003). While the FRP shell use to protect the concrete core from degradation, due to its confinement characteristics, it responses a portion of the axial loads by applying a confining constraint. When the load is applied, lateral movement occurs in the concrete core and the FRP shell responds to lateral movement, thereby increasing the axial capacity of the concrete (Pando et al., 2006). This advantage of the FRP shell on a short tubular FRP element filled with concrete has been studied by (Fam and Rizkalla, 2001a).

On the other hand, due to the lack of sufficient studies on the structural behavior of reinforced recycled plastic piles, manufacturers often provide information on the performance of these piles (Pando et al., 2006). However, recent studies show good results

on the structural behavior of these piles (Pando et al., 2006). Some literary works on the structural behavior of composite piles under axial loading are presented below.

Robinson and Iskander (2008) conducted a research study to determine the stiffness, flexibility, settlement and bearing capacity behaviors of axially loaded composite piles. The study included in-situ static and dynamic tests with on-site Standard Penetration Tests (SPT) and Cone Penetration Tests (CPT). Four different types of composite piles (concrete-filled fiberglass shell piles, polyethylene piles reinforced with steel bars, polyethylene piles reinforced by fiberglass bars and solid polyethylene piles) were used to conduct static and dynamic tests. The research study showed that plastic piles had the potential to be an option to traditional pile applications under axial loading. However, they believe that further study should be done to consider durability and long-term creep behavior.

Roberts and Brandner (2010) conducted comprehensive study included full-scale field load testing, monitoring of long-term vertical movement and model analysis to study the axial behavior of the recycled plastic piles. The test results showed that the recycled plastic piles (RPPs) could easily support the lightly-loaded structures, approximately at 6 mm of pile head settlements. While the design load of these structures for a single pile in order to 110 kPa to 155 kPa. Despite many benefits over traditional piling, the low friction coefficient makes plastic piles also have a potential to be an alternative to traditional piling in expansive clay and shale soils.

Bozorg-Haddad et al. (2012) experimentally conducted an accelerated testing method to predict the compressive creep of recycled high-density polyethylene (HDPE) composite pile. The experiments were performed based on the equivalence of strain energy density (SED) between conventional constant-stress creep tests and stress-strain tests, at different strain rates. Test results showed that the HDPE pile loaded in compression at an ultimate stress of 6.9 MPa, will creep by less than 1% for an estimated service of 100 years. Based on conventional stress-strain tests, the ultimate strength capacity of the HDPE piles used in the study was ranged from 15 to 28 MPa. However, relied on the SED test method, the expected ultimate strength capacity of HDPE piles loaded in compression will be reduced to 11.7 MPa after 100 years of service. The predicted ultimate strength based on SED represents the 40-75% of the obtained value based on conventional stress-strain tests.

Gathimba Naftary et al. (2014) conducted an experimental program included axial compression tests to investigate the compressive strength of concrete-filled un-plasticized

polyvinyl (UPVC) pipes. The test results showed that (UPVC) pipes can significantly increase the concrete compressive strength. The compressive strength increased from 1.18 to 3.65 times the unconfined compressive strength. The enhancement in compressive strength was dependent on the strength of the concrete core and wall-thickness of plastic pipes. They recommended that low-strength concrete confined by PVC pipes tend to be more ductility and may have the potential for earthquake-resistant applications.

1.6. Effect of Installation Methods on Pile Bearing Capacity

The principles of soil mechanics that are used to estimate the bearing capacity of shallow foundations are quite different from those, which are used in the design of pile foundations. In a shallow foundation, it is possible to inspect and take samples over the entire surface of the proposed site to ensure that the bearing capacity of the foundation soil is sufficient to support the applied loads. In addition, modern installation techniques can limit disturbances in soil foundations to a few centimeters below the level of the excavation trench, so that the foundation soil is not affected by the construction process significantly and remains almost undisturbed (Das, 2010).

The conditions and factors that dominate the pile bearing capacity are quite different from those of the shallow foundation, no matter what type of pile installation (i.e., driving and drilling) is performed, the surrounding soil and the soil under the pile toe is affected and disturbed by the installation process (Das, 2010).

In the case of the bored pile, due to the drilling process, the soil is disturbed in both zones under the pile toe and at the pile-soil interface, so that the soil becomes lesser to some distances and thus the pile bearing capacity is reduced. But in the case of driven piles, due to the impact of the driving process, the soil is pushed away in the pile-soil interface area and in the pile toe contact area; therefore, pile point capacity is increased while its shaft capacity is reduced causes to losses its contact with soil in some areas, this reduction of pile shaft capacity studied for the first time by Vesic (1970) in terms of friction fatigue. In both installation methods, the bearing capacity of the piles increases with time, but this increase is much larger and significant in the case of driven piles (Das, 2010).

Several theoretical and empirical studies have been conducted to investigate the effect of pile driving on the bearing capacity of a single pile, including its effect on increasing sand density at certain distances under the pile toe and in the surrounding soils, thus increasing the internal friction angle, density and stiffness, especially in the case of

loose and medium dense sand. Based on field tests, this improvement in sand density was estimated at approximately 2.5 times the pile diameter in the surrounding zone (Das, 2015). While the bearing capacity of a single pile driven into sand is generally predicted using the bearing capacity theories based on soil shearing resistance, without considering that soil condition is affected by the driving process (Das, 2010).

Due to the influence of the pile driving operation, an increase in the relative density is achieved and the compacting effect cannot be easily ignored, resulting in a significant effect on the soil characteristics as a function of the bearing capacity of the soil. The increase in the ultimate bearing capacity of a single pile driven in the sand depends on the compaction level due to the driving process (Meyerhof, 1959).

The improvement in the pile bearing capacity occurs as a result of some factors such as the dissipation of the excess pore water pressure, the aging of the soil which leads to increase the stiffness of the soil resulting in the improvement of the cohesion and the interface friction angle, or in the case of concrete and steel piles, due to chemical or electrochemical effects caused by hardening and corrosion of concrete and steel, respectively, in areas that are in contact with the ground. However, it is not possible to explain the mechanism of long-term pile set-up (i.e., an increase in the pile bearing capacity) driven in the granular soils only depends on the dissipation of the excess pore water pressure generated by the driving impact, and as it dissipates in a few hours or days after pile installation. There is still no clear mechanism to clearly represent this phenomenon, but it can be divided into three possible time-dependent reasons (Chow et al., 1997): (a) formation of bond between surface of pile materials and sand particles resulting from chemical influences especially in case of steel piles, (b) an increase in stiffness, dilation, and shear strength of the soil caused by soil aging (Mitchell and Solymar,1984; Schmertmann, 1991), and (c) continuous changes in surrounding soil stress in terms of long-term pile set-up where the effect of soil arching is reduced due to the behavior of creeping soil particles around the pile shaft, resulting in an increase in radial stress on the soil-pile interface area. Each of these mechanisms begins immediately after the pile is being installed and is, to a certain degree, and a part of the short-term set-up that occurs during the dissipation of excess pore water pressure. However, it is not yet known which of these mechanisms is the main reason under different circumstances, and the other question is how long these mechanisms will last (Axelsson, 1998).

In the case of pile group foundations, the construction process of the adjacent piles has a significant effect on the bearing capacity characteristics and the load-settlement behavior of the pile in the group that has already been driven. The "soil mechanics" approach used to estimate the bearing capacity of the piles is based on the fact that the total axial capacity of the pile to the vertical axial applied loads is the sum of two components. First, is the friction resistance of the pile-soil interface (i.e., pile shaft capacity) and the second, is the soil bearing capacity at the pile toe. Understanding the axial behavior of piles is quite complex, even if the bearing capacity of the piles has been accurately estimated, it is still difficult to predict the problems taken into account in the installation process of the pile at depths indicated by empirical or semi-empirical calculation methods. For example, if the exact length of the pile can be accurately calculated to be driven into the ground to support the applied loads, the energy required by the hammer for this installation is always highlighted, as well as whether the pile can be installed successfully without any significant damage resulting from the driving impact (Das, 2010).

1.7. Estimation of Pile Bearing Capacity

The load-displacement behavior and bearing capacity of a single pile are highly dependent on the stiffness and shear strength characteristics of the surrounding soil and the pile-soil interface (Poulos, 1989). However, the bearing capacity of a pile and its settlement under certain conditions are first estimated on the basis of the theoretical principles of soil mechanics. But to verify the theoretical estimates that involve with the high level of uncertainties, field load tests are usually conducted, especially in large projects. While field load tests are the most effective methods, they take a lot of time and cost and are therefore undesirable especially in low-budget projects. Although they are used in analytical methods to determine load-displacement behavior by using field failures, as well as, makes analysis methods to be used as an option for pile analysis with the available field data.

High levels of uncertainty in the prediction of axial pile capacity increase the tendency to perform field load tests, but it is still impossible in field load tests to independently measure the pile shaft capacity. In addition, very few studies on experimental models have also been conducted to investigate the independent contribution of pile shaft capacity to the ultimate load-bearing capacity of a pile installed in sand.

Despite considerable research on the analysis and design of pile foundations in recent decades, there are still gaps in knowledge regarding of pile shaft behavior, and the results available in the literature do not match the actual behavior of the pile shaft capacity. Due to the effect of uncertainties associated with axial behavior, a high degree of conservatism is often taken into account in the design of pile foundations. The prediction of ultimate pile bearing capacity installed in the sand (i.e., the pile shaft and end bearings capacity) is first theoretically estimated based on primarily on interface shear box test and direct shear box test results, and after installation because of the complexity of the pile axial behavior resulting from installation methods and type of loads, in practice, on the basis of empirical methods (i.e., in-situ standard and cone penetration test results) and/or field load tests the ultimate pile bearing capacity is estimated again.

Usually, researchers and designers rely on the interface shear box test to evaluate shear strength parameters that are required to estimate pile shaft capacity. Although the working mechanism of the interface shear test is very different from the actual behavior of the pile shaft in the field. However, the factors that control the shear strength parameters in the interface shear test were almost defined in the literature such as surface roughness, moisture content, soil composition, density, surface hardness , relative roughness (surface roughness of the material/soil particle mean size (D50)), the levels of normal stress, amount of coarse-grained soil in the whole soil mass and soil granular shapes (angular or round), and shearing rate and have been studied by several researchers (Potyondy, 1961; O'Rourke et al., 1990; Frost and Han, 1999; Pando et al., 2002a; Sakr et al., 2005; Al-Mhaidib, 2006; Aksoy et al., 2016; Almallah et al., 2018).

But the main factor that is not clearly defined is the shear mechanism in the soil-pile interface zone; despite the aforementioned factors, in the interface shear box test the thickness of the soil sample compared to the applied normal load especially in low relative densities (i.e., in a case of high void ratio), as well as the load direction, perfectly control the shear failure criteria. In the interface shear box test due to the applied load, the soil sample becomes denser and denser throughout the test, this increase is in favor of low-to-high density. This is why it is impossible to find obvious failures of shear-displacement relationships in the interface shear test. This means that in the interface shear box test, the shear stress-displacement relationship always increases and their behavior does not reach the clear point of failure as has been observed in the field load tests, where at a limit, it remains constant or decreases. Field load tests have already confirmed this fact; where the

shaft friction resistance (i.e., pile shaft capacity or pile skin friction resistance) increases with increasing displacement of the pile to a depth where the embedment length of the pile reaches 15 to 20 times its diameter (Das, 2015).

When the pile is subjected to axial vertical loads, a vertical displacement is observed at the pile head, which consists of elastic compression of the pile material body and settlement of soil layers beneath the pile toe. However, the elastic compression of pile in case of friction pile is very small compared to soil settlement. While the pile is in contact with the ground, a relative displacement between the pile-soil structure is sufficient to mobilize the friction force between the pile interface and the surrounding soil.

The author believes that the most reliable statement that can be said to describe the pile shaft behavior is as follows: at the beginning, when the load is applied to the pile head and the pile starts to penetrates into the ground a relative displacement of the pile-soil structure (i.e., pile displacement minus surrounding soil displacement) occurs. Which makes the pile to take some soil particles down with itself; as a result, the surrounding soil becomes denser and the pile shaft capacity increases with the pile displacement. When enough soil particles are moved down, the surrounding soil density reaches its optimal state under certain conditions and an ideal hollow shaft of soil is formed around the pile. Beyond this, the surrounding soil does not easily receive soil particles coming with the displacement of the pile. Thus, the pile shaft friction resistance to the applied load reaches its maximum state, which then decreases in case of low relative density, or remains constant or decreases in case of medium to high relative densities. After the pile shaft capacity is failed, the applied load is mainly supported by the soil under the pile toe.

For the above reasons, this study is aimed at providing bearing capacities behavior and to focus in particular on the interface shear behavior, depends on model experiments, as well as, theoretical methods and finite element analysis, of two concrete-filled (FRP and PVC) pipe piles at different relative densities of the model sand.

1.8. Objectives and Scope

In the current study, the axial capacities (i.e., total or ultimate bearing capacity, base capacity or base resistance, and shaft capacity) of two composite piles made of concrete-filled FRP and PVC pipe piles (note: concrete core is self-consolidated concrete) are investigated and both piles are installed in the model sandy soil at different relative

densities (i.e., D_r = 10%, 40%, 65%, and 90%). The main objectives of this study can be expressed as below:

1. Conducting axial bearing capacities (i.e., pile base resistance, end-bearing capacity and pile shaft capacity) in terms of load-displacement behavior (i.e., p-y) of the single-model composite piles at different conditions of the model sand (i.e., D_r = 10%, 40%, 65% and 90%).
2. Using the most common bearing capacity equations to determine the pile base resistance and pile end-bearing capacity of composite piles by using direct shear test results and then compare with the experimental results.
3. Determination of the interface friction angles of the composite piles using interface shear testing, and then also, using experimental results of pile shaft capacity, to determine the coefficient of lateral earth pressure (K) using values of (δ) measured from the interface shear box test.
4. Assessment of the interface friction angles (δ) of composite piles using coefficient of lateral earth pressure (K_p) by substituting experimental results of pile shaft capacity, and then make a comparison with the (δ) results measured from the interface shear box test.
5. Model of experimental work in a computer environment by a finite element programming approach, to simulate the PVC pile/sand and FRP pile/sand system based on experimental model tests using PLAXIS 3D software.
6. Finally, to recommend future researchers on this subject.

2. THEORETICAL BACKGROUND

2.1. Introduction

In the past, theoretical approaches have not been well documented and also there was no comprehensive bearing capacity theory to estimate the bearing capacity of foundation engineering as it currently exists. Therefore, the pile foundation was designed on the basis of a combination of experimental methods and past experiences. However, in the last century, several theories have been proposed to estimate the bearing capacity of a pile foundation, but the high level of uncertainty associated with the axial behavior of piles is still addressed with this issue. The complexity of the pile behavior has led to Terzaghi and Peck (1967) stated that the "…theoretical refinements in dealing with pile problems are completely out of place and can be safely ignored…". In addition, Randolph (2003) stated that ".... is consistent with my belief that we may never be able to estimate axial pile capacity in many soil types more accurately than about ±30%. We, therefore, need to rely on pile tests to refine pile design.... ".

Furthermore, Randolph (2003) stated that "Scientific approaches to pile design have advanced enormously in recent decades and yet, still, the most fundamental aspects of pile design-that of estimating the axial capacity-relies heavily upon empirical correlations.".

In order to eliminate the effect of uncertainties in prediction of axial pile behavior field load tests are usually recommended. Depends on current design methods (Fleming et al., 1992) and, because of inherent uncertainties, involves estimating pile bearing capacity and prediction of settlement behavior (Chow, 1997; Anonymous, 1999; Wheeler, 2000), field load tests are recommended to confirm the actual bearing capacity of the pile. For that reasons mentioned above, field load tests are required during the construction process to estimate the real bearing capacity of a pile. Despite their important role in pile design, time and cost are two major obstacles to field load tests that push the researcher to provide alternative design methods to predict pile bearing capacity such as empirical and numerical methods.

In recent decades, the load-displacement behavior of model piles has been studied by several researchers to study the axial and lateral behavior of a single pile or group piles under different soil conditions and for various research purposes (Vesic, 1963, 1964; Kerisel, 1964; Robinsky and Morrison, 1964; Hanna and Tan, 1973; Tan and Hanna, 1974; Das et al., 1977; Chaudhuri and Symons, 1983; Kraft, 1991; Shin et al., 1993; Randolph et

al., 1994; Foray et al., 1998; Al-Mhaidib, 2001; Mayoral et al., 2005; Nanda and Patra, 2011; Igoe et al., 2011; Manandhar and Yasufuku, 2013; Al-Busoda and Al-Rubaye, 2015; Leong et al., 2015; Fattah et al., 2016).

Some of the general bearing capacity theories that have been presented by many researchers to estimate the ultimate bearing capacity of shallow foundations are usually used to predict pile point or end-bearing capacity, as well as, to predict pile base capacity. The most common bearing capacity equations that are used to predict the axial behavior of piles are: (i.e., Terzaghi (1943), Hansen (1970), Janbu (1976), Meyerhof (1976), and Coyle and Castello (1981).

As the pile point or end-bearing capacity, several methods have been proposed to estimate the shaft capacity of a pile installed in sand for drilled and driven piles. In this study, the general pile shaft capacity equation (Burland, 1973) is used to predict piles shaft capacity using the estimated interface friction angle (δ) from the interface shear box test with considering several considerations of the coefficient of lateral earth pressure (K).

This Chapter presents a sufficient theoretical background to assess the piles bearing capacities (i.e., total or ultimate bearing capacity, point bearing or end bearing capacity, and shaft capacity of the single-model composite piles) based on evaluation procedures of traditional pile bearing capacity equations.

2.2. Pile Foundations

Pile foundations are a kind of deep foundation, they are long columnar elements mostly made of timber, steel, and reinforced concrete. Piles are often used to carry loads from heavy structures to deeper soil layers and in cases where the soil at a reasonable depth is not even suitable to support normal superstructure loads without an excessive settlement or because of stability problems such as high-rise building applications. Pile transfer the vertical loads to the desired ground depth either by pile point or pile end bearing capacity, and/or pile skin friction resistance (i.e., pile shaft friction resistance or pile shaft capacity). Although pile foundations need more time and costs than shallow foundations, a considerable development in offshore energy resources structure, an increase in demand for high-rise buildings, emphasize the need to build pile foundations with a higher load carrying capacity and penetrate piles to a deeper depth (Bowles, 1996). Pile foundations are mainly classified according to the material, installation process, and functions. Piles are divided into (timber, steel, reinforced concrete, and composite piles) and (driven, bored or

jacket piles), based on materials and installation process, respectively. Depending on the length and function (i.e., by which mechanism the load is transferred to the foundation soil layers), piles are also divided into several categories: (1) end-bearing piles, (2) friction piles, (3) compaction piles, (4) tension piles and (5) sheet piles.

2.2.1. End Bearing Piles

If site explorations record that the rock layers or rock-like materials can be founded at a reasonable depth (Figure 2.1.a.), in such a case piles are often extended and rested on the surface layer of rocks or rock-like materials. In this kind of pile foundation, the pile acts as a column and its ultimate capacity is fully taken from the bearing capacity of the underlying soil layers at the bottom of the pile toe; thus, the piles are called end or point bearing piles. The key point to transfer the total loads from the superstructure safely is that the pile must be rested exactly on the desired rock layers or rock-like materials and its sufficient length should be well established. If hard soil strata encountered instead of bed-rocks, the piles are often lengthened a few meters into the hard soil strata (Figure 2.1.b.) (Das, 2015).

2.2.2. Friction Piles

If bed-rock layers or rock-like materials cannot be found at a reasonable depth, the length of the end-bearing piles becomes larger than the normal size, so in such a case, the end-bearing piles are economically unacceptable. Therefore, the piles are installed in the ground soils to the desired depth which is already determined based on both site exploration and the design approaches (Figure 2.1.c) (Das, 2015).

The working principle of friction piles is quite different from the end-bearing piles. Friction pile transfers the applied loads from the friction resistance (i.e., shaft capacity) between the soil-pile interface. The friction force is mobilized with a relative displacement between the pile and surrounding soils (Das, 2015).

This kind of pile is called friction pile because most of its load bearing capacity is derived from the pile-soil interface friction resistance. However, the term of friction pile is referred to literature, but this term is a misnomer: because in the clay soil conditions most of the friction resistance is derived from adhesion (Das, 2015).

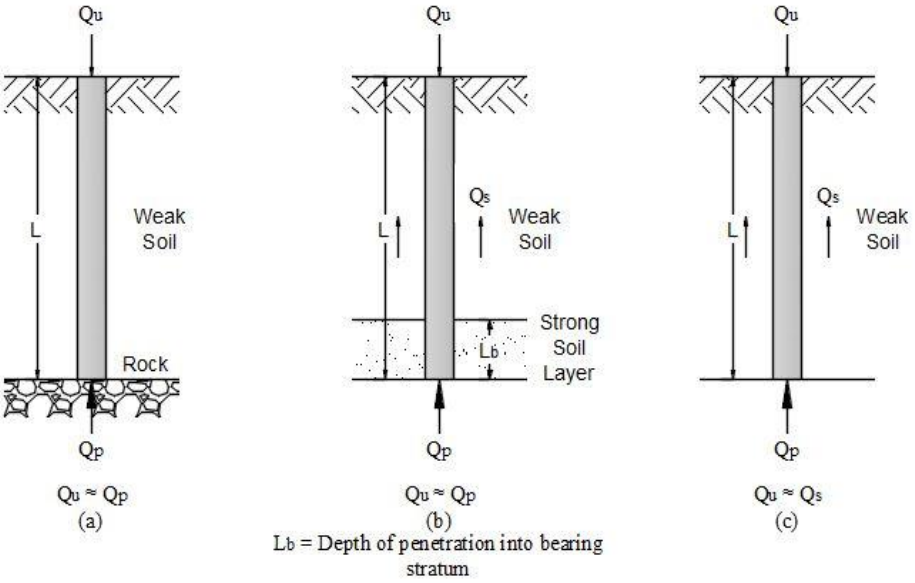

Figure 2.1. (a) and (b) end bearing piles; (c) friction pile.

Dimension parameters of the friction piles are estimated based on the shear strength parameters of the pile-soil interface, the type and amount of applied loads. To estimate the required length of friction piles, the engineer or designer must have a good knowledge of the behavior of the soil-pile interface, good judgment, and experience (Das, 2015).

2.2.3. Compaction Piles

However, piles are mostly used to load-bearing applications, but sometimes for the purpose of soil improvement, piles are driven into the coarse-grained soil for some distances to achieve the required bearing capacity of the soil layers near the ground surface. These piles displace or push the surrounding soil during the driving process, as a result, soil density is increased, so these kinds of piles are called compaction piles. Determine the dimension parameters of these piles depends on (a) the initial relative density of the soil foundation, (b) the required relative density to be achieved after compaction or driven the piles, and (c) the depth of soil layers required to be compacted. These piles are usually short piles. However, several field tests are required to make a decision to determine the appropriate length of these piles (Das, 2015).

2.2.4. Tension Piles

Tension piles are also called anchor or uplift piles. These piles are used to resist uplift loads when the superstructure is exposed to horizontal loads such as wind loads, earth side slope forces, earthquakes and sea waves. In these cases, uplift forces are developed on piles and cause to pull out or extract piles from the ground soil (Das, 2015).

2.2.5. Sheet Piles

Unlike other piles, sheet piles are used to support the lateral pressure of soft or weak soil, or water flow. Sheet piles are used in some cases or for certain purposes such as building of retaining walls, to support the side walls of the foundation trench, to protect the side soil of the river from erosion and coastal soils from the sea waves, isolate of adjacent foundations and to improve the bearing capacity of the foundation soils through the soil confinement and support it against lateral movements under vertical loading (Das, 2015).

2.3. Pile in Sand

The prediction of the axial capacity of piles is known as being the area of greatest uncertainty in foundation design (Randolph et al., 1994). However, several methods have developed to eliminate the effect of uncertainty in the design of pile foundations, the appropriateness and accuracy of current design methods are often questioned (Randolph, et al., 1994; Olson, 2002). These methods have been developed based on some simplifying assumptions or empirical approaches with respect to soil layers (i.e., soil stratigraphy), soil-pile-structure interaction and distribution of soil resistance along the pile. Therefore, these methods or approaches are not directly useful in the design of pile foundations (Eslami and Fellenius, 1997).

High level of uncertainty in the design of pile foundation challenges the prediction of axial capacity of a driven pile into sandy soil (Randolph et al., 1994). Due to the uncertainties associated with predicting the axial and lateral behavior of the pile, after the pile installation process is completed, field load tests are usually carried out to assess the actual bearing capacity of the pile, while the ultimate bearing capacity is first estimated using theoretical methods. Despite the necessity of field tests especially static load tests, but it is still not possible to separate the independent contribution of the pile shaft capacity from the pile point or end-bearing capacity in the field load tests, with the exception of

very few field load tests using instrumented piles for research purposes such as Coyle and Castello (1981). For this reason, a semi-empirical approach (i.e., standard penetration test and cone penetration test) is often applied to separate the point bearing capacity of a single pile, but these tests are not useful where a pile foundation is very deep.

Most useful approaches in prediction of pile bearing capacity are static analysis, dynamic analysis, dynamic testing, pile load test and in-situ testing. However, in the design recommendations of static analysis, the concept of critical depth is often suggested, but it is an ideal concept and is not supported either by theoretical or reliable empirical and it conflicts with physical laws (Shooshpasha, et al., 2013). Pile bearing capacity in the dynamic analysis is determined based on the wave mechanics of the hammer to the pile-soil system. This approach includes some uncertainty such as the effect of the hammer impact of pile - soil structure, changes in soil shear strength parameters during pile driving and in pile load tests. Despite these uncertainties, it can be used only by an experienced person and pile capacity remains unknown until pile driving is finished (Rausche et al., 1985). Field static load testing is the best method to estimate the pile bearing capacity, but time and costs are common constraints in field tests especially for small projects. Recently, in-situ testing methods (i.e., Cone Penetration Test and Standard Penetration Test) have been increasingly used in geotechnical design. This is due to the fast progress of in-situ testing tools and a better understanding of soil behavior.

2.4. Pile Design

However, several methods have been proposed to estimate the pile axial capacity, but still, it remains complex and it is still questioned. The pile axial capacity is first estimated using theoretical methods, then because of high levels of uncertainty, after the pile installation process, the actual bearing capacity of a pile is estimated by performing field tests, in particular, static load tests.

2.4.1. Ultimate Pile Bearing Capacity

In such a soil as in the current study, when the pile cannot be found on rock or rock-like materials (i.e., hard or stiff soil stratum) due to the lack of these strong layers at a reasonable depth or for economic reasons the ultimate bearing capacity of a single pile is often estimated from the combination of both pile point or end-bearing capacity and pile

shaft capacity. In such a case the ultimate axial bearing capacity of a single pile can be estimated in the equation below:

$$Q_u = Q_p + Q_f \quad (2.1)$$

Where;

Q_u = ultimate bearing capacity of a single pile,

Q_p = pile point or end-bearing capacity,

Q_f = shaft friction resistance or pile shaft capacity.

2.4.2. Pile Point Capacity

The pile point or end-bearing capacity of a single pile is often determined using the most well-known bearing capacity equations such as (i.e., Terzaghi (1943), Hansen (1970), Janbu (1976), Meyerhof (1976), and Coyle and Castello (1981). These methods are extensions of the rigid plasticity theory approaches for surface footings (Gui and Muhunthan, 2006). In field load tests, it has been found that the vertical displacement of the pile up to 10% to 25% of its diameter is necessary for the pile to reach its maximum end-bearing capacity (Das, 2015).

2.4.2.1. Terzaghi (1943)

The first comprehensive theory proposed by Terzaghi (1943) to evaluate the bearing capacity of the rough shallow foundation and his theory is still used to estimate the pile end-bearing capacity (Figure 2.2.). However, the Terzaghi equation is recognized to provide conservative results but is still widely used due to its simplicity. Terzaghi in his theory suggested that a foundation with its depth (D_f) equal or less than its width is shallow. The researchers then reported that the foundation, which its depth greater than its width by (3-4 times), it can also be considered a shallow foundation.

In Terzaghi's theory, the foundation soil was divided into two planes with three zones with different shear patterns. The zone ACD indicates active Rankine state with angles of ACD and CAD are supposed to be equal to internal friction angle. He assumed that walls of AD and CD are pushed the soil mass outward and upward thus the passive failure is happened in both sides. In addition, the other zones are two radial shear zone of ADF and

CDE, and two triangular Rankine passives of AFH and CEG. The planes of AF and AD are inclined towards left and right sides at angle of ($\alpha = 45^\circ - \varphi/2$) and ($\alpha = 45^\circ + \varphi/2$) with horizontal plane, respectively. In Terzaghi theory, when the foundation is loaded, the triangular zone (ACD) immediately under the foundation is moved downward, as a result, the two other soil volumes (ADFH) and (CDEG) are moved outward and upward with the soil failure surface at the bottom level of the foundation.

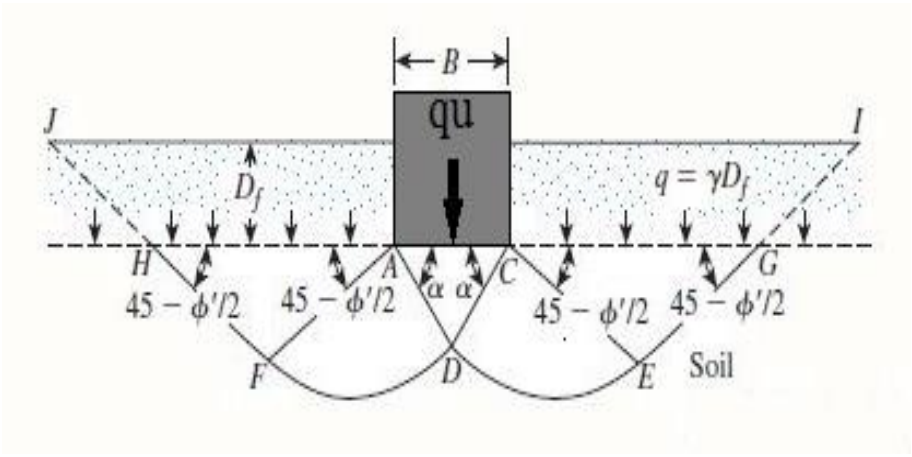

Figure 2.2. Terzaghi bearing capacity theory.

Terzaghi bearing capacity equation for circular foundation in sand can be expressed as follow:

$$Q_p = A_p.(q\,.N_q + 0{,}5\,.\gamma\,.\mathrm{B}\,.N_\gamma\,.S_\gamma) \tag{2.2}$$

where;

Q_p = ultimate point bearing or end-bearing capacity of the pile,

A_p = pile point area,

q = effective overburden soil pressure at the pile toe (γ_f x D_f),

γ_f = dry unit weight of foundation soil above the pile toe,

D_f = depth of foundation soil above the pile toe,

γ = dry unit weight of foundation soil at the pile toe,

B = pile diameter or least dimension of the pile,

N_q and N_γ = bearing capacity factors,

S_γ = shape factor.

The value of Sγ in the last term of the Terzaghi bearing capacity equation for different foundation shapes is given in (Table 2.1.).

Table 2.1. Shape factor (S_γ) in the last term of Terzaghi's equation.

Shape Factor	Circular	Square	Strip
S_γ	0.6	0.8	1

By substituting S_γ in the (equation 2.2) Terzaghi bearing capacity equation can be rewritten as below:

$$Q_p = A_p.(q\,.N_q + 0{,}3\,.\gamma\,.\mathrm{B}\,.N_\gamma) \tag{2.3}$$

To estimate the ultimate bearing capacity of a shallow foundation, Terzaghi ignored the overburden soil shear strength parameters and only considered its weight as overburden pressure acting positively on the soil bearing capacity beneath the foundation level. In addition, he estimated bearing capacity factors depends only on the shear strength parameters of the soil layers under the foundation tip. Furthermore, estimating the actual value these dimensionless bearing capacity factors (N_q and N_γ) is very difficult, for this reason, Terzaghi evaluated these bearing capacity factors using an approximation method (soil weightless theory).

Based on the soil weightless theory Terzaghi proposed the following equation to estimate bearing capacity factors:

$$N_q = \frac{e^{2\left(\frac{3\pi}{4}-\frac{\varphi}{2}\right)tan\,\varphi}}{2\,cos^2(45+\frac{\varphi}{2})} \tag{2.4}$$

$$N_\gamma = \frac{1}{2}tan\,\varphi \quad (\frac{K_{p\gamma}}{cos^2\varphi} - 1) \tag{2.5}$$

where;

φ = internal friction angle of the soil at the pile toe,

$K_{p\gamma}$ = coefficient of passive earth pressure, some back computed typical values of $K_{p\gamma}$ are given in (Table 2.2.).

Several researchers have also been used the soil weightless theory to estimate bearing capacity factors such as (Prandtl, 1920; Reissner, 1924; Meyerhof, 1951; Vesic 1973). The only thing that is always different among all the above researchers is the N_γ,

while the differences get smaller for the other bearing capacity factors such as (N_c and N_q). Ukritchon et al. (2003) reported that this difference in the estimate of N_γ by several researchers is related to the uncertainties in estimating this bearing capacity factor. Terzaghi's bearing capacity factors for various internal friction angles are given in (Table 2.2.).

Table 2.2. Terzaghi's bearing capacity factors with some typical values of $K_{p\gamma}$ (adopted from Bowles 1996).

Values of N_γ for φ of 0º, 34º, and 48º are original Terzaghi values and used to back				
φ^o	N_c	N_q	N_γ	$K_{p\gamma}$
0	5.7*	1.0	0.0	10.8
5	7.3	1.6	0.5	12.2
10	9.6	2.7	1.2	14.7
15	12.9	4.4	2.5	18.6
20	17.7	7.4	5.0	25.0
25	25.1	12.7	9.7	35.0
30	37.2	22.5	19.7	52.0
34	52.6	36.5	36.0	
35	57.8	41.4	42.4	82.0
40	95.7	81.3	100.4	141.0
45	172.3	173.3	297.5	298.0
48	258.3	287.9	780.1	
50	347.5	415.1	1153.2	800.0
*$N_c = 1.5\ \pi + 1$ [see Terzaghi (1943), p. 127.]				

2.4.2.2. Meyerhof (1963 and 1976)

After the first comprehensive bearing capacity theory proposed by Terzaghi in (1943), Meyerhof (1948) criticized Terzaghi's theory and stated that the failure mechanism presented by Terzaghi is not consistent with the observed ground movement. While Terzaghi's bearing capacity, theory is possible only for continuous, square and circular foundations, it did not consider a case of rectangular foundation when ($0 < B/L < 1$), and it is only applicable to vertical loading.

The other thing that has been criticized by Meyerhof is the shear strength parameters of the soil above the bottom of the foundation that were ignored by Terzaghi in the estimation of bearing capacity factors. In addition, Meyerhof believed that Terzaghi's theory provides conservative values for the bearing capacity of the foundation soil.

Meyerhof (1963) has proposed another general bearing capacity theory. Meyerhof's bearing capacity theory includes both vertical and inclined loads. For the case of vertical loading, he proposed the depth factor (d_c) with the term N_c, the shape factor (s_q) and the depth factor (d_q) with the term N_q and the depth factor (d_γ) with the term N_γ, while these factors were not considered by Terzaghi.

Meyerhof's bearing capacity theory for cohessionless soil in case of vertical loading, as in this study, can be written as follows:

$$Q_p = A_p.(q \ .N_q.d_q.s_q + 0{,}5\,.\gamma \ .B\,.N_\gamma.d_\gamma.s_\gamma) \tag{2.6}$$

Where;

Q_p= ultimate point bearing or end-bearing capacity of the pile,

A_p= pile point area,

q = effective overburden soil pressure at the pile toe (γ_f x D_f),

γ_f = dry unit weight of foundation soil above the pile toe,

D_f = depth of foundation soil above the pile toe,

γ = dry unit weight of foundation soil at the pile toe,

B = pile diameter or least dimension of the pile,

N_q and N_γ = bearing capacity factors,

d_q and d_γ = depth factors,

s_q and s_γ = shape factors.

Meyerhof's depth factors, shape factors and bearing capacity factors can be written as follows:

For φ >10°

$$d_q = d_\gamma = 1 + 0{,}1\sqrt{K_p}\,(\frac{D''}{B''}) \tag{2.7}$$

and

$$s_q = s_\gamma = 1 + 0{,}1\,K_p\,\frac{B''}{L''} \tag{2.8}$$

where;

K_p = coefficient of passive earth pressure,

D" = embedment depth of the pile,

B" = short dimension of the pile,

L" = long dimension of the pile,

$$K_p = tan^2(45 + \frac{\varphi}{2}) \quad (2.9)$$

and

$$N_q = e^{\pi \, tan \, \varphi} \quad tan^2(45 + \frac{\varphi}{2}) \quad (2.10)$$

$$N_\gamma = \left(N_q - 1\right) tan(1.4 \, \varphi \quad) \quad (2.11)$$

where;

φ = internal friction angle of the soil at the pile toe.

In 1976, based on field tests, Meyerhof reported that the end-bearing or pile point capacity increases with an increase in the pile embedment length to a depth where (L_b/D') reaches its critical state $(L_b/D')_{cr}$ (note: L_b= embedment depth of pile and D'= pile diameter, and in such a case as in this study for homogeneous soil, L_b is equal to L). Beyond this limit $(L_b/D')_{cr}$, the pile end-bearing capacity remains constant even if L_b<L (Figure 2.3.). From field tests it has been found that $(L_b/D')_{cr}$ is between16 to 18 (Das, 2015).

In general, the second term in the (equation 2.6) is neglected for piles because it gives a very small value, except in the case of piers or piles of large diameter. (Note: in this study the second term in (equation 2.6) is used to estimate the piles base capacity, and results are given in Chapter Five in (Table 5.6.).

Thus, Meyerhof's bearing capacity equation for pile point or pile end-bearing capacity can be rewritten as below:

$$Q_p = A_p . q_p = \ A_p . q \quad . N_q^* \quad (2.12)$$

Where;

Q_p = ultimate point bearing or end-bearing capacity of the pile,

A_p = pile point area,

q = effective overburden soil pressure at the pile toe (γ_f x D_f),

γ_f = dry unit weight of foundation soil above the pile toe,

D_f = depth of foundation soil above the pile toe,

N_q^* = Meyerhof's bearing capacity factor for pile foundations (1976). Meyerhof's bearing capacity factors from φ 20 to 45º are given in (Table 2.3.).

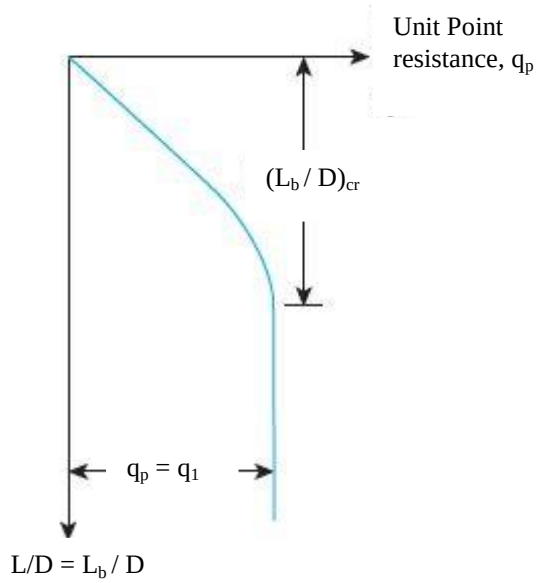

Figure 2.3. The nature of variation of unit point resistance in a homogeneous sand.

Table 2.3. Meyerhof's bearing capacity factors with φ from 20º to 45º (adopted from Das, 2015).

φº	N_q*	φº	N_q*	φº	N_q*
20	12.4	29	46.5	38	231.0
21	13.8	30	56.7	39	276.0
22	15.5	31	68.2	40	346.0
23	17.9	32	81.0	41	420.0
24	21.4	33	96.0	42	525.0
25	26.0	34	115.0	43	650.0
26	29.5	35	143.0	44	780.0
27	34.0	36	168.0	45	930.0
28	39.7	37	194.0		

According to the Meyerhof method for the pile point capacity, the pile capacity increases until (L_b/D') reaches its critical state (L_b/D')$_{cr}$, beyond this limit it remains constant. Therefore, he provided a limit value for the pile point capacity, which can be expressed in the equation as follow:

$$Q_p = A_p . q_p = A_p . q \ \ . N_q^* \leq A_p . 0{,}5 \, . p_a . N_q^* . \tan \varphi \qquad (2.13)$$

Where;

A_p = pile point area,

q = effective overburden soil pressure at the pile toe (γ_f x D_f),

γ_f = dry unit weight of foundation soil above the pile toe,

D_f = depth of foundation soil above the pile toe,

N_q^* = Meyerhof's bearing capacity factor for pile foundations (1976) (Table 2.3.).

p_a = atmospheric pressure (100 kN/m^2),

φ = soil internal friction angle of the bearing soil at the pile point level.

2.4.2.3. Coyle and Castello (1981)

Coyle and Castello (1981) proposed pile point capacity equation for driven pile into sand based on 24 full-scale pile load tests. They conducted field load tests using instrumented piles and separated the independent contribution of the pile base and pile shaft capacity from the ultimate pile bearing capacity. Coyle and Castello's pile point capacity equation can be written as below:

$$Q_p = A_p . q \quad . N_q^* \tag{2.14}$$

Where;

Q_p = ultimate point bearing or end-bearing capacity of the pile,

A_p = pile point area,

q = effective overburden soil pressure at the pile toe (γ_f x D_f),

γ_f = dry unit weight of foundation soil above the pile toe,

D_f = depth of foundation soil above the pile toe,

N_q^* = bearing capacity factor.

The bearing capacity factor (N_q^*) of the Coyle and Castello method versus embedment ratio (L/D) for an internal friction angle between 30º and 40º is given in (Figure 2.4.).

2.4.2.4. Janbu (1976)

Janbu (1976) proposed another bearing capacity factor N_q^* for estimating pile point capacity. The Janbu bearing capacity factor includes the effective surface friction angle (η), ranging from 60 ° for soft clay to 105 ° for dense sand, while other researchers did not take

this angle into account and they assumed that the soil failure surface extends only to the level at the bottom of the pile tip.

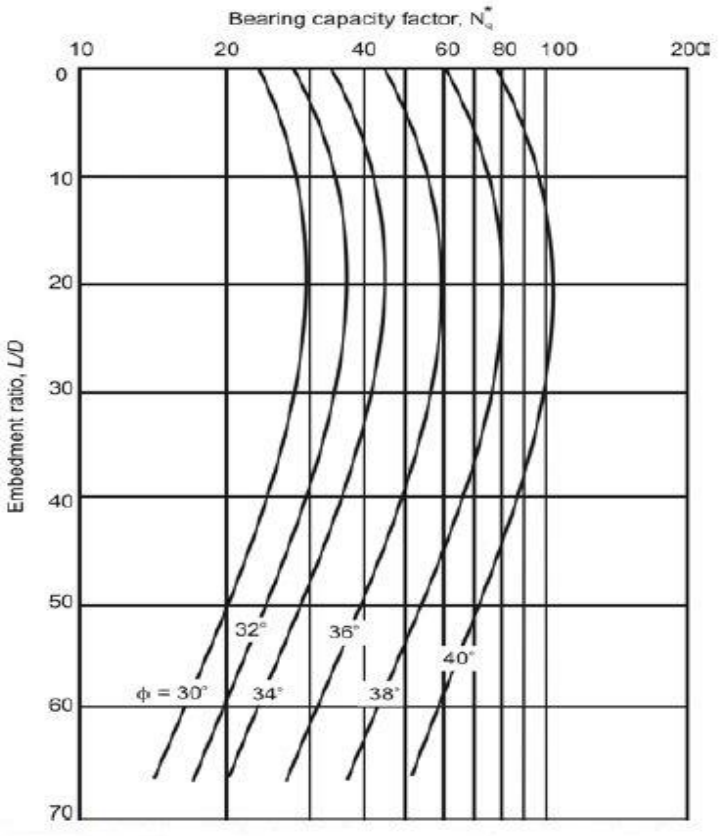

Figure 2.4. Variation of N_q^* with embedment ratio (Coyle and Castello 1981).

Janbu's pile point capacity equation can be written as follow:

$$Q_p = A_p . q \quad . N_q^* \tag{2.15}$$

Where;

Q_p = ultimate point bearing or end-bearing capacity of the pile,

A_p = pile point area,

q= effective overburden soil pressure at the pile toe (γ_f x D_f),

γ_f = dry unit weight of foundation soil above the pile toe,

D_f = depth of foundation soil above the pile toe,

N_q^* = bearing capacity factor.

Janbu's bearing capacity factor can be written as follow:

$$N_q^* = (\tan \varphi \quad + \sqrt{1 + tan^2 \varphi \quad})^2 \ (e^{2\eta \quad \tan \varphi \quad}) \tag{2.16}$$

where;

φ = soil internal friction angle at the pile toe,

η = surface angle in radian at the pile toe.

Janbu suggested that the surface friction angle is between 60º for soft clay and 105º for dense sand. However, the model sand used in this study presented an unusual internal friction at D_r = 90% compared to the literature related to the work on the sandy soil, which is equal to 52.4º. Mostly the engineer recommends this angle between 60º to 90º. In this study, pure model sand at different relative densities (i.e., D_r = 10%, 40%, 65%, and 90%) is used. Therefore, for the loosest state D_r = 10 and the densest state, D_r = 90%, 70º and 90º are considered, respectively. For the other two, D_r = 40% and 65%, 74º and 80º are considered, respectively.

Janbu's bearing capacity factor (N_q^*) versus internal friction angle for different consideration of (η) is given in (Figure 2.5.).

2.4.2.5. Hansen (1970)

Hansen (1970) proposed the general bearing capacity theory for two soil cases (0 < φ and φ = 0), which seems to be an extension for the Meyerhof (1951). Hansen considered the different situation for loading on the foundations in each of the previous cases: (a) no horizontal load component or, if it exists, in the width direction, (b) a horizontal load component in the direction of the foundation length or in both directions (width and length). The Hansen extension also included the base factor for the possibility in which the foundation is inclined with respect to the horizontal and for situations in which the foundation is found on the inclined ground. Hansen's bearing capacity theory has the possibility of use in both shallow and deep foundations, as there is a D/B factor in the Hansen depth factors.

Hansen's bearing capacity equations for vertical loading can be written as follow:

$$Q_p = A_p.(q \ .N_q'.d_q.s_q + 0{,}5\,.\gamma \ .B'.N_\gamma.d_\gamma.s_\gamma) \tag{2.17}$$

where;

Q_p = ultimate point bearing or end-bearing capacity of the pile,

A_p = pile point area,

q= effective overburden soil pressure at the pile toe (γ_f x D_f),

γ_f = dry unit weight of foundation soil above the pile toe,

D_f = depth of foundation soil above the pile toe,

d_q, d_γ = depth factors,

S_q, S_γ = shape factors,

γ = dry unit weight of soil at the pile toe,

B' = pile diameter, or least dimension of the pile (note; in this study, B' = B there is no eccentricity in vertical load),

N_q' , N_γ = bearing capacity factors.

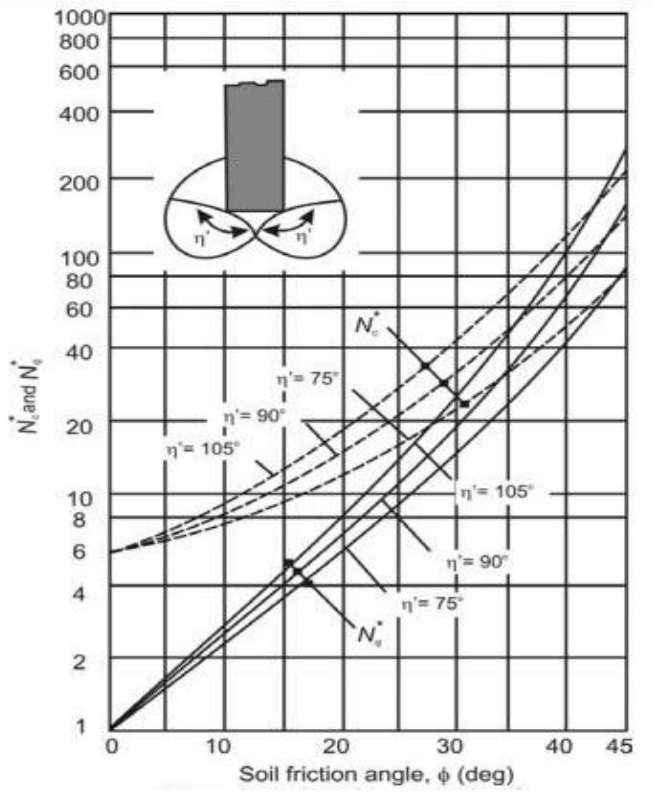

Figure 2.5. Variation of N_q^* with soil internal friction angle (Janbu 1976).

Hansen's bearing capacity factors, shape and depth factors can be written as follows:

$$N_q = e^{\pi \tan \varphi'} \tan^2(45 + \frac{\varphi'}{2}) \quad (2.18)$$

$$N_\gamma = 1.5\left(N_q - 1\right) \tan \varphi' \quad (2.19)$$

For all φ;

$$s_q = 1 + \frac{B'}{L'} \sin \varphi \quad (2.20)$$

and for all φ when $\frac{D}{B} > 1$;

$$d_q = 1 + 2\tan\varphi\ (1 - \sin\varphi)^2 \tan^{-1}\frac{D}{B} \quad (2.21)$$

note; $\tan^{-1}\frac{D}{B}$ should be calculated in radians,

for all φ ;

$$s_\gamma = 1 - 0.4\ \frac{B'}{L'} \geq 0.6 \quad (2.22)$$

$$d_\gamma = 1 \quad (2.23)$$

where;

φ = internal friction angle of soil at the pile toe,

D = pile embedment length,

B = pile diameter or least dimension of the pile,

B' = width of the pile cross section,

L' = length of the pile cross section.

Figure 2.6. Shows the variation of Hansen's bearing capacity factors versus soil internal friction angle.

2.4.3. Pile Shaft Capacity

The axial behavior of the pile is quite complex, in particular, pile shaft behavior. Therefore, there is something to be considered, when estimating pile shaft capacity:

1. In the case of driving pile into the sand due to the impact of the driving process, the soil surrounding the pile gets denser to some diameters as much as 2.5 times of pile diameters **(**Figure 2.7**)**, thus pile bearing capacity is increased. However, under certain conditions, bored piles have a lower bearing capacity compared to driven piles. Another case is pile shaft friction resistance or pile shaft capacity in loose sandy soil gets higher value with higher displacement piles compared to low displacement piles (Das, 2015).

2. It is important to know how long the pile length should be included in determining shaft friction resistance or shaft capacity. In the field load tests, it has been found that shaft friction resistance increases with pile embedment to a depth of 15-20 times pile diameter and its behavior is a non-linear behavior **(**Figure 2.8.**)**, beyond this limit the shaft friction resistance or shaft capacity does not increase with depth (Das, 2015).

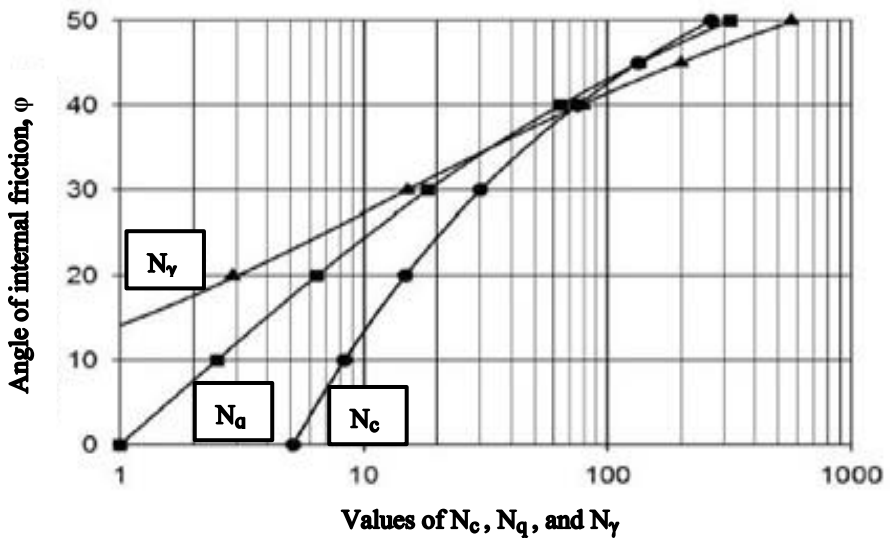

Figure 2.6. Variation of bearing capacity factors with soil internal friction angle (Hansen 1970).

In theoretical approaches, designers are often used, approximation values of (δ), and interface shear box test to estimate interface friction angle, to predict the shaft friction resistance or pile shaft capacity. While the interface friction angle is usually measured based on the interface shear box test, and it gives unreasonable results, especially in the case of loose sand. One example of this subject is the high value of the interface friction angle at low relative density compared to high relative density; this is confirming the existence of uncertainty in the interface shear box test. For example, at the beginning of the interface shear test when the normal load is applied the sand is directly displaced, as a result, sand specimen density is increased. In addition, when the interface shear box test machine is operated vertical displacement is also observed due to normal loading and making the sand get denser and denser. This behavior is in favor of relatively low densities of higher ones.

The friction force that is mobilized in the contact area between the pile and the surrounding soil is a significant component of the ultimate pile capacity to carry the applied vertical axial loads, especially for rough surface piles installed in sand. The interface friction angle is mainly measured using the interface shear box test. Considerable studied has been carried out by several researchers to estimate the interface friction angle between various pile materials and different types of soils by using various testing method such as pullout test, interface shear box test and ring shear test (Potyondy, 1961; O'Rourke

et al., 1990; Frost and Han, 1999; Pando et al., 2002a; Sakr et al., 2005; Al-Mhaidib, 2006; Aksoy et al., 2016; Almallah et al., 2018).

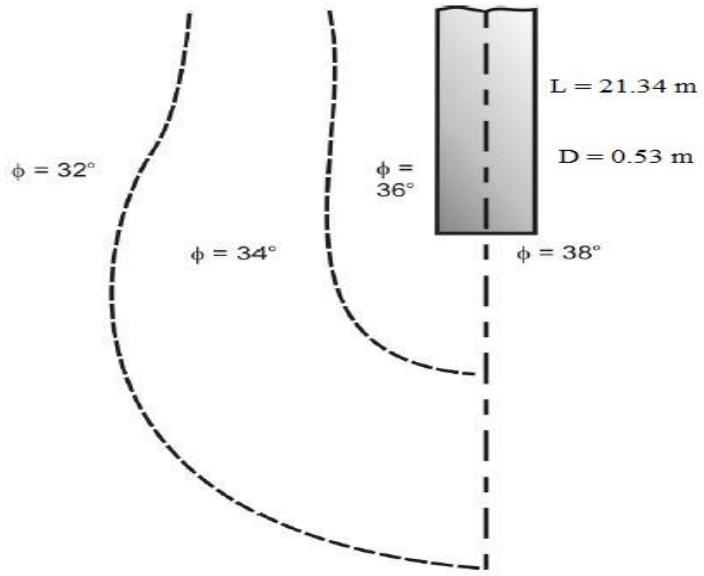

Figure 2.7. Effect of a driven pile on the soil surrounding (after Meyerhof, 1961).

The ultimate pile shaft capacity (Q_f) for a pile installed in a homogeneous sandy soil as in the current study (i.e., pure model sand), can be written as follows:

$$Q_f = \Sigma\, p\,.\,\Delta L\,.\,f \tag{2.24}$$

Where;

Q_f = ultimate pile shaft friction resistance or ultimate pile shaft capacity,

p = pile perimeter or circumference,

ΔL = change in pile embedment length,

f = unit skin friction resistance,

The unit skin friction in equation (2.24) can be written as follow:

$$f = K.\sigma_0'\,.\,tan\,\delta \tag{2.25}$$

where;

f = unit skin friction resistance,

K = coefficient of lateral earth pressure,

σ_0' = mean effective vertical pressure at the desired depth (γ_z x D_z),

γ_z = dry unit weight of foundation soil at the desired depth,

D_z = the desired depth of foundation soil,

δ = pile-soil interface friction angle.

From field tests, it has been observed that the pile shaft capacity increases with an increase of the pile embedment length to a critical depth (L') (Figure 2.8.b) where L' is equal to 15 to 20 times pile diameter, beyond, it remains constant. Usually, for a conservative estimate L' is considered equal to, L' ≈15D (Das, 2015).

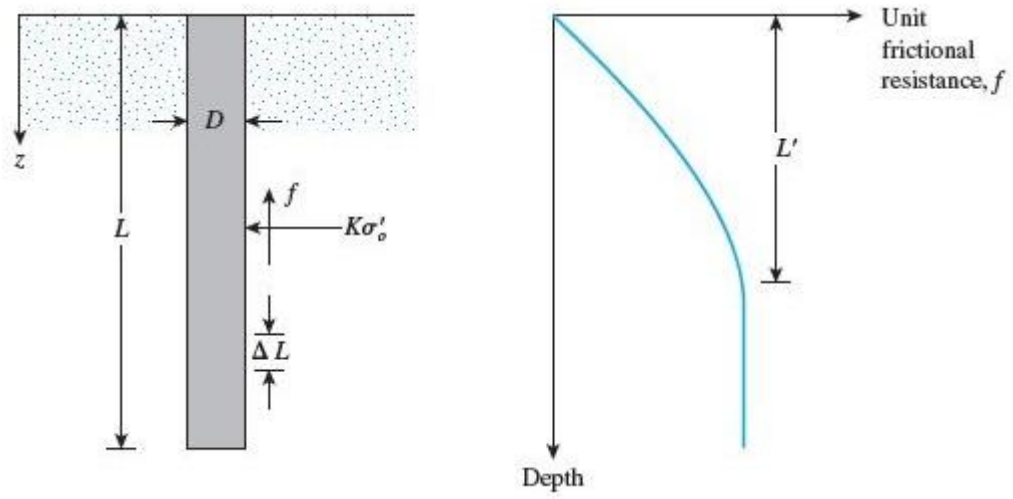

Figure 2.8. (a) Typical piles in sand (b) Shaft friction resistance behavior with pile depth (Das, 2015).

In this study the general pile shaft capacity equation (Burland, 1973) is used to estimate pile shaft capacity with a different consideration of coefficient of lateral earth pressure (K).

2.4.3.1. Burland (1973)

Burland (1973) has proposed a method for estimating the pile shaft capacity installed in clay and it is also used for a pile installed in sand.

Pile shaft capacity equation can be written as follows:

$$Q_f = f_{av}.pL = (K.\sigma'_0.tan\,\delta \quad .p\,.L') \tag{2.26}$$

Where;

Q_f = pile shaft capacity or pile shaft friction resistance,

K = coefficient of lateral earth pressure,

σ'_0 = mean effective vertical soil pressure at the desired depth,

δ = pile-soil interface friction angle,

p = pile perimeter or circumference,

L' = critical pile embedment length ≤ 15D,

D = pile diameter.

In the estimation of the pile shaft capacity, two factors govern the estimation significantly: the factors are coefficient of lateral earth pressure (K) and interface friction angle (δ). In Chapter one, subsection (1.5.1.), despite many uncertainties, but sufficient studies have been presented on the (δ). In addition, for the other factor (K), it is difficult to be accurately estimated, because the value of K is changed with the depth. For this reason, several researchers have presented many approximations of the K value and these approximation values are presented in (Table 2.4.).

Table 2.4. Some recommended values of K (adopted from Bowles 1996).

Pile type	K	K
Bored or jetted	$\approx K_o = 1 - \sin\varphi$	$K = K_a = \tan^2(45 - \frac{\varphi}{2})$
Low-displacement driven	$\approx K_o = 1 - \sin\varphi$ or $1.4(1 - \sin\varphi)$	$K = K_p = \tan^2(45 + \frac{\varphi}{2})$
High-displacement driven	$\approx K_o = 1 - \sin\varphi$ or $1.8(1 - \sin\varphi)$	$K = K_p = \tan^2(45 + \frac{\varphi}{2})$

In addition, as already explained in this Chapter, subsection (2.4.2.3.), Coyle and Castello relied on 24 full-scale field load tests using instrumented piles, they estimated the independent contribution of the pile shaft capacity to the ultimate pile bearing capacity. Based on field load tests they proposed a K value which is the function of both the internal friction angle and pile embedment ratio. Figure 2.9. shows variation of K with L/D (redrawn after Coyle and Castello, 1981).

However, several different considerations are taken into account for the value of (δ). For example, Terzaghi and Peck (1948) and Coyle and Castello (1981) have suggested that $\delta = 0.67\varphi$ and $\delta = 0.8\varphi$, respectively. Several other researchers reported that (δ) is between 0.5 to 0.8φ (Das, 2015). But in the current study, the real measured values of (δ) from the interface shear box test are considered, with different consideration of (K) value such as (K_o, $1.4K_o$, K_p, and Coyle and Castello's K).

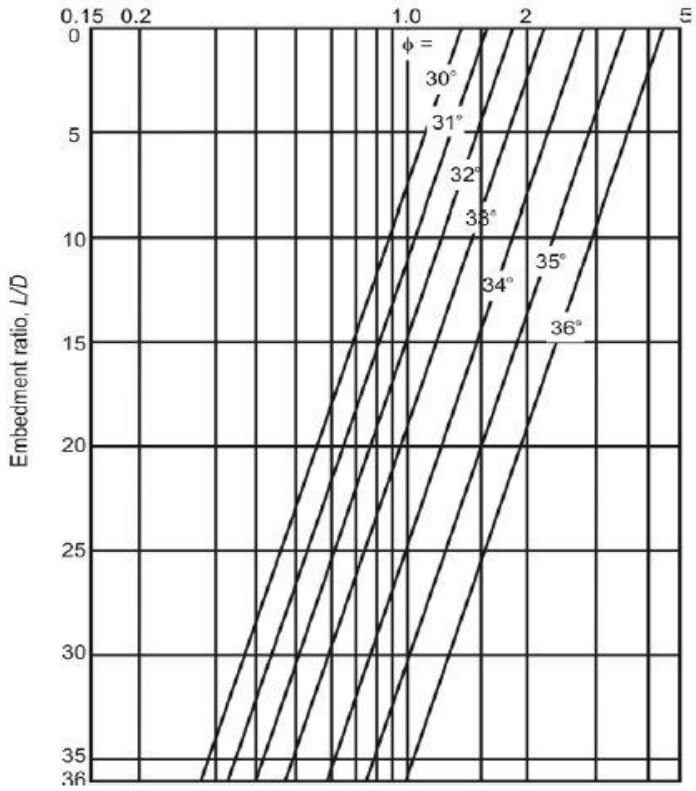

Figure 2.9. Variation of *K* versus *L*/D (redrawn after Coyle and Castello, 1981).

3. EQUIPMENT AND METHODOLOGY

3.1. Introduction

In this Chapter, sufficient details are provided on equipment and materials that are used to measure the axial capacities of single-model composite piles (i.e., total or ultimate bearing capacity, base resistance or base capacity, and shaft capacity) in terms of (p – y) behavior under vertical loading at different relative densities of model sand (i.e., D_r = 10, D_r = 40%, D_r = 65%, and D_r = 90%). The aim of this experimental program is to determine the bearing capacities of single-model composite piles, particularly to determine the piles shaft capacity. Most researchers have relied on the interface shear box test to estimate the pile-soil interface friction angle. Although very few researchers have studied on the single model pile foundation to estimate pile bearing capacity and in particular to study pile shaft capacity. The shear strength parameters (φ and δ) of the foundation sandy soil and pile-sand interface are required to estimate the ultimate pile bearing capacity of a single pile installed in sandy soil. Details of the experimental equipment used in this study are briefly summarized below:

3.2. Relative Density of Model Experiments

In order to determine the relative density of the model sand (i.e., maximum and minimum relative density). About 1 kg of sand is taken randomly and is then oven dried for 24 hours, then according to ASTM D4253 - 16 the relative density of model sand is determined.

In addition, in order to determine the relative densities of the model sand that are required to perform model experiments, a wooden box (42x27.8x11.2 cm) is used. In each case, D_r = 10%, D_r = 40%, D_r = 65%, and D_r = 90%, a number of trial and error experiments should be performed. For example, for D_r = 10%, sand is normally poured from a height of (10 to 15cm) into the wooden box using a flexible plastic pipe. But for D_r = 40%, D_r = 65%, and D_r = 90%, to conduct appropriate experiments of trial and error with a minimum errors or mistakes, at first, the model tank should be filled for some layers with considering the certain layer thicknesses and compaction periods (i.e., for D_r = 40% each hammer point (15 x 15 cm) at each (10 cm) sand layer is compacted for just a moment, for D_r = 65% each hammer point (15 x 15 cm) at each (10 cm) sand layer is compacted for two

seconds, and for D_r = 90%, each hammer point (15 x 15 cm) at each (5 cm) sand layer is compacted for 8 seconds). In the last layer, the wooden box should be placed in the center of the model tank and the sand is then poured. After that, the entire soil layer is compacted under a certain relative density at a height of the wooden box (Figure 3.1. b). To perform a good trial and error experiment, at least one other layer must be prepared above the wooden box level in the case where D_r = 40% and 65%, and at least two layers where D_r = 90 % (Figure 3.1. c). Care should be taken to apply the appropriate compaction to the wooden box, for example, the hammer base should be exactly placed inside the inner dimensions of the wooden box (Figure 3.1. b and Figure 3.1. c). This procedure is repeated for each relative density of some trials. At the end of each trial, the wooden box is weighed and the soil sample is then taken to determine moisture content which is required to measure the dry density of the model sand. A Proter brand electro-pneumatic hammer with a tamper plate (15 x 15 cm) is used for the purpose of compacting model sand (Figure 3.1.a). To avoid crushing sand particles during the compaction process, a plastic base (15 x 15 x 2 cm) is attached to the tamper plate by detachable screw bolts (Figure 3.1.a).

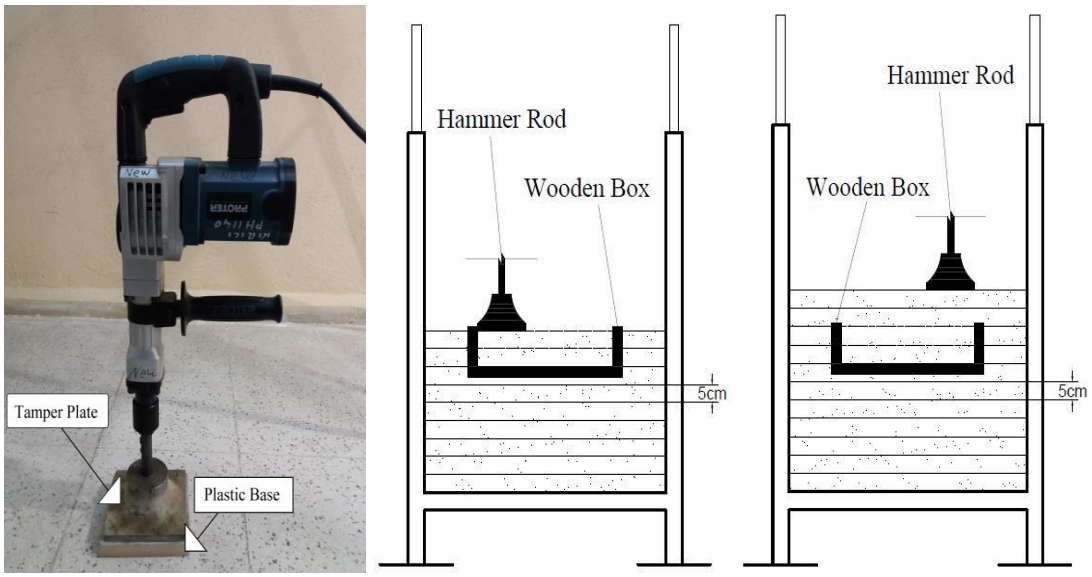

(a) (b) (c)

Figure 3.1. (a) The Proter hammer (b) and (c) an experiment of trials and error for finding model experiment relative density in case where D_r = 90%.

3.3. Load Test System

A series of laboratory experiments are conducted to measure the load-bearing capacities of axially loaded piles. The single-model composite piles are installed in the

center of the specially designed steel tank and loaded vertically in the center of the piles under different conditions of the model sand. Sufficient details of the single-model composite piles load tests setup, as well as, the soil model tank and other facilities are shown in (Figure 3.2.). All the bearing capacity test system accessories are described below.

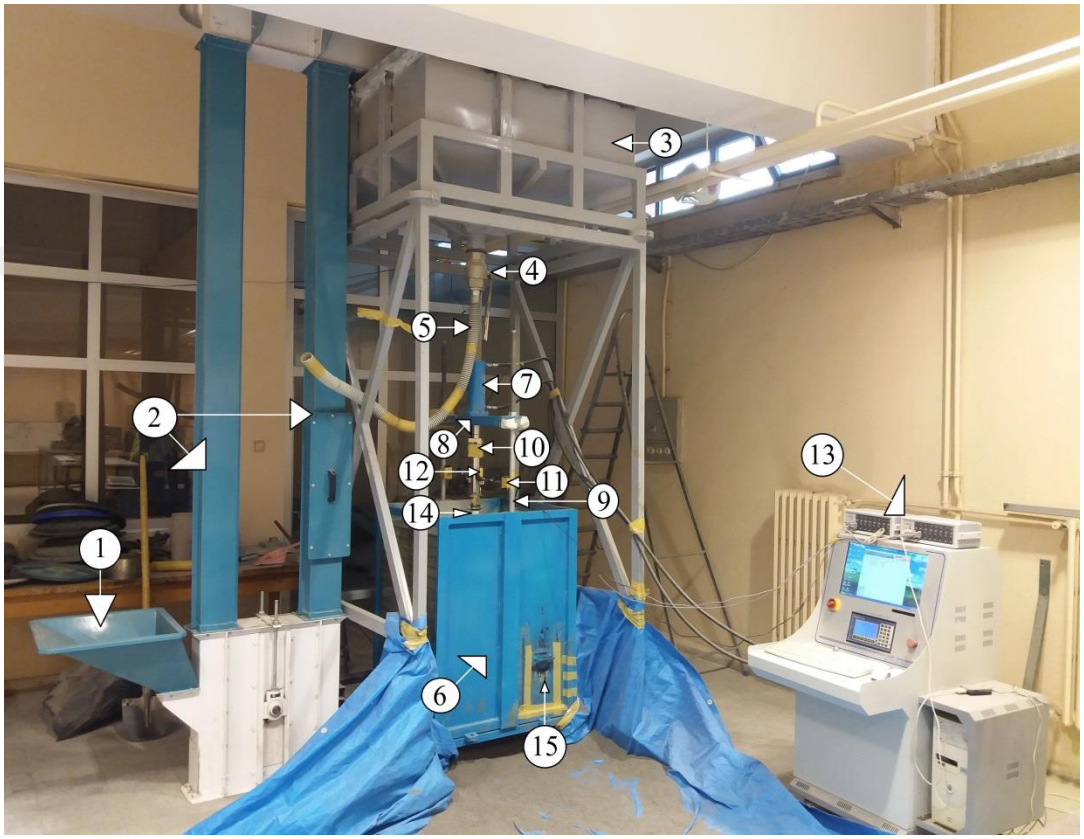

Figure 3.2. Bearing capacity test system : 1. Funnel, 2. vertical bucket elevator, 3. Hopper, 4. Valve, 5.Flexible plastic pipe, 6. Model tank, 7. Hydraulic jack, 8. Loading beam, 9. Steel pipe column, 10.Load cell, 11. Magnetic holder, 12. LVDT, 13. Data acquisition system, 14. Single-Model pile and 15. Emptying gate

3.4. Hydraulic Jack and Loading Machine

A specially designed steel tank (75x75x100 cm) is used in this study. A rectangular steel loading frame supported by two steel pipe columns is used to set up the test system and its loading capacity of more than 2.5 ton. Screw bolts are used to install the hydraulic jack on the loading frame at the center of the model tank. The hydraulic machine is operated electrically and mechanically controlled, and its capacity is 30 kN. Loading frame and other accessories are shown in (Figure 3.3.).

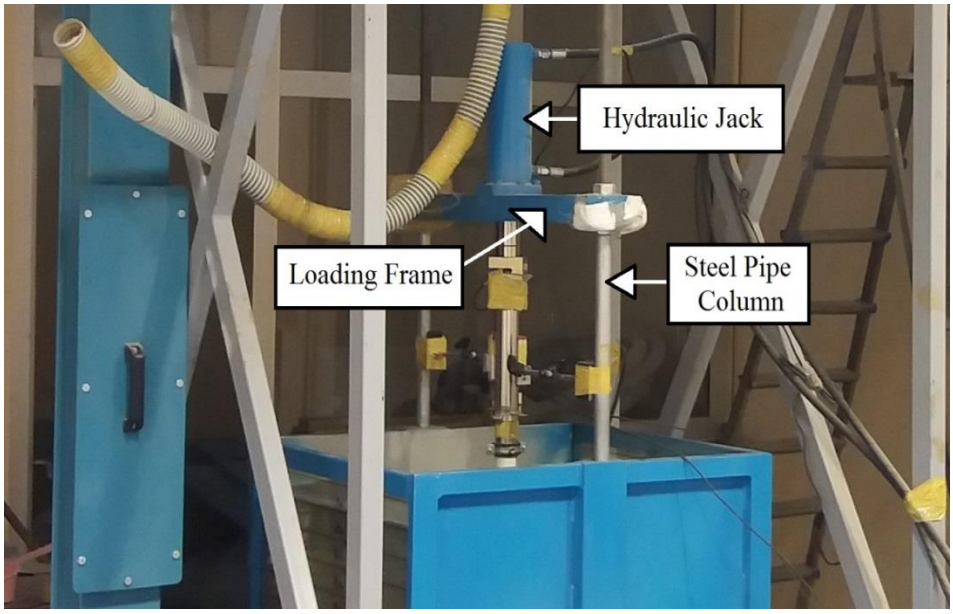

Figure 3.3. Loading frame and other accessories.

3.5. Soil Model tank

A specially designed steel tank is used in this experiment to determine the bearing capacities of the single-model composite piles to conduct (p – y) behavior. The model tank was made from steel, and its dimension parameters are (75 x 75 x 100 cm) as shown in (Figure 3.4.c.). In order to conduct a specific test, the sand is poured into a medium-sized box funnel (Figure 3.4.a.) at a height of 60 cm above ground. The bunch elevator of 340 cm height (Figure 3.4.a.) is used to transfer the appropriate sand to the other funnel box or hopper at the top of the system frame (Figure 3.4.b.).

When the appropriate sand is transferred and stored at the top funnel or sand hopper, a flexible plastic tube is used to pour the sand into the model tank (Figure 3.4.b.). By performing an axial load test on a single-model composite pile, a behavior (p – y) is conducted. After each experiment is finished, the model tank is emptied by opening a small gate on the underside of the model tank (Figure 3.4.c.). The model system is illustrated schematically in (Figure 3.5.).

3.6. Single-Model Composite Piles

In this study, concrete-filled PVC and FRP pipe piles are used (Figure 3.6.a). The piles are 50 mm in diameter and 600 mm in length (500 mm in embedding length). The FRP composite pile used in this study is a semi-rough FRP pipe pile and the PVC

composite pile is a smooth PVC pipe pile. The typical properties of single-model composite piles are given in (Table 3.1.).

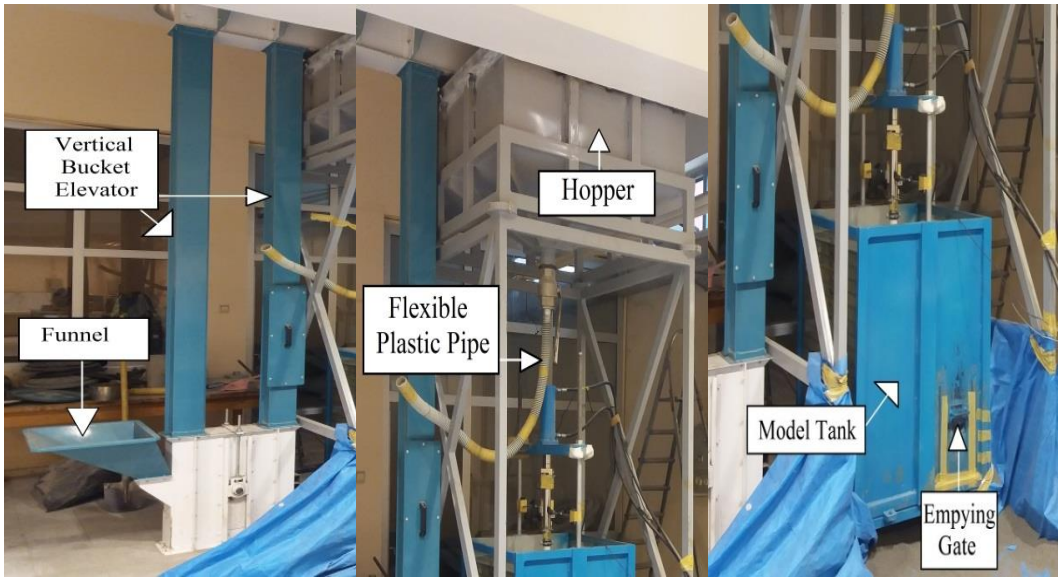

(a) (b) (c)

Figure 3.4. (a) Vertical bucket elevator, (b) hopper and flexible plastic pipe, and (c) soil model tank.

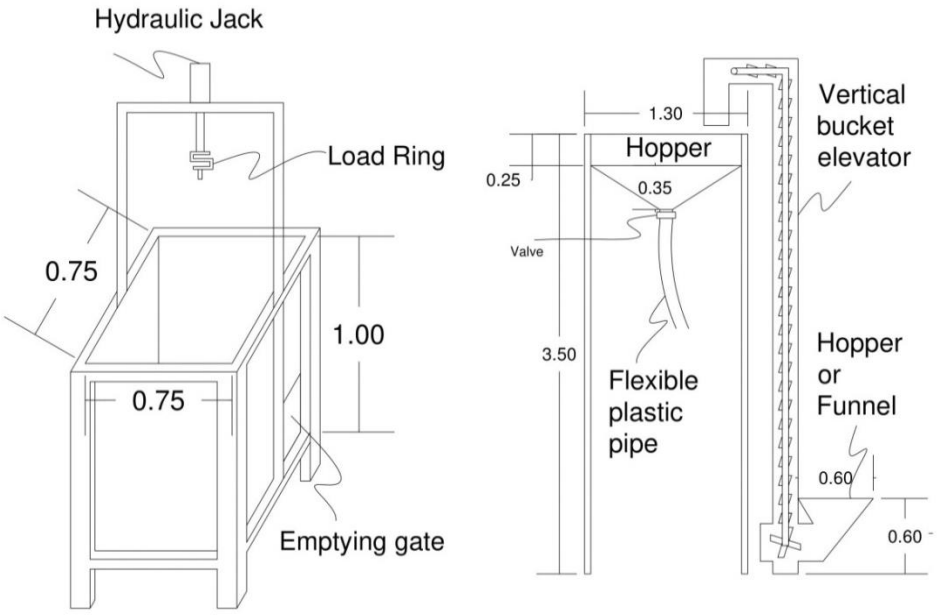

(a) (b) (c)

Figure 3.5. (a) Soil model tank, (b) hopper and flexible plastic pipe, and (c) Vertical bucket elevator.

Table 3.1. Typical properties of single-model composite piles.

Properties	PVC pile	FRP pile
Compression strength (Mpa)	66.19	200
Tensile strength (Mpa)	0.0414 – 0.0527	240
Tensile Elasticity Modulus (Gpa)	2.48 – 3.3	23
Density (gr/cm^3)	1.3 – 1.49	1.8

The aim of using these composite piles in this study is to determine the ultimate bearing capacity, pile base resistance and especially to estimate pile shaft capacity of these piles. In order to conduct model experiments, some important points must be taken into account, such as the diameter and length of the pile, the width or diameter of the model tank, as well as, depth of the soil between the pile bottom and the base of the model tank.

In this study, the dimension parameters of the single-model composite piles were selected based on the recommendations reported by Bolton et al. (1999). These researchers proposed two recommendations to avoid the bearing capacity of the model pile by the boundary effect of the model soil tank and scale effect of both model sand and model pile. First, to avoid any contact between the failure zones of the model sand (i.e., the surrounding soil and soil beneath the pile) and the side wall of the model soil tank, the ratio of the diameter of the model soil tank to the diameter of the model pile (D_{tank}/D_{pile}) must be greater than 8. Second, to keep pile bearing capacities away from the scale effect, the model pile diameter must be greater than 20 x D_{50} size. In this study, the ratio of (D_{tank}/D_{pile}) = 15 > 8 and piles diameter = 50 mm > ($20xD_{50}$ = 9.5 mm), thus the pile bearing capacity is avoided from the boundary and scale effect, respectively. In spite of this, for both single-model composite piles to have the same base behavior, a galvanized steel plate is attached to their base (Figure 3.6.b). Several dimensional parameters of the model piles and soil tanks that have been used by the other researchers to measure the bearing capacity of the model pile in terms of load-displacement (i.e., p-y) behavior are given in (Table 3.2.).

Another important point must be considered in model experiments is, how deep the stress isobar or pressure bulb extends under the bottom of the pile due to the applied loads. Based on the design recommendations of foundation engineering, the pressure bulb induce due to applied loads, can be effectively extended into the soil foundation layers at a depth of 1.5 to 2B (note: B is the short dimension of the foundation and in this study is the pile

diameter). For this reason, piles are also installed at a depth of 400 mm (400 mm = 8D>2B or 2D) above the base of the model tank. Thus, the model tank which is used in this study has sufficient depth and the bearing capacity of the single-model composite piles is avoided by the effect of the pressure bulb of more than 4 times (8D > 2D).

(a) (b)

Figure 3.6. (a) Single-model composite piles, and (b) Galvanized steel plate attached to the bottom of the single-model composite piles.

3.6.1. Load-Displacement Measurement of Single-Model Composite Piles

In order to measure the vertical displacement of the single-model composite piles, two Linear Variable Displacement Transducer (LVDT) are used. A pipe clamp is used to install two small strong steel L-shape angle bracket bar (50 x 50 mm) on both sides of the pile head (i.e., the left and right sides of the piles head), and then the light-weight LVDTs are placed on it. Magnetic holders are used to support LVDTs that are installed next to piles. The LDVTs measurement capacity used in this study is 50 mm. In order to measure the applied load from the machine, a Keli brand S-type 5tons capacity load cell is used. The load cell is connected to the computer via data loggers and automatically registers the applied load. The amount of load and vertical displacement are measured and recorded in the computer environment by the data acquisition system. The load cell beam and some other accessories are shown in (Figure 3.7.).

Table 3.2. Several dimension parameters of model experiments used by some researchers (Taylan, 2013).

Reference	Soil model tank diameter (mm)	Model pile diameter (mm)	Soil model tank to model pile diameter ratio
Vesic (1963, 1964)	2450	50.8 - 171.5	14.29 - 48.23
Hanna and Tan (1973) Tan and Hanna (1974)	610 x 610	15.7 - 38	16.05 – 38.85
Das et al. (1977)	475 x 610	25.4	18.7
Chaudhuri and Symons (1983)	1100	25.4 - 50	22 – 43.31
Kerisel (1964)	6400	40 - 320	20 - 160
Robinsky and Morrison (1964)	501 x 711	20.5 - 37.5	24.44 – 13.36
Shin et al. (1993)	457 x 457	25.4	17.99
Al-Mhaidib (2001)	450	30	15
Mayoral et al. (2005)	510	51	10
Nanda and Patra (2011)	750	32	23.44
Present Study	750x750	50	15

3.6.2. Load Tests Procedure

A number of model experiments are conducted to determine the bearing capacities (i.e., total or ultimate, base resistance or base capacity, and shaft capacity) of single-model composite piles in the model sand. The appropriate procedures for measuring the bearing capacities of single-model composite piles are detailed in subsections below.

3.6.2.1. Conducting Ultimate Piles Bearing Capacity Model Experiments

The sufficient procedures that is used in this study to prepare soil foundation in the model tank for ultimate bearing capacity experiments can be presented as follow:

1. In order to conduct the ultimate bearing capacity of single-model composite piles, the model tank is filled to a depth of 90 cm for each relative density under a certain condition. For example, for D_r = 10% (Figure 3.8.) the model tank is filled to the required depth (i.e., 90cm) by pouring model sand normally from a height of 10 to 15 cm using a flexible plastic pipe. In addition, for D_r = 40% and 65% (Figure 3.9.), the

required depth of the model tank is filled in 10 cm soil layers by pouring model sand from a height of not more than 5 cm. Then, each hammer point of (15 x 15 cm) in each (10 cm) sand layer is compacted for a moment (less than one second) and two seconds for D_r = 40% and 65%, respectively. But in the case of D_r = 90% (Figure 3.10.), the model sand is poured from a height of 10 cm and the thickness of the sand layers is 5 cm, and each hammer point of (15 x 15 cm) in each (5 cm) sand layer is compacted for 8 seconds. As already given in Chapter Three, section (3.2.) a Proter brand electro-pneumatic hammer with a tamper plate (15 cm x 15 cm) is used to compact the model sand.

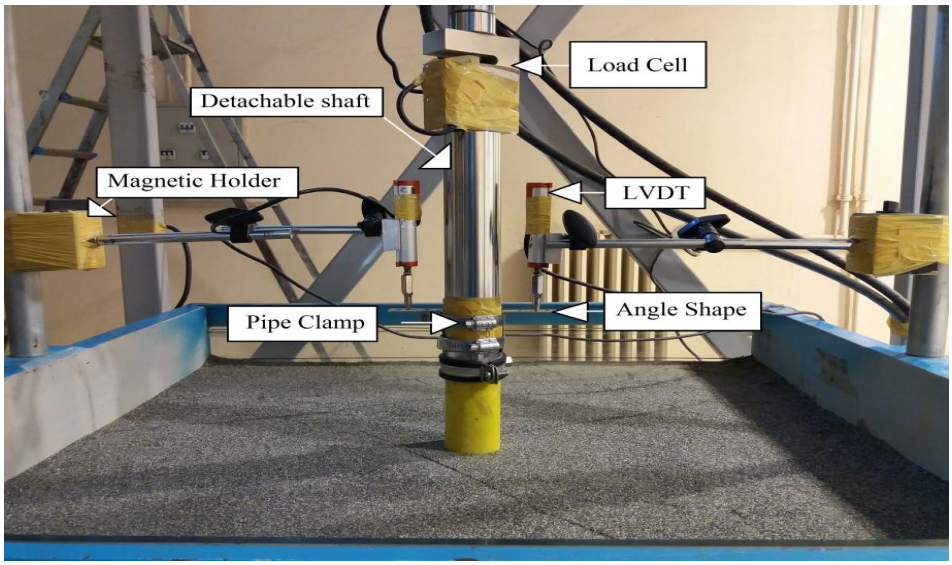

Figure 3.7. Load cell beam and other accessories.

2. When the soil tank is filled to a depth of 40 cm, a sensitive adjustment or leveling is applied using a bubble balance in the case of D_r = 10%, and using a bubble balance with a 10 cm thick circular base plate in the case where D_r = 40%, 65%, and 90%. After that, the single-model composite piles are attached to the Keli S beam-type 5tons capacity load cell via the detachable screw connection.

3. The piles are then lowered carefully to a level touches only on the ground.

4. The procedure is continued under the instructions explained in point 1.

5. Single-model composite piles are then loaded axially on their heads through a hydraulic jack. An electric machine is used to operate the hydraulic jack which is electrically operated and controlled mechanically.

6. The ultimate bearing capacity of single-model composite piles in terms of (p-y behavior) is measured by means of Keli S beam-type capacity of 5 tons and two LVDTs on the left and right side of the pile head. The data are recorded in the computer by means of two data loggers. A brief summary of the sand compaction procedures is given in (Table 3.3.).

Table 3.3. A brief summary of the sand compaction procedures.

Relative Density (D_r,%)	Compaction Process	Dry Unit Weight (γ_d), (kN/m^3)	Void Ratio (e)
10	The model tank is filled to the required depth (i.e., 90 cm for ultimate bearing capacity and pile shaft capacity, and 40 cm for the pile base resistance). The model sand is poured normally using a flexible plastic pipe from a height of 10 up to 15 cm, care should be taken, any mistake will change the relative density significantly.	14.6	0.86
40	The model tank is filled to the required depth, as explained above in the D_r = 10% (i.e., 90cm and 40cm). The model sand is poured by means of a flexible plastic pipe from a height of not more than 5 cm for each 10 cm layer of sand. Then each point of (15 * 15 cm) in each layer of 10 cm sand is compacted for a moment (less than one second).	15.5	0.75
65	The same procedure is carried out as already given for D_r = 40%, except for each point of (15 * 15 cm) in each layer of 10 cm of sand is compacted for 2 seconds.	16.3	0.66
90	The model tank is filled to the required depth, as explained above in the D_r = 10% (i.e., 90cm and 40cm). The model sand is poured by means of a flexible plastic pipe from a height of 10 to 15 cm for each 5 cm layer of sand. Then each point of (15 * 15 cm) in each layer of 5 cm sand is compacted for 8 seconds.	17.3	0.57

To ensure that single-model composite piles are installed vertically, a steel shaft is used of appropriate length and in the same diameter that piles have. The steel shaft is already screwed at one end and mechanically adjusted at the other end. The shaft is connected to the load cell via a detachable screw connection and at the other end the special type of glue such as EPOXY 5 MINUTE is used to attach the steel shaft with the pile head. An object of suitable height is placed under the pile base for the purpose of setting it up and the Styrofoam is also placed to keep the pile during the setup process. When the epoxy is prepared and placed on top of the pile, the pile is placed at the top of that object which is already placed inside the model tank. After that, the pile is loaded for

some amount just for the purpose of setting it up. During this process, the water bubble balance is used to check the pile verticality in all sides (Figure 3.11.).

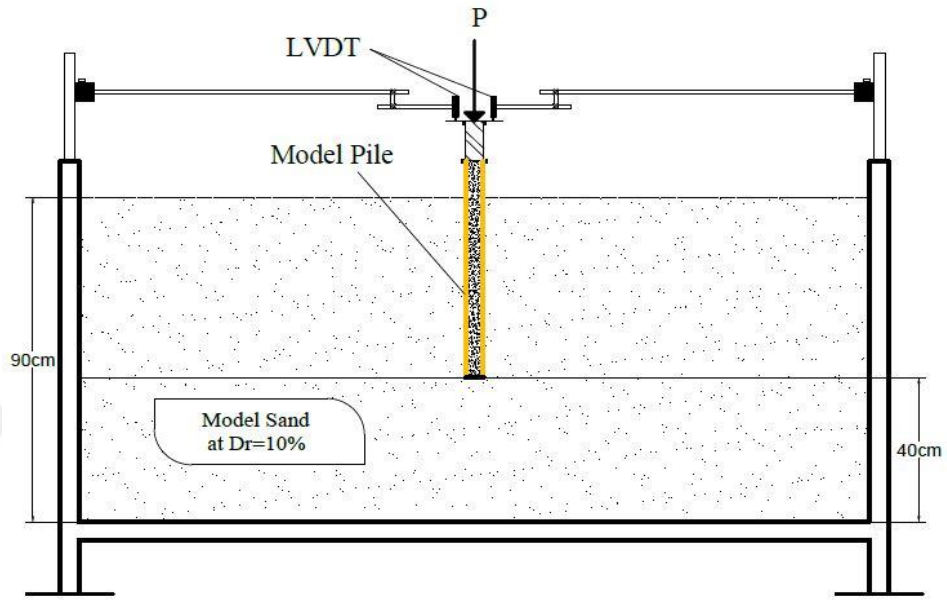

Figure 3.8. A single-model composite pile installed in the model tank to conduct the ultimate bearing capacity model experiment at D_r = 10%.

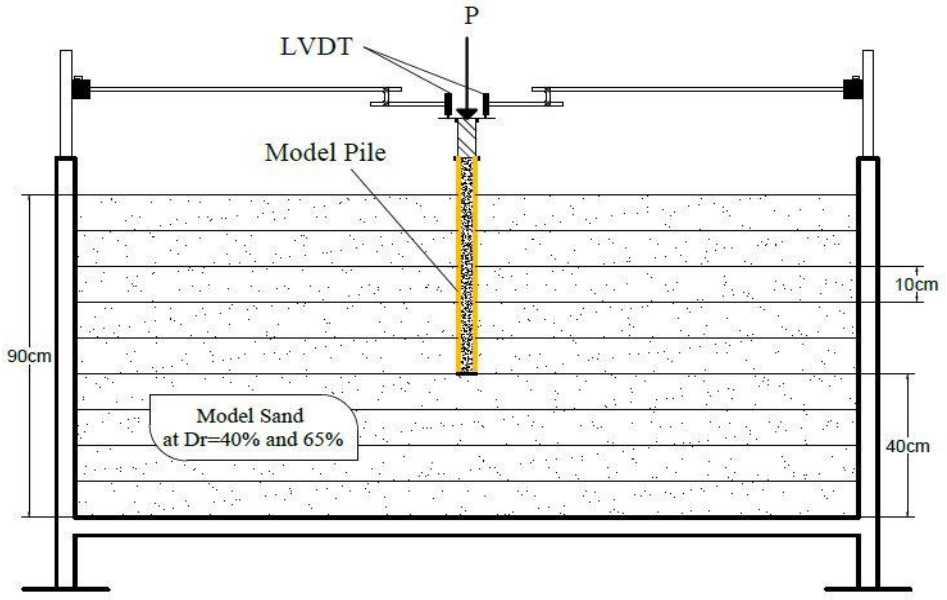

Figure 3.9. A single-model composite pile installed in the model tank to conduct the ultimate bearing capacity model experiment at D_r = 40% and 65%.

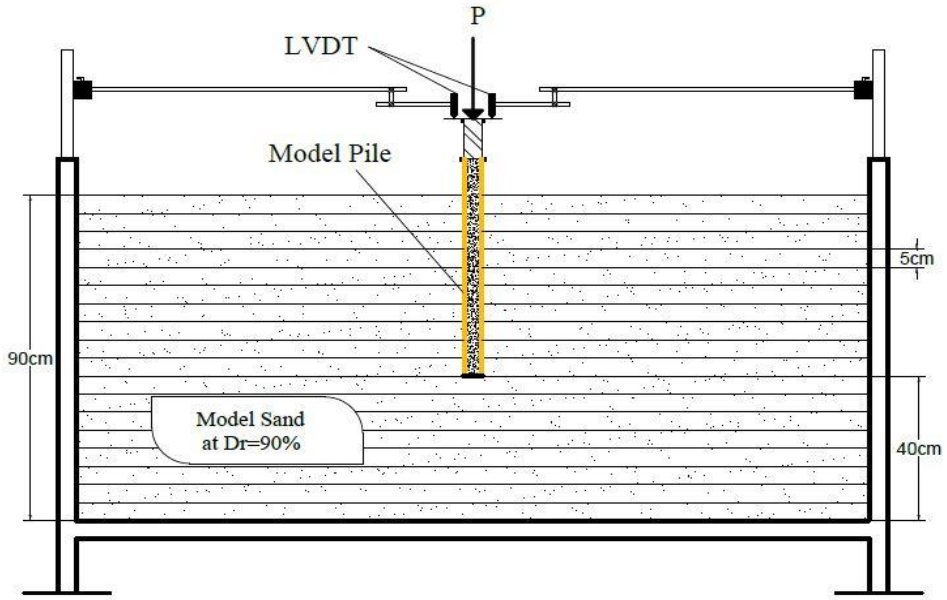

Figure 3.10. A single-model composite pile installed in the model tank to conduct the ultimate bearing capacity model experiment at D_r = 90%.

The pipe clamp (Figure 3.11.) is also used besides the epoxy to provide proper bonding between piles and detachable steel shaft. In this study, the hydraulic machine is a load control device and single-model composite piles are loaded at different loading speeds depending on the relative densities until the displacement of the pile reaches 40 mm.

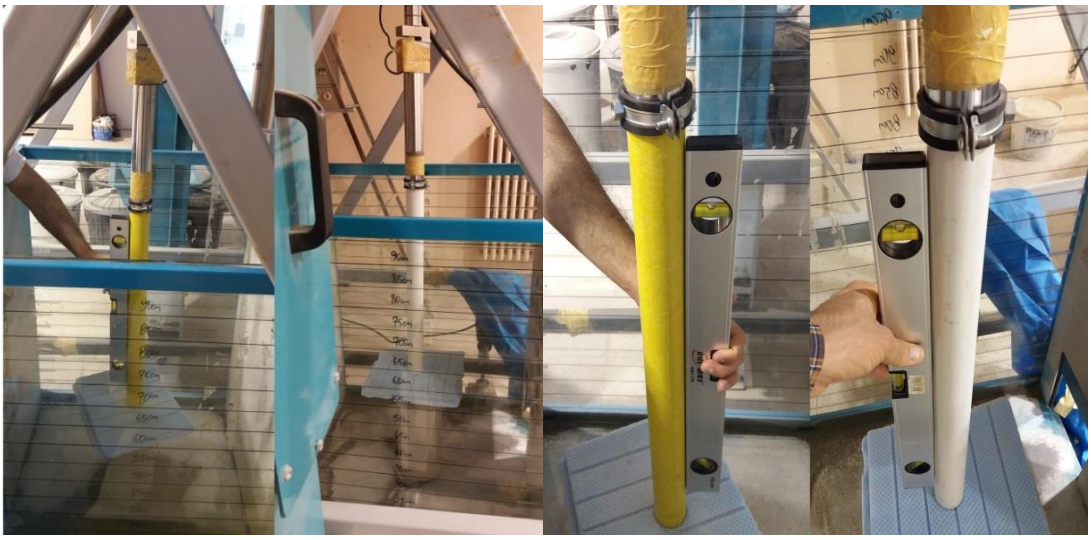

Figure 3.11. Piles set up before conducting model experiments.

3.6.2.2. Conducting Piles Base Capacity Model Experiments

In order to perform pile base capacity or pile base resistance model experiments, the model tank is filled to a depth of 40 cm. To prepare the model sand for a given relative density, the same instructions given earlier in the procedures of the ultimate bearing capacity experiments (subsection 3.6.2.1) are followed. When the required depth of the model tank is reached, a sensitive adjustment or leveling is applied using a bubble balance in the case of D_r = 10%, and using a bubble balance with a 10 cm thick circular base plate in the case where D_r = 40%, 65%, and 90%, the piles are then lowered carefully to the level touches only on the ground (Figure 3.12.), then the load is applied.

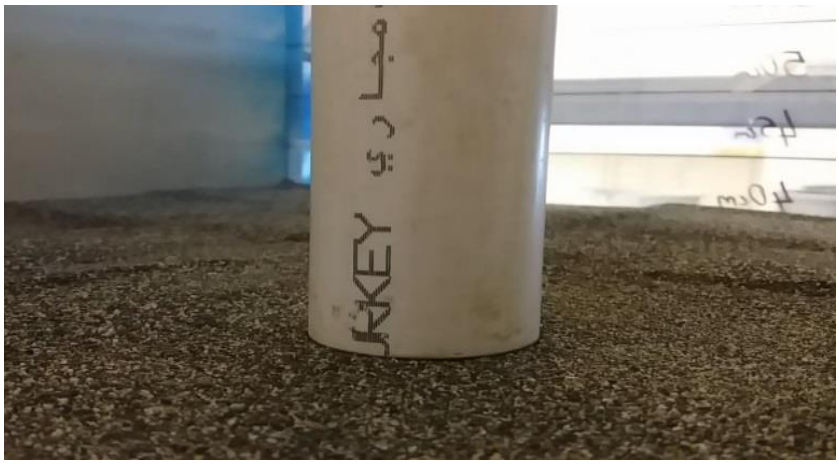

Figure 3.12. The PVC compsite model pile installed in the model tank to conduct the pile base capacity model experiment and touched only on the ground.

Typical installations of single-model composite piles to conduct a pile base capacity at different relative densities of model sand are shown in (Figure 3.13 to 3.15).

3.6.2.3. Conducting Piles Shaft Capacity Model Experiments

The test procedure of pile shaft friction resistance or pile shaft capacity can be summarized as follows:

1. A normal type of semi-solid Styrofoam (Figure 3.16.a.) is used in pile shaft capacity experiments to make a cubic shape (15 x 15 x 8 cm), with a hole of diameter (5.3 to 5.5 cm) in the center of the Styrofoam body. The most important thing in the pile shaft capacity experiments is how to provide sufficient gap between the bottom of the pile and sand, as well as between the pile and the side wall of the Styrofoam body, to keep

the pile away from contacts when filling the model tank and performing model experiments. For this reason, the Styrofoam body must be installed in the exact location.

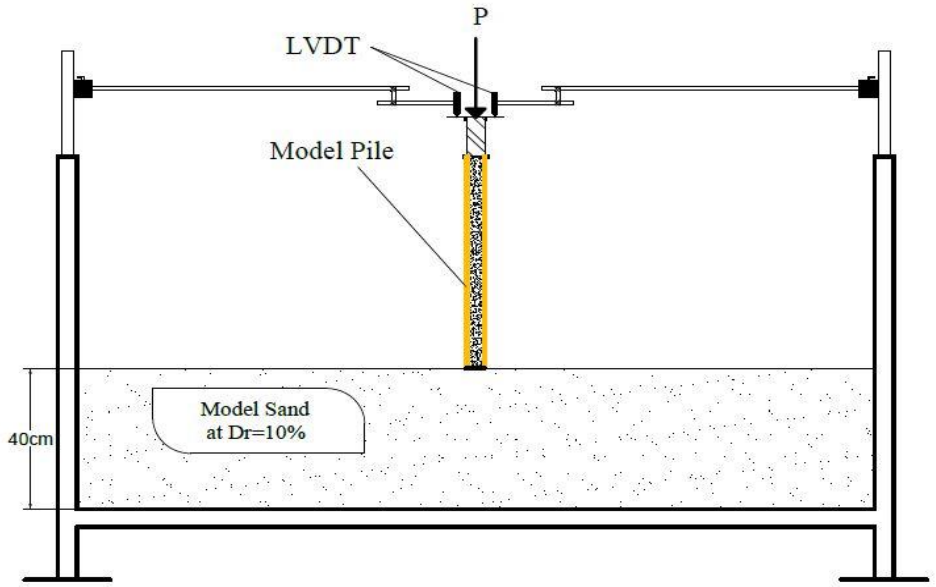

Figure 3.13. A single-model composite pile installed in the model tank to conduct the pile base capacity model experiment at D_r = 10%.

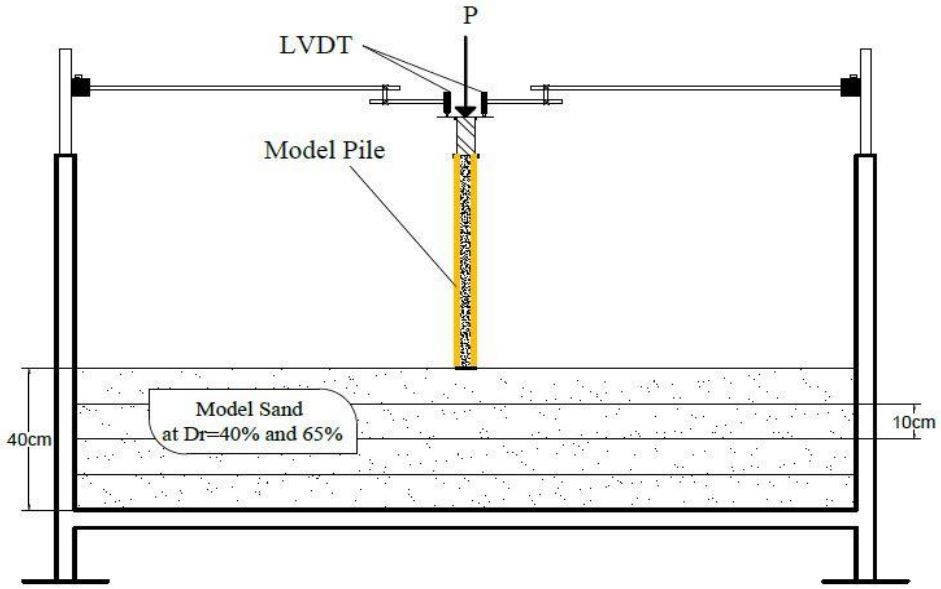

Figure 3.14. A single-model composite pile installed in the model tank to conduct the pile base capacity model experiment at D_r = 40% and 65%.

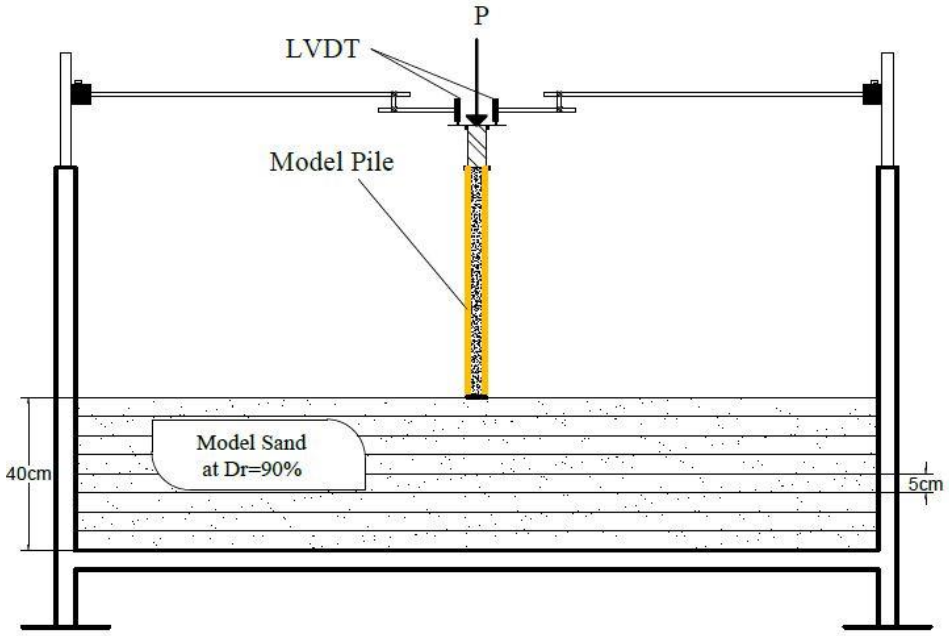

Figure 3.15. A single-model composite pile installed in the model tank to conduct the pile base capacity model experiment at D_r = 90%.

2. To prevent unexpected movements of the Styrofoam body during filling the model tank and performing model experiments that can change the results significantly. The hard soil layer is prepared at D_r = 90% under the Styrofoam body (note: look at point 1 of the procedure for measuring the ultimate bearing capacity of single-model composite piles to find out how D_r = 90% is reached, subsection 3.6.2.1.).

3. Then, the Styrofoam body is placed and the pile is lowered into the hole of the Styrofoam body to the level touches only on the ground, after that, the sand surrounding the Styrofoam body at a height of (8 cm) is prepared under certain conditions, the pile is then uplifted to the desired position, in a manner where the pile penetration of (1.5 to 2 cm) is maintained inside the Styrofoam hole.

4. To avoid entering any sand particles into the hole of Styrofoam body during filling the model tank and conducting model experiments, a filter is prepared with a height of 2cm and placed on top of the Styrofoam body (i.e., 8 cm height of Styrofoam body and 2 cm height of the filter is equal to 10 cm, which is equal to the thickness of one soil layer in D_r = 40% and 65%, and two soil layers in D_r = 90%). For this purpose, a normal type of pipe clamp is installed around the pile, and to avoid any contact between the clamp and the pile, a normal type of sponge is wrapped around the pile, then the clamp is fixed on the sponge. After that, the sponge-clamp system is covered with a normal type of

adhesive tape, and then a normal type of papers are placed on the sponge-clamp system. These papers were already covered with adhesive tape and have a hole of the same diameter or a little smaller than that the piles. In fact, these papers provide the proper filter and the clamp-sponge system is only used to support them. Figure (3.16.b) indicates what the filter consists of and how to prepare the filter around the pile is shown in (Figure 3.17.).

(a) (b)

Figure 3.16. (a) Styrofoam body, and (b) other accessories that were mentioned in point 1, 2 and 5.

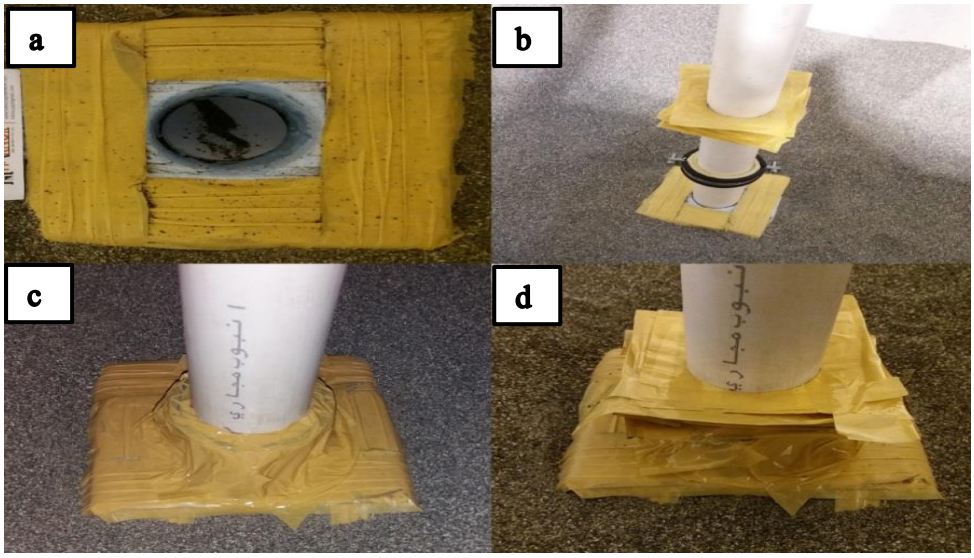

Figure 3.17. (a to b) How to prepare the filter around a single-model composite pile for conducting a shaft capacity model experiment.

5. Finally, the same instructions that were already detailed in the ultimate bearing capacity procedure experiments (subsection 3.6.2.1.) are followed to prepare the soil surrounding the pile shaft at different relative densities.

Figure (3.18 to 3.20) illustrate an installed single-model composite pile to perform pile shaft capacity model experiments at different relative densities of model sand.

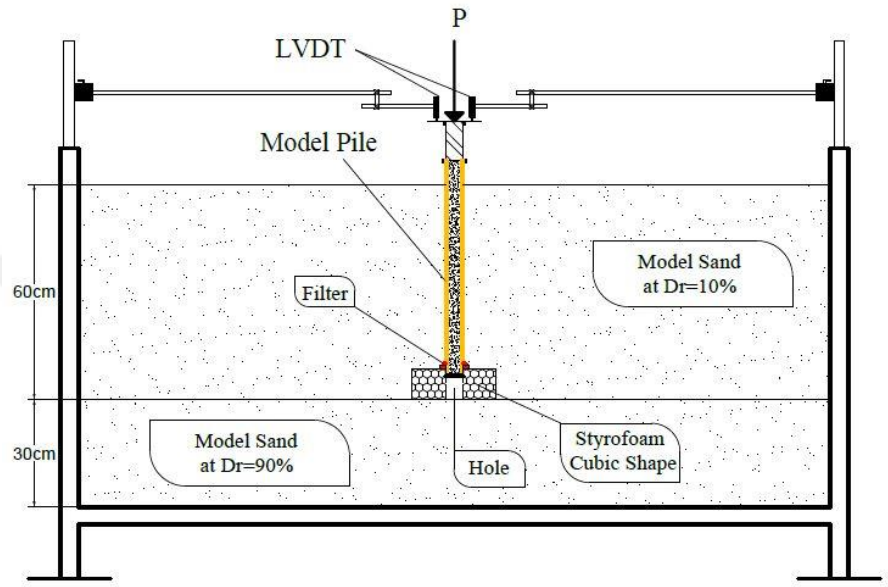

Figure 3.18. A single-model composite pile installed in the model tank to conduct the pile shaft capacity model experiment at D_r = 10%.

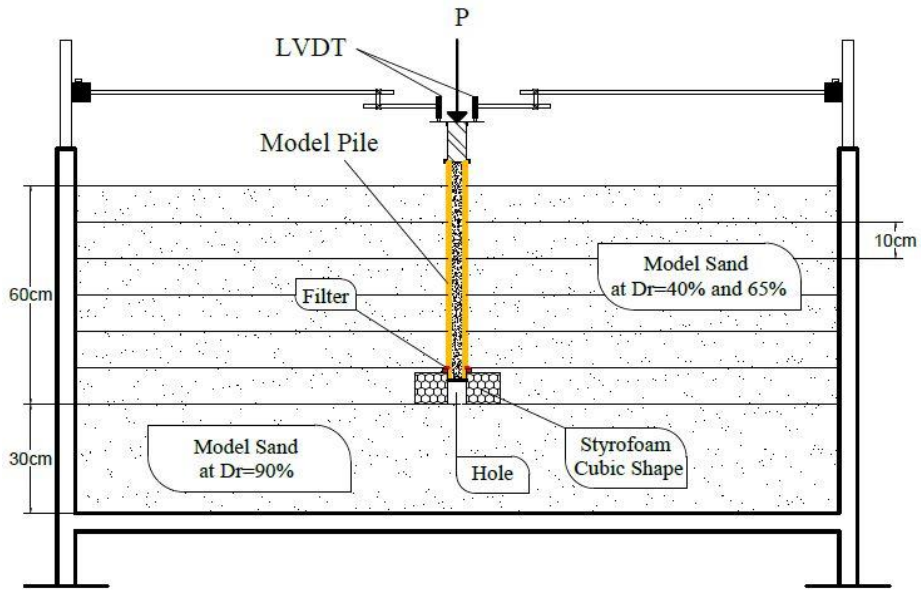

Figure 3.19. A single-model composite pile installed in the model tank to conduct the pile shaft capacity model experiment at D_r = 40% and 65%.

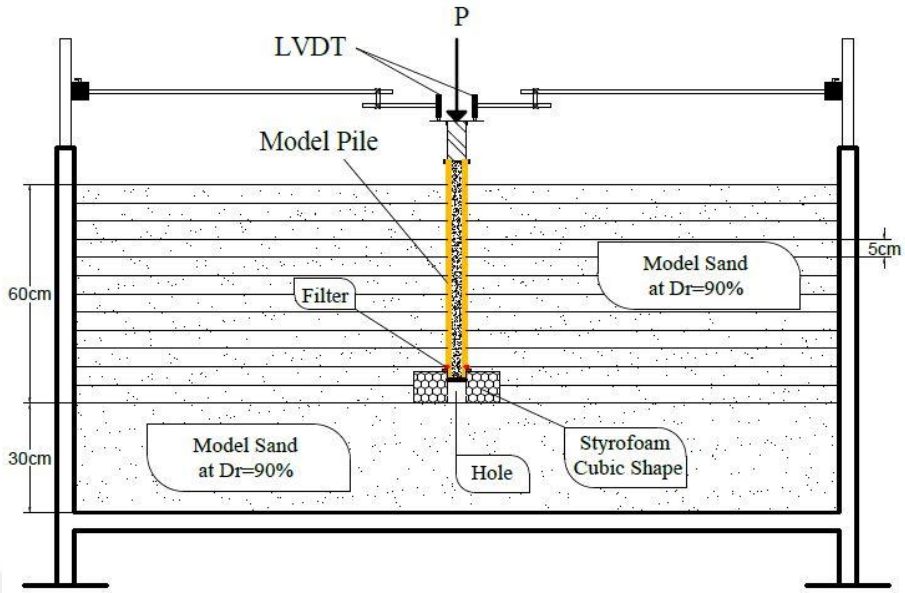

Figure 3.20. A single-model composite pile installed in the model tank to conduct the pile shaft capacity model experiment at D_r = 90%.

At the end of each model experiment, the quality or efficiency of the filter system has been checked. In critical conditions where the relative density was 65% and 90%, the particles entering the Styrofoam body hole were not reached up to 1 gr (Figure 3.21). This means that the filter has worked effectively.

Figure 3.21. Checking the quality or efficiency of the filter system.

3.7. Effect of Loading Rate

Many researchers have studied the effect of loading rate on the pile bearing capacity. Dijkstra (2004) reported that the loading rate can significantly affect the pile bearing capacity installed in unsaturated sand. AL-Mhaidib (1999) reported that the axial bearing capacity of single-model pile installed in sand increases with increasing loading rate, as single-model piles the axial bearing capacity of model pile group installed in sand also increases with the loading rate (AL-Mhaidib, 2006a). In the literature, researchers have used different loading rates, but in general, it is recommended to be no more than 2 mm/min and often 1 mm/min is recommended. For this reason, in this study, the loading rates of ultimate bearing capacity and base resistance experiments of single-model piles are maintained at about 1 to 1.30 mm/min. This range was chosen because the hydraulic jack that is used in this study is not a displacement control: therefore, it is impossible to exactly reach the required load rate (i.e., 1 mm/min). In addition, due to the sensitivity of the independent contribution of the pile shaft capacity experiments, the loading rate is 1 mm/min for the loosest state (D_r = 10%) and 0.5 mm/min for the densest state (D_r = 90%), and for the other two (D_r = 40% and 65%) is between 0.5 and 1 mm/min.

3.8. Direct Shear Test Device

The traditional direct shear box test and interface shear box test apparatus is used to measure the internal friction angle (φ) of the model sand and interface friction angle (δ) of the composite piles according to the ASTM D3080-72 (1989) and ASTM D5321/D5321M-14 (2014) guidelines, respectively. These shear strength parameters (φ and δ) of sand and pile-sand structure are required to estimate the ultimate bearing capacity, base capacity or base resistance, and shaft capacity of single-model composite piles. Figure 3.22 and 3.23 illustrate how the φ and δ of soil are measured in the direct shear box test and interface shear box test, respectively.

In order to measure the (φ) of the model sand, the direct shear box (DSB) (60mm * 60mm * 20mm) is filled with the model sand in different relative densities. During the preparation of the model sand specimens, the DSB depth is divided into three equal layers for applying the appropriate compaction, especially in the case of D_r = 65% and D_r = 90%.

But to measure the interface friction angles between the composite piles and the model sand, two plates of the same composite material must be prepared in the same

dimensions as the DSB (60 mm * 60 mm) and 10 mm in height. The interface shear box tests are conducted by placing the composite plates into the lower part of the interface shear box test, and then installing the upper part by using bolts. The model sand are then poured into the upper part of the shear box and compacted with respect to a certain relative density. In the determination of both (φ and δ), the test machine is operated at strain shearing of 0.5mm/min and under three normal loading case (20 kg, 40kg and 60 kg).

3.9. Surface Roughness Test Device

In study, in order to determine the surface roughness of single-model composite piles the Mitutoyo SJ-201 test device is used for a measuring distance of 4 mm. However, the PVC and FRP single-model composite piles that are used in this study are smooth and semi-rough materials, respectively. But, to represent the actual piles installed in the field and to simulate the effect of the driven process on the piles surface roughness, the surface roughness tests are conducted after performing the load-displacement model experiments.

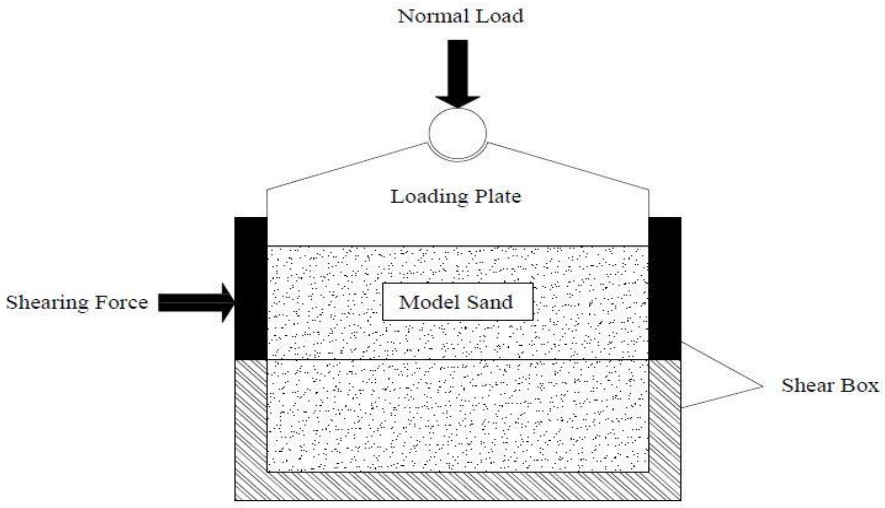

Figure 3.22. Schematic diagram of the internal friction angle test setup.

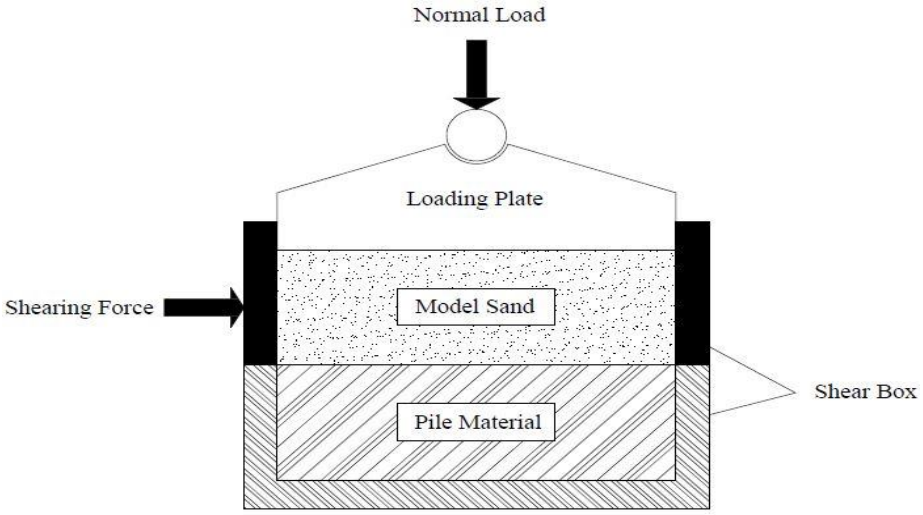

Figure 3.23. Schematic diagram of the interface friction angle test setup.

4. EXPERIMENTAL RESULTS

4.1. General Description

Two composite single-model composite piles were already described and installed in the specially designed model steel tank with sufficient accessories. The model sand was compacted at different relative densities. The single-model composite piles were then loaded to measure their load versus displacement behavior (i.e., p-y behavior). In this Chapter, the required experimental results are given in two sections (4.2. and 4.3.). In the first, appropriate laboratory experiments and properties of the model sand are presented. In the second, the experimental p-y behavior is presented for single-model composite piles.

4.2. Soil Properties Tests

In order to determine the index properties of model sand and shear strength parameters of model sand and pile-sand structure, a number of laboratory experiments were conducted.

4.2.1. Sieve Analysis and Specific Gravity Tests

In the literature, in the case of sandy soils, the maximum particle size (1 mm) was often used to measure the load-displacement behavior of model foundations (i.e., shallow foundation model, piles model, anchor piles model, etc.) (Terzi et al., 2009; El Sawwaf, 2010; Bağrıaçık and Laman, 2011; Kahyaoğlu et al., 2012). The sandy soil used in this study is pure sand and has already been prepared by geotechnical laboratory staff with a granular size ranging from 0.074 mm to 1 mm.

The grain size distribution and specific gravity of the model sand had been obtained through sieve tests that were carried out according to ASTM D422-63 (1989) and ASTM D854-83 (1989), respectively. The model sand is SP according to the unified soil classification system. The representative soil sample was taken from the whole model sand and oven dried for 24 hours. The grain size distribution curve of the model sand is shown in (Figure 4.1.). The sand index properties related to this subsection are given in (Table 4.1.).

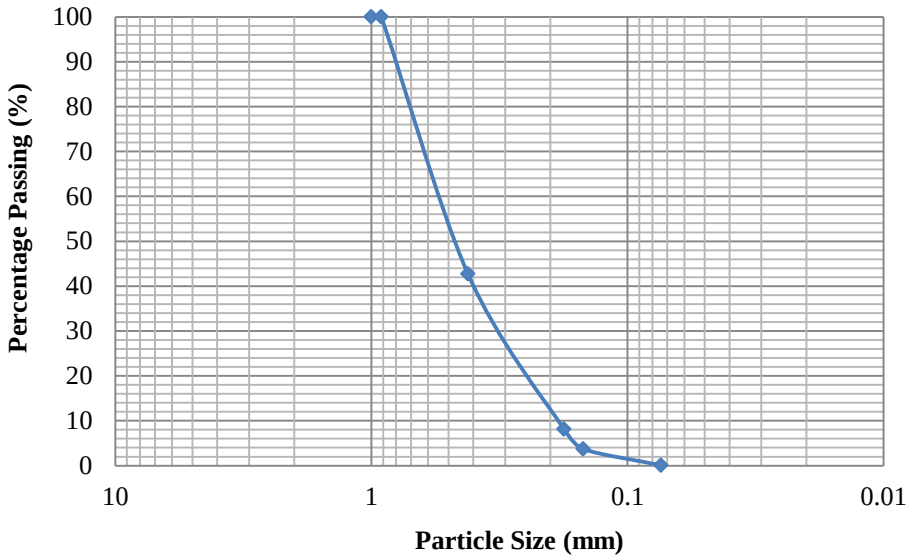

Figure 4.1. Grain size distribution of the model sand.

4.2.2. Relative Density Tests

In order to determine the relative density of the model sand (i.e., maximum and minimum relative density). About 1 kg of sand was taken randomly and then oven dried for 24 hours. According to ASTM D4253 – 16 the relative density of model sand was determined. But in order to estimate the relative densities of the model experiments, look at Chapter Three, section (3.2.). The relative density parameters of the model sand for model experiments are given in (Table 4.1.).

4.2.3. Direct Shear Tests

The traditional direct shear box testing device was used with shear box (60mm * 60mm * 20mm) to determine shear strength parameters of model sand and pile-model sand structure. The internal friction angles (φ) of the sandy soil and piles-soil interface friction angles (δ) were measured with different relative densities for three normal stress conditions (54.5, 109 and 163.5 kPa), according to ASTM D3080-72 (1989) and ASTM D5321/D5321M-14 (2014), respectively. In the current study, 0.5 mm/min is the constant shearing rate for all specimens. These shear strength parameters are necessary to estimate bearing capacity of the single-model composite piles in model sand. Shear strength parameters (φ and δ) of the model sand and sand-piles are also given in (Table 4.1.).

Table 4.1. Index properties of the model sand, and shear strength parameters of the model sand and single-model composite piles.

Relative Density, D_r %	10%	40%	65%	90%
Soil internal friction angle, φ	41.0°	44.3°	48.7°	52.4°
Soil-FRP interface friction, δ	23.7°	26.2°	28.3°	28.2°
Soil-PVC interface friction, δ	26.1°	28.7°	31.4°	30.3°
Dry unit weight, γ_{dry} (kN/m^3)	14.6	15.5	16.3	17.3
Specific gravity, G_s	2.77			
Minimum dry unit weight, $\gamma_{d.min}$, (kN/m^3)	14.30			
Maximum dry unit weight, $\gamma_{d.max}$, (kN/m^3)	17.66			
Void ratio, e	0.86	0.75	0.66	0.57
Maximum void ratio, e_{max}	0.90			
Minimum void ratio, e_{min}	0.54			
Maximum – Minimum grain size, D_{max}-D_{min} (mm)	1 - 0.074			
D10, (mm)	0.19			
D30, (mm)	0.325			
D50, (mm)	0.475			
D60, (mm)	0.55			
Coefficient of uniformity, C_u	2.9			
Coefficient of curvature, C_c	1.01			

4.2.4. Surface Roughness Tests

In fact, there are many factors that govern the interface friction behavior between soils and pile materials. Surface roughness is an important factor that has a significant effect on the interface friction behavior and has been studied by several researchers such as (Potyondy, 1961; Frost and Han, 1999; Pando et al., 2002a; Al-Mhaidib, 2006; Almallah et al., 2018). The surface roughness plays a role in improving the interlocking between pile surface and surrounding soils, a rougher pile material shows better interlocking, thus, pile settlement at failure decreases, as a result, the effect of lateral earth pressure on pile surface and coefficient of lateral earth pressure (K) is increased, which increases the pile shaft capacity (Sadrekarimi et al., 2009).

In this study, to determine the surface roughness of pile materials, the Mitutoyo SJ-201 was used for a measuring distance of 4 mm. The test results are given in (Figure 4.2.) and (Table 4.2.).

The surface roughness parameters (Ra and Ry) are estimated using the following equations:

$$\text{Ra} = \frac{1}{N}\sum_{i=1}^{N}|Y_i| \tag{4.1}$$

$$Ry = Y_p + Y_v \tag{4.2}$$

Where;

Ra = is the arithmetic mean of the absolute values of the profile deviation (Yi) of the measured distance from the mean line,

Ry = is the sum of the height of the highest peak (Yp) and the depth of the deepest valley (Yv) of the measured distance from the mean line.

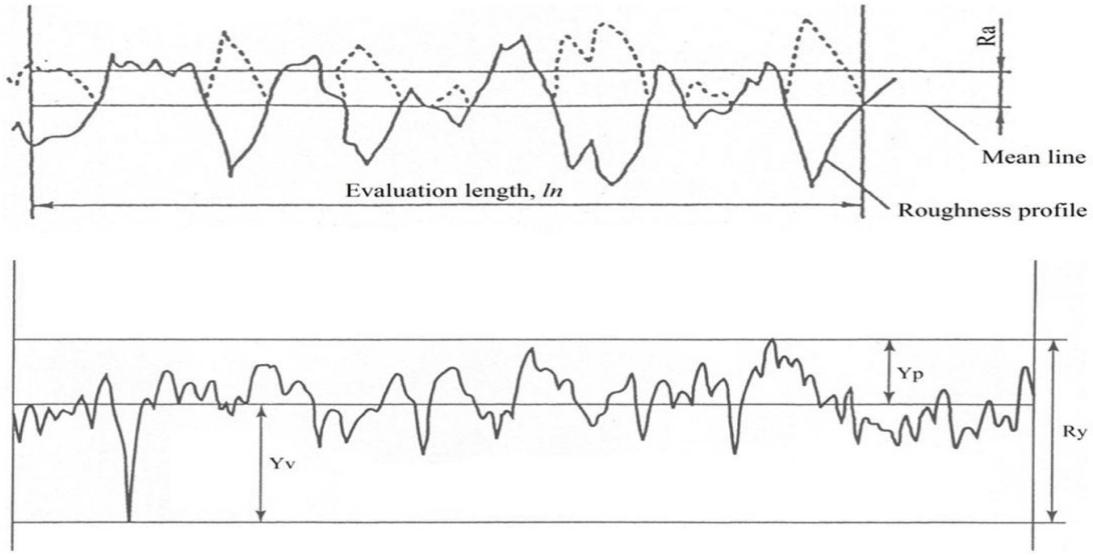

Figure 4.2. Surface roughness test graphs.

Table 4.2. Surface roughness parameters of single-model composite piles.

Model Piles	Ra (µm)	Ry (µm)
FRP Pile	1.63	8.84
PVC Pile	1.78	12.83

4.3. Load-Displacement Behaviors of Single-Model Composite Piles

Several load-displacement model experiments were performed to conduct bearing capacities (i.e., total or ultimate bearing capacity, base resistance or base capacity, and shaft capacity) of single-model composite piles at different relative densities of model sand (i.e., D_r = 10%, 40%, 65%, and 90%). The dimension parameters of composite piles are (50 mm and 600 mm) in diameter and length, respectively. Piles embedment length was 50 mm. The appropriate details for pile installation and load testing procedures were already presented in Chapter Three, see subsections (3.6.2.1 to 3.6.2.3).

Note: in this study, it has been assumed that there are two options for a pile foundation (i.e., concrete-filled FRP and PVC pipe piles) under certain conditions. Therefore, the ultimate bearing capacity, base resistance or base capacity, and shaft capacity of both single-model composite piles were chosen at the same settlement.

4.3.1. Ultimate Piles Bearing Capacity Model Experiments

A number of load-displacement model experiments were conducted to measure the ultimate bearing capacity of single-model composite piles at different relative densities of model sand (i.e., D_r = 10%, 40%, 65%, and 90%). The experimental load-displacement behaviors (i.e., p – y) of the ultimate bearing capacity of the single-model composite piles at different relative densities of model sand are shown in (Figure 4.3. to 4.6.). In addition, the experimental results of the ultimate piles bearing capacity are given in (Table 4.3.). For more details about load-displacement model experiments see (Appendix 1 and 2).

Note: The values of ultimate bearing capacity in (Table 4.3.) included the detachable shaft weight, and all (mm and kN) are represented settlement at model failures and ultimate bearing capacity of single-model composite piles, respectively.

Table 4.3. Experimental ultimate bearing capacity (Q_u, kN) results of single-model composite piles.

	Model Sand							
	D_r = 10%		D_r = 40%		D_r = 65%		D_r = 90%	
Model Piles	mm	kN	mm	kN	mm	kN	mm	kN
FRP Pile	4.95	0.287	8.1	2.128	9.55	6.201	10	12.122
PVC Pile	4.95	0.358	8.1	2.250	9.55	6.532	10	12.894

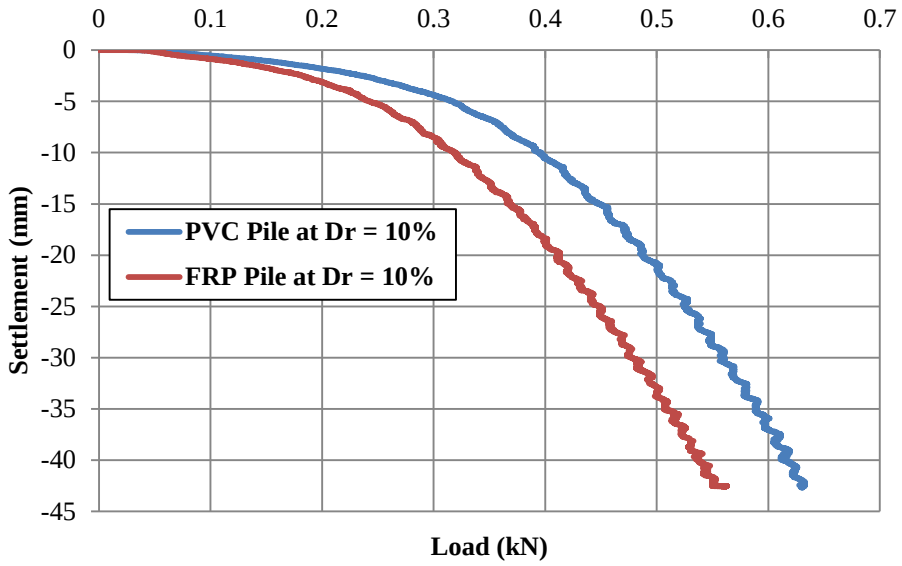

Figure 4.3. Load-displacement behavior of single-model composite piles in the ultimate bearing capacity model experiments at D_r = 10%.

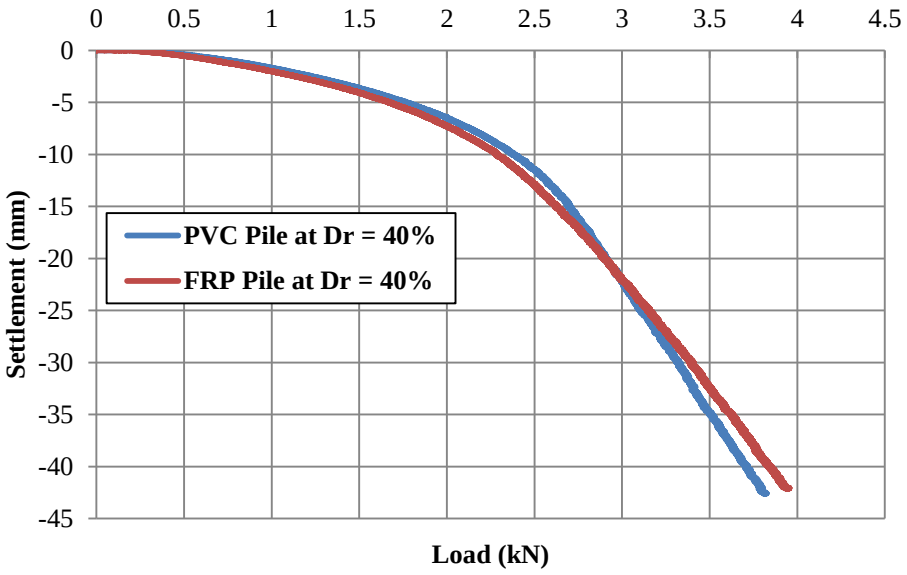

Figure 4.4. Load-displacement behavior of single-model composite piles in the ultimate bearing capacity model experiments at D_r = 40%.

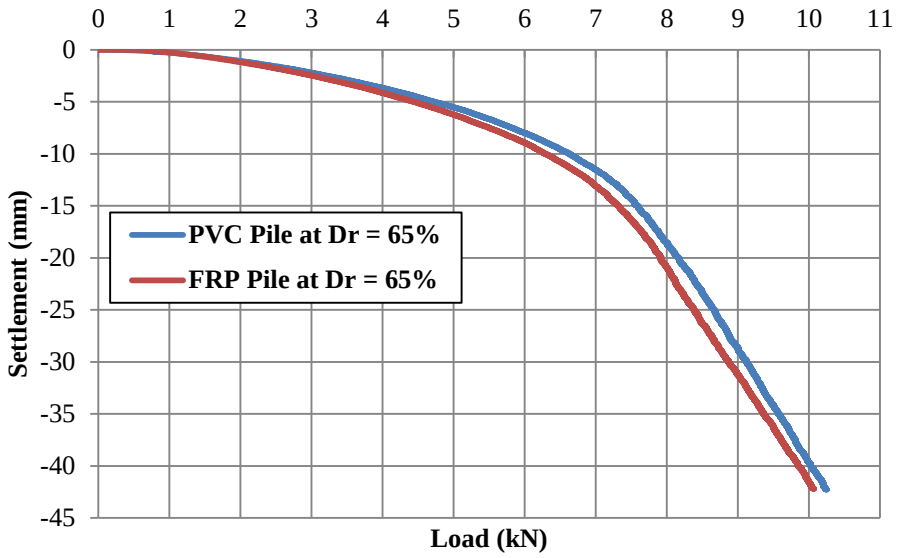

Figure 4.5. Load-displacement behavior of single-model composite piles in the ultimate bearing capacity model experiments at D_r = 65%.

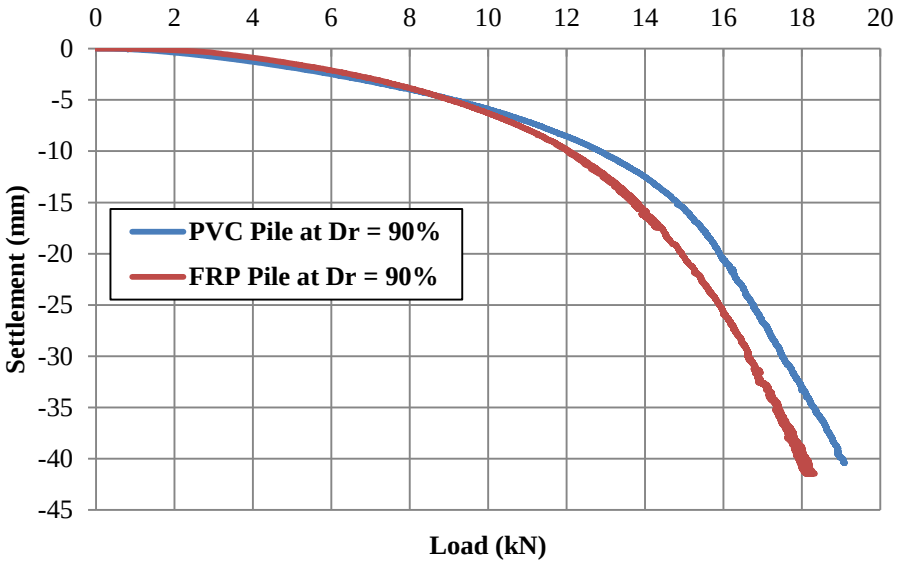

Figure 4.6. Load-displacement behavior of single-model composite piles in the ultimate bearing capacity model experiments at D_r = 90%.

4.3.2. Piles Base Capacity Model Experiments

A number of load-displacement model experiments were carried out to measure the base bearing capacity of the single-model composite piles at different relative densities of model sand (i.e., D_r = 10%, 40%, 65%, and 90%). The experimental load-displacement behaviors (i.e., p – y) of the base bearing capacity of single-model composite piles at

different relative densities of the model sand are shown in (Figure 4.7.) and are given in (Table 4.4.), for more detail see (Appendix-3).

Note: The values of piles base capacity or piles base resistance in (Table 4.4.) included the weight of the detachable shaft and single-model composite piles, and all (mm and kN) are represented settlement at model failures and base capacity of single-model composite piles, respectively.

Table 4.4. Experimental base capacity (Q_b, kN) results of single-model composite piles.

	Model Sand							
	D_r = 10%		D_r = 40%		D_r = 65%		D_r = 90%	
Model Piles	mm	kN	mm	kN	mm	kN	mm	kN
FRP and PVC Pile	4.508	0.075	3.502	0.269	3.403	0.568	3.056	0.872

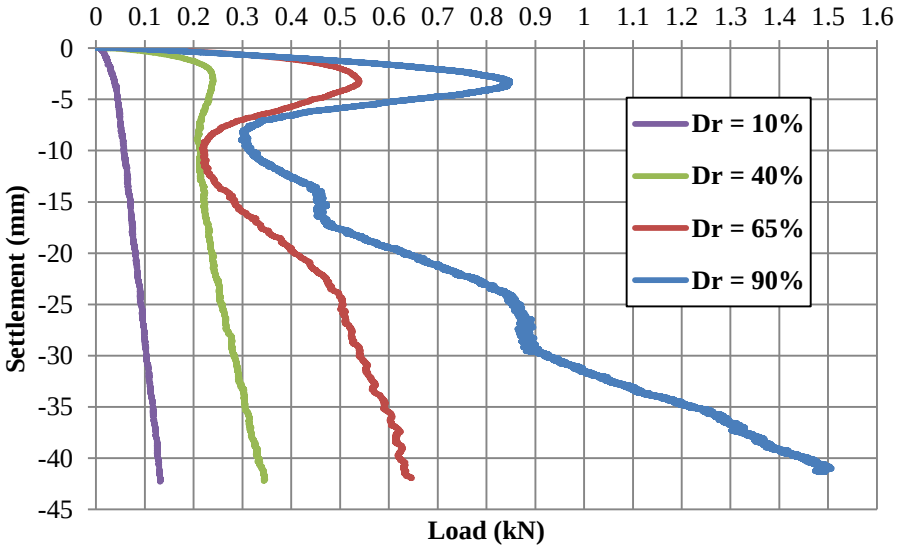

Figure 4.7. Load-displacement behavior of single-model composite piles in the base capacity model experiments.

4.3.3. Piles Shaft Capacity Model Experiments

Like ultimate piles bearing capacity and piles base capacity model experiments, several load-displacement experiments were performed to measure the independent contribution of shaft capacity or shaft friction resistance of the single-model composite

piles at different relative densities of model sand. The soil surrounding the single-model composite piles was prepared in four relative densities (D_r = 10%, 40%, 65%, and 90%), and piles shaft capacity in terms of (p – y behavior) were conducted. Prior to any shaft friction resistance loading experiments, the penetration resistance of the filter system or Styrofoam-Filter penetration resistance to the single-model composite piles was measured through penetration loading experiments in terms of (p – y) behavior. The experimental results of the shaft friction resistance or shaft capacity (note: the results are net shaft friction resistances, i.e., total shaft friction resistance (i.e., shaft friction resistance of the single model composite piles plus resistance of the filter system to penetrate them) minus the penetration resistance of the filter system for single-model composite piles) of the single model composite piles are given in (Table 4.5.).

In addition, total shaft friction resistance or total shaft capacity (i.e., pile shaft friction resistance and Styrofoam-Filter penetration resistance or filter system penetration resistance) in terms of (p – y) behavior for concrete-filled PVC and FRP pipe piles are shown in (Figure 4.8. to 4.11.). For more detail see (Appendix 4 and 5).

Note: The net shaft capacity values of single-model composite piles in (Table 4.5.) excluded the weight of the detachable shaft, and all (mm and kN) are represented settlement at model failures and shaft capacity of single-model composite piles, respectively.

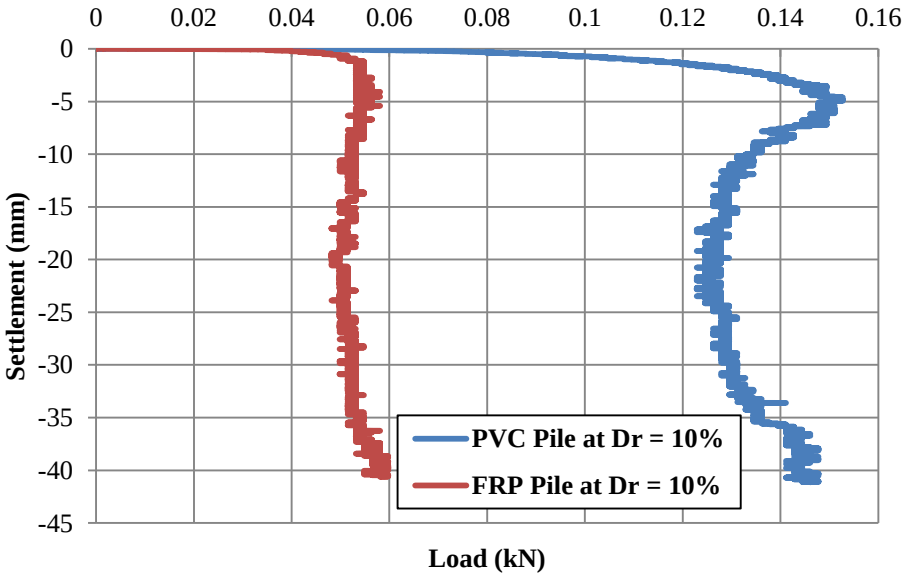

Figure 4.8. Load-displacement behavior of single-model composite piles in the total shaft capacity model experiments at D_r = 10%.

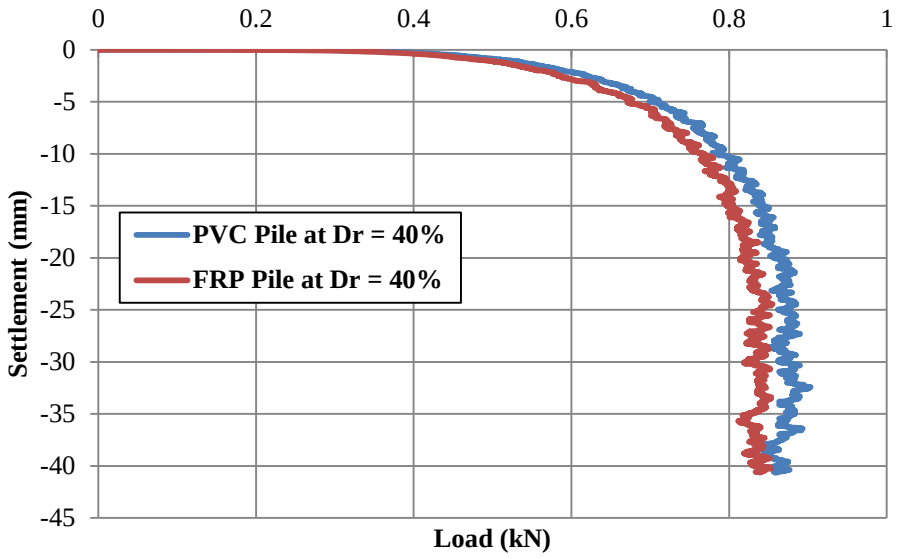

Figure 4.9. Load-displacement behavior of single-model composite piles in the total shaft capacity model experiments at D_r = 40%.

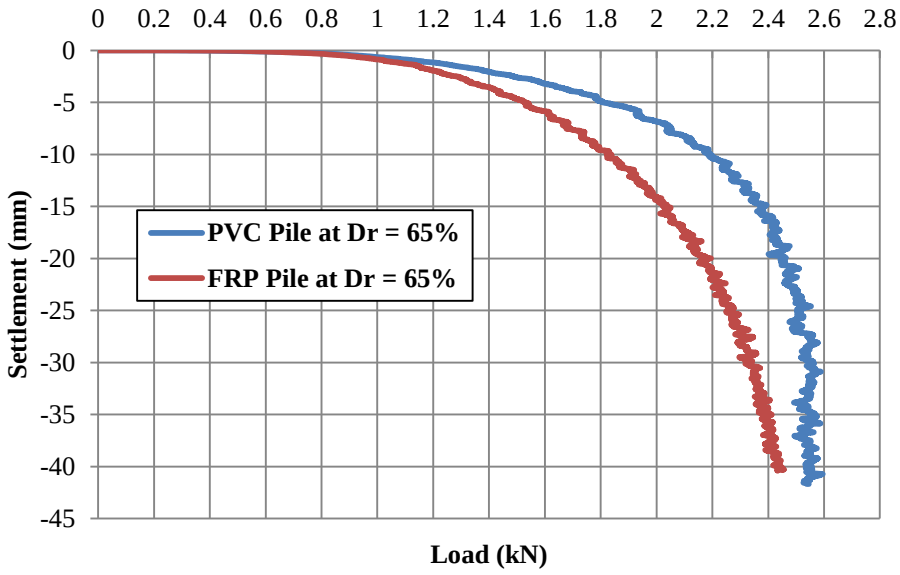

Figure 4.10. Load-displacement behavior of single-model composite piles in the total shaft capacity model experiments at D_r = 65%.

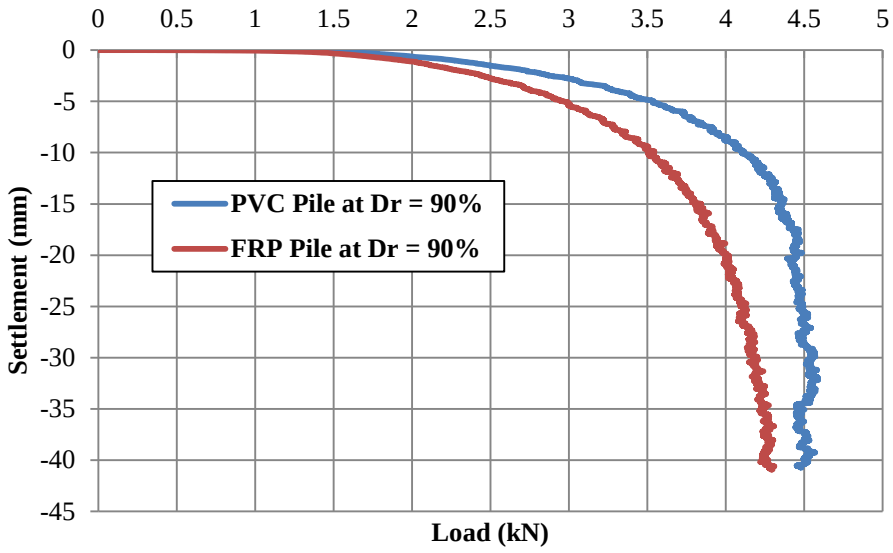

Figure 4.11. Load-displacement behavior of single-model composite piles in the total shaft capacity model experiments at D_r = 90%.

Table 4.5. Experimental shaft capacity (Q_f, kN) results of single-model composite piles.

	Model Sand							
	D_r = 10%		D_r = 40%		D_r = 65%		D_r = 90%	
Model Piles	mm	kN	mm	kN	mm	kN	mm	kN
FRP Pile	4.95	0.068	8.1	0.649	9.55	1.793	10	3.514
PVC Pile	4.95	0.090	8.1	0.777	9.55	2.144	10	4.099

4.4. Back-Calculation for Piles Shaft Capacity Parameters

In this study, the back-calculation for pile shaft capacity parameters (i.e., K and δ) is done in two ways, using Burland method (Chapter Two, subsection (2.4.3.1.), equation 2.26). First, using the measured values of interface friction angle (δ) from interface shear box test for back estimation of (K) value. Second, the K_p is used for back estimation of (δ). The back-calculated results for (K) and δ values are given in (Table 4.6. and 4.7.), and (Table 4.8. and 4.9.), respectively.

Table 4.6. Back-calculated results of pile shaft capacity parameter (K) of single-model FRP composite pile.

	FRP Model Pile					
	Settlement, m	D_f, m	γ, kN/m^3	Q_f, kN	δ^o	K
D_r = 10%	4.95 x 10^{-3}	0.50	14.60	0.068	23.7	0.53 ≅ 0.50
D_r = 40%	8.10 x 10^{-3}	0.50	15.50	0.649	26.2	4.19 ≅ 4.0
D_r = 65%	9.55 x 10^{-3}	0.50	16.30	1.793	28.3	10.01 ≅ 10.0
D_r = 90%	10 x 10^{-3}	0.50	17.30	3.514	28.2	18.54 ≅ 18.50

Table 4.7. Back-calculated results of pile shaft capacity parameter (K) of single-model PVC composite pile.

	PVC Model Pile					
	Settlement, m	D_f, m	γ, kN/m^3	Q_f, kN	δ^o	K
D_r = 10%	4.95 x 10^{-3}	0.50	14.60	0.090	26.1	0.63 ≅ 0.60
D_r = 40%	8.10 x 10^{-3}	0.50	15.50	0.777	28.7	4.51 ≅ 4.50
D_r = 65%	9.55 x 10^{-3}	0.50	16.30	2.144	31.4	10.56 ≅ 10.50
D_r = 90%	10 x 10^{-3}	0.50	17.30	4.099	30.3	19.84 ≅ 19.80

Table 4.8. Back-calculated results of pile shaft capacity parameter (δ) of single-model FRP composite pile.

	FRP Model Pile					
	Settlement, m	D_f, m	γ, kN/m^3	Q_f, kN	K_p	δ^o
D_r = 10%	4.95 x 10^{-3}	0.50	14.60	0.068	4.815	2.76 ≅ 3.0
D_r = 40%	8.10 x 10^{-3}	0.50	15.50	0.649	5.632	21.13 ≅ 21.0
D_r = 65%	9.55 x 10^{-3}	0.50	16.30	1.793	7.041	37.45 ≅ 37.5
D_r = 90%	10 x 10^{-3}	0.50	17.30	3.514	8.629	49.04 ≅ 49.0

Table 4.9. Back-calculated results of pile shaft capacity parameter (δ) of single-model PVC composite pile.

	PVC Model Pile					
	Settlement, m	D_f, m	γ, kN/m^3	Q_f, kN	K_p	δ^o
D_r = 10%	4.95 x 10^{-3}	0.50	14.60	0.090	4.815	3.66 ≅ 4.0
D_r = 40%	8.10 x 10^{-3}	0.50	15.50	0.777	5.632	23.69 ≅ 23.50
D_r = 65%	9.55 x 10^{-3}	0.50	16.30	2.144	7.041	42.48 ≅ 42.50
D_r = 90%	10 x 10^{-3}	0.50	17.30	4.099	8.629	53.34 ≅ 53.50

In addition, the interface friction angles measured from the interface shear box test (ISB) and estimated from the back-calculation (BC) using the model experiment failures are shown in (Figure 4.12) as a function of relative density.

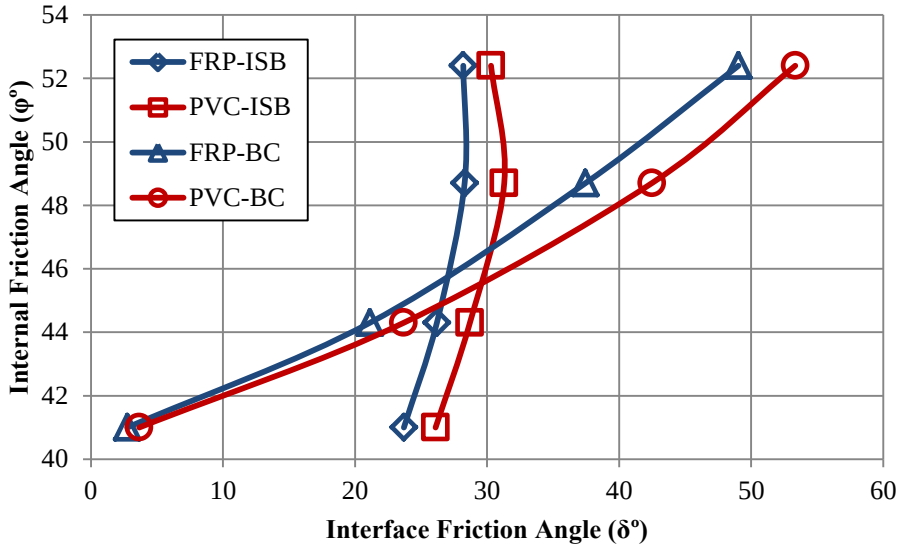

Figure 4.12. Interface friction angle measured from ISB and estimated from BC versus relative density.

5. RESULTS AND DISCUSSION

5.1. Experimental Results

5.1.1. Direct Shear Test and Surface Roughness Test Results

The experimental results of direct shear box tests and interface shear box tests (i.e., internal friction angles and interface friction angles) are given in (Table 5.1.) and are shown in (Figure 5.1. and 5.2.). The internal friction angle (φ) of the model sand is increased with the increase of the relative density, and the variation of the internal friction angle with the relative density is linear behavior from D_r = 10% to D_r = 40%, and from D_r = 40% to D_r = 90% has become a non-linear behavior. But the piles-sand interface friction angle (δ) is increased with an increase in relative density up to D_r = 65% and reaches its optimum value. Then at D_r = 90% it remains constant or decreases slightly, and their behavior is a semi-linear relationship.

Table 5.1. Shear strength parameters of model sand and single-model composite piles.

	D_r = 10%	D_r = 40%	D_r = 65%	D_r = 90%
Model Sand, φº	41	44.3	48.7	52.4
FRP Model Pile, δº	23.7	26.2	28.3	28.2
PVC Model Pile, δº	26.1	28.7	31.4	30.3

In addition, the measured surface roughness parameters (Ra and Ry) of single-model composite piles are given in (Table 5.2.). However, the original surface roughness of the FRP single-model composite pile is greater than that of the PVC single-model composite pile and the PVC single-model composite pile is a soft material compared to FRP single-model composite pile. But in order to consider the effect of the driven process on piles surface behavior, and to simulate the single-model piles to the actually installed piles in the field, the surface roughness tests were performed after performing load-displacement model experiments. This is why the PVC single-pile composite pile has shown a higher surface roughness than FRP single-model composite pile.

Table 5.2. Surface roughness parameters of single-model composite piles.

Model Piles	Ra (μm)	Ry (μm)
FRP Pile	1.63	8.84
PVC Pile	1.78	12.83

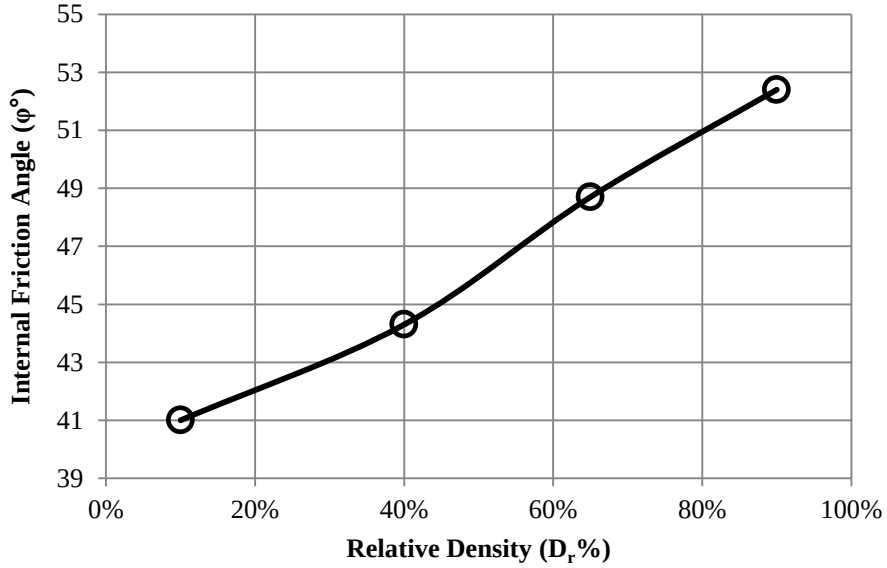

Figure 5.1. Variation of internal friction angle with relative density.

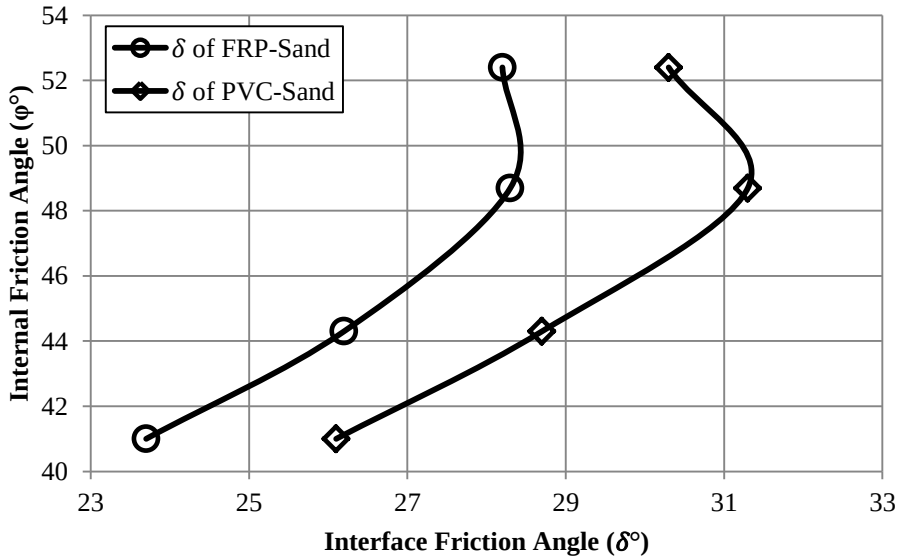

Figure 5.2. Variation of piles-sand interface friction angle with relative density.

5.1.2. Model Experiments

5.1.2.1. Ultimate Piles Bearing Capacity

The model experiment results were obtained from a number of single-model composite piles axial loading experiments are shown in (Figures 5.3 and 5.4) and are given in (Table 5.3.). The test results showed that the ultimate bearing capacity of single-model composite piles is increased with increasing relative density and its behavior is a non-linear relationship. In addition, piles settlement is also increased with increasing relative density in a non-linear relationship, but its behavior contrary to the ultimate bearing capacity.

Moreover, at the beginning of the ultimate bearing capacity experiments, the piles displacement was stopped for a period while the load was recorded for a quantity. This is attributed to the pile shaft behavior, because there was no soil disturbance around the pile, as a result, a quantity of load was required to develop a relative displacement between the surrounding soil and the pile interface under certain conditions.

Note: The ultimate bearing capacity of single-model composite piles in (Table 5.3.) included the detachable shaft weight. In addition, all (mm and kN) are represented settlement at model failures and ultimate bearing capacity of single-model composite piles, respectively.

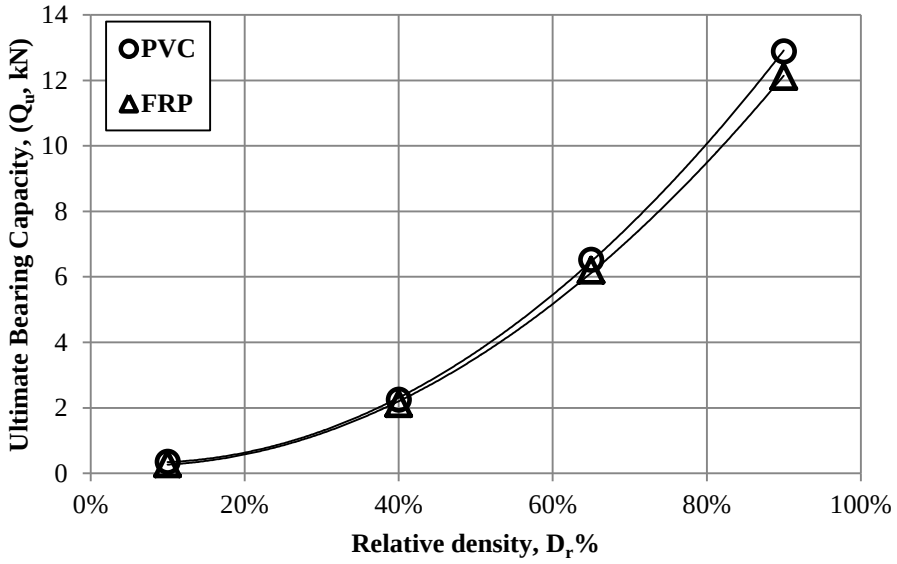

Figure 5.3. Ultimate bearing capacity-relative density behavior of single-model composite piles in model experiments.

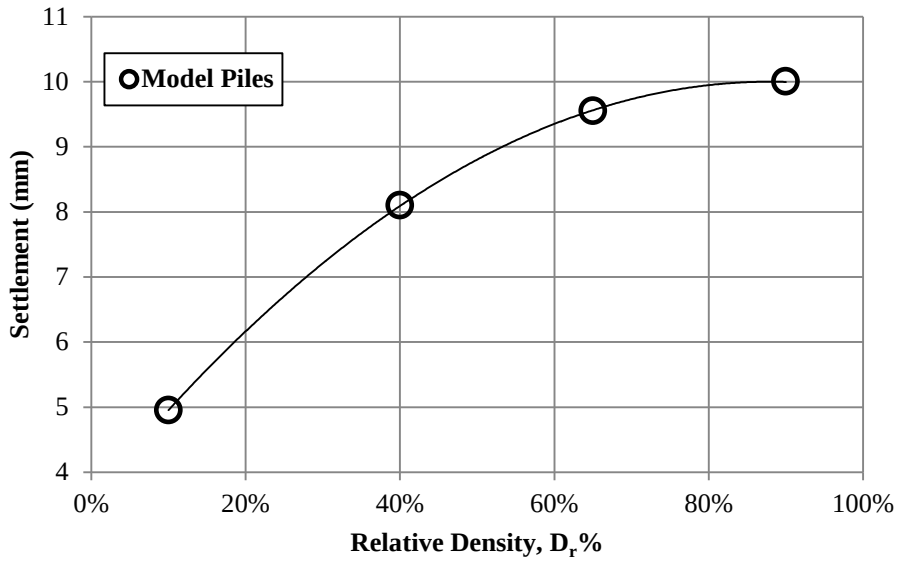

Figure 5.4. Displacement-relative density behavior of single-model composite piles in the ultimate bearing capacity model experiments.

Table 5.3. Ultimate bearing capacity (Q_u, kN) of single-model composite piles measured from model experiments.

	D_r = 10%		D_r = 40%		D_r = 65%		D_r = 90%	
Model Piles	mm	kN	mm	kN	mm	kN	mm	kN
FRP Pile	4.95	0.287	8.10	2.128	9.55	6.201	10	12.122
PVC Pile	4.95	0.358	8.10	2.250	9.55	6.532	10	12.894

5.1.2.2. Piles Base Capacity

The results were obtained from single-model base bearing capacity experiments are shown in (Figure 5.5. and 5.6.), and are also given in (Table 5.4.). As with ultimate bearing capacity, the piles base bearing capacity is also increased with increasing relative density in a non-linear relationship. But piles displacement (i.e., settlement) is decreased with increasing relative density in a non-linear relationship.

Note: The base capacity of single-model composite piles in (Table 5.4.) included the detachable shaft weight. In addition, both piles have the same weight and same base behavior, so base capacity of them taken the same. Although, all (mm and kN) are represented settlement at model failures and base capacity of single-model composite piles, respectively.

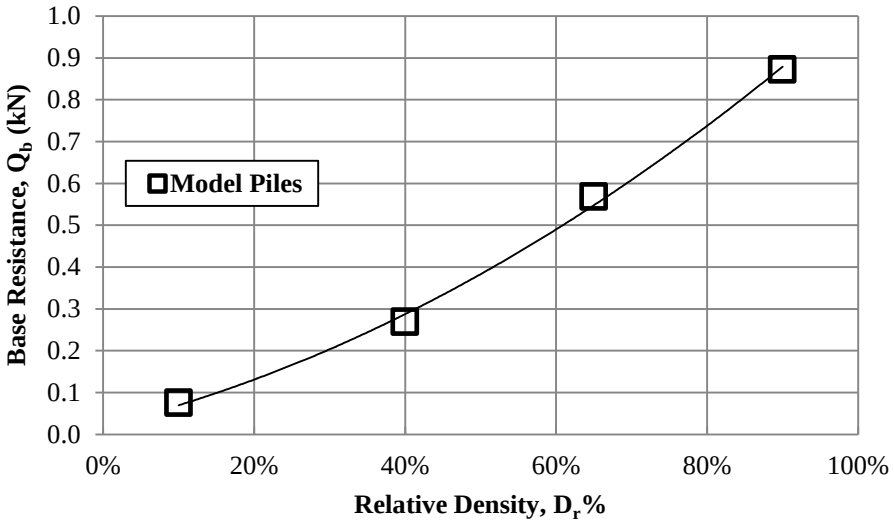

Figure 5.5. Base capacity-relative density behavior of single-model composite piles in model experiments.

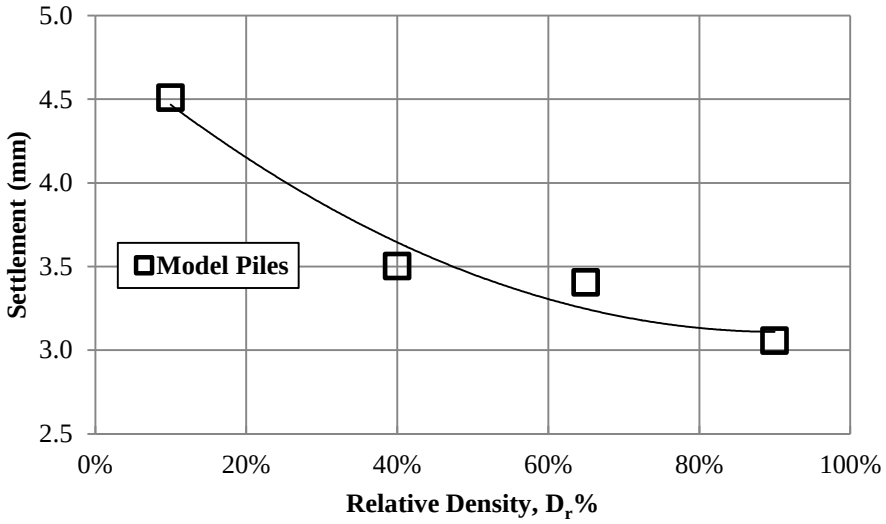

Figure 5.6. Displacement-relative density behavior of single-model composite piles in the base capacity model experiments.

Table 5.4. Base capacity (Q_b, kN) of single-model composite piles measured from model experiments.

	D_r = 10%		D_r = 40%		D_r = 65%		D_r = 90%	
Model Piles	mm	kN	mm	kN	mm	kN	mm	kN
	4.508	0.075	3.502	0.269	3.403	0.568	3.056	0.872

5.1.2.3. Piles Shaft Capacity

The results obtained from the model experiments of the piles shaft capacity or piles shaft friction resistance are given in (Table 5.5.) and are shown in (Figure 5.7. and 5.8.). The test results most likely appeared with the same behavior as it was already observed in ultimate bearing capacity experiments, and the friction behavior in the model experiments is quite different from that of the interface shear box test. Furthermore, piles shaft capacity is increased with an increase of the relative density in a non-linear relationship. In addition, piles displacement (i.e., settlement) at failure is increased with an increase of the relative density in a non-linear relationship.

Although, at the beginning of the independent contribution of the pile shaft capacity experiments, due to the pile shaft behavior, the same behavior roughly with the same amount was observed and already explained in the ultimate bearing capacity experiments, where the pile displacement was stopped for a period, while the load was recorded for a quantity. This is attributed to the non-disturbance of the soil around the pile, so that a quantity of load was required to develop a relative movement between the surrounding soil and the pile interface under certain conditions.

Note: The shaft capacity of single-model composite piles in (Table 5.5.) is the net shaft capacity (i.e., total shaft capacity minus Styrofoam-Filter penetration or filter system penetration resistance) and excluded the detachable shaft weight. In addition, all (mm and kN) are represented settlement at model failures and shaft capacity of single-model composite piles, respectively.

Table 5.5. Net shaft capacity (Q_f, kN) of single-model composite piles measured from model experiments.

	D_r = 10%		D_r = 40%		D_r = 65%		D_r = 90%	
Model Piles	mm	kN	mm	kN	mm	kN	mm	kN
FRP	4.95	0.068	8.10	0.649	9.55	1.793	10.00	3.514
PVC	4.95	0.090	8.10	0.777	9.55	2.144	10.00	4.099

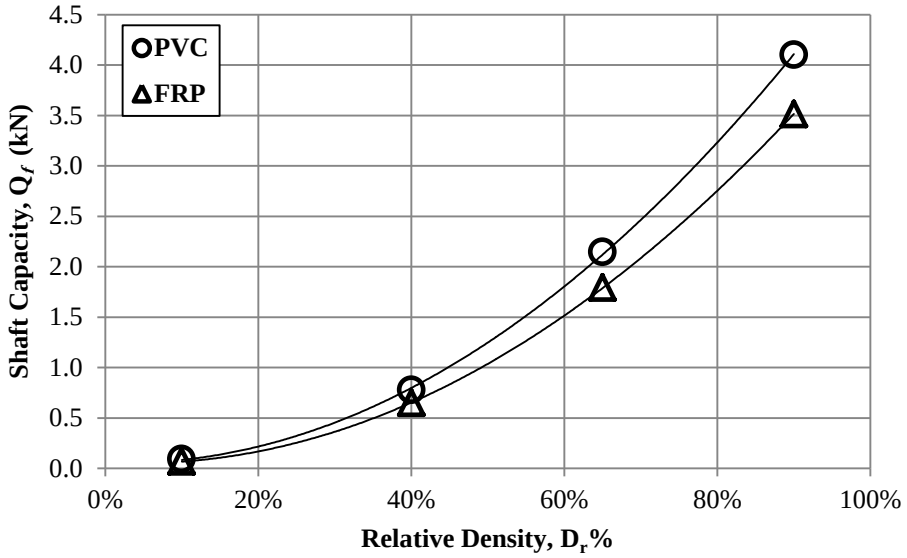

Figure 5.7. Shaft capacity-relative density behavior of single-model composite piles in model experiments.

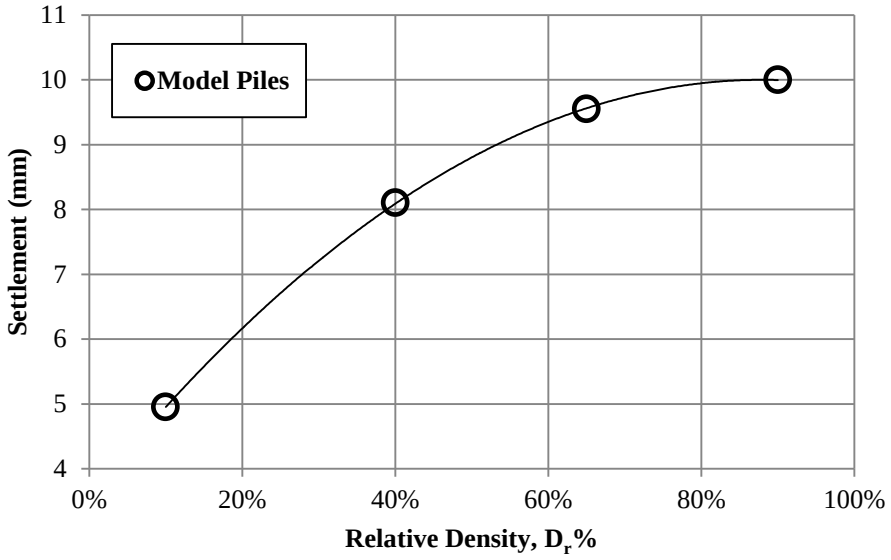

Figure 5.8. Displacement-relative density behavior of single-model composite piles in the shaft capacity model experiments.

5.2. Theoretical Results

5.2.1. Piles Base Capacity

In the current study, the base bearing capacity (Q_b) of single-model composite piles was assessed using the Terzaghi (1943), Meyerhof (1963) and Hansen (1970) method. The theoretical results of the piles base capacity are given in (Table 5.6.).

Note: Because both single-model composite piles have the same diameter and length, as well as, have about the same weight, their theoretical base capacity or base resistance was taken the same as it was also taken into account in the model experiments.

Table 5.6. Theoretical base capacity (Q_b, kN) results of single-model composite piles.

FRP & PVC Piles	Terzaghi (1943)	Meyerhof (1963)	Hansen (1970)
D_r = 10%	0.05	0.39	0.041
D_r = 40%	0.12	0.913	0.081
D_r = 65%	0.426	3.152	0.207
D_r = 90%	1.003	10.749	0.510

5.2.2. Piles Point Capacity

In this study, Terzaghi (1943), Meyerhof (1976), Coyle & Castello (1981), Janbu (1976) and Hansen (1970) were used to estimate the point capacity or end-bearing capacity (Q_p) of single-model composite piles at different relative density of model sand. The theoretical results of (Q_p) for single-model composite piles are given in (Table 5.7.).

Note: Because both single-model composite piles have the same diameter, length, and the same embedment length, as well as, have about the same weight, their theoretical point capacity or end-bearing capacity was taken the same.

Table 5.7. Theoretical point capacity (Q_p, kN) results of single-model composite piles.

Model Piles	Terzaghi (1943)	Meyerhof (1976)	Coyle & Castello (1981)	Janbu (1976)	Hansen (1970)
D_r = 10%	1.56	6.023	1.58	0.579	2.339
D_r = 40%	2.506	12.483	2.416	1.070	4.042
D_r = 65%	5.038	26.735	3.888	2.719	8.779
D_r = 90%	9.385	40.269	5.866	8.718	18.748

5.2.3. Piles Shaft Capacity

In order to predict shaft capacity of single-model composite piles, the interface friction angles measured from interface shear box test were used with different

considerations of coefficient of lateral earth pressure (K). The theoretical shaft capacity (Q_f) results of single-model composite piles are given in (Table 5.8. and 5.9.).

Table 5.8. Theoretical shaft capacity (Q_f, kN) results of single-model FRP composite pile.

FRP Pile – Pile Shaft capacity				
Model Sand	Q_f, ($K = K_o$)	Q_f, ($K = 1.4\ K_o$)	Q_f, (Coyle and Castello's K)	Q_f, ($K = K_p$)
D_r = 10%	0.043	0.061	0.942	0.608
D_r = 40%	0.045	0.063	1.782	0.846
D_r = 65%	0.043	0.06	3.365	1.218
D_r = 90%	0.038	0.053	5.006	1.578

Table 5.9. Theoretical shaft capacity (Q_f, kN) results of single-model PVC composite pile.

PVC Pile – Pile Shaft capacity				
Model Sand	Q_f, ($K = K_o$)	Q_f, ($K = 1.4\ K_o$)	Q_f, (Coyle and Castello's K)	Q_f, ($K = K_p$)
D_r = 10%	0.048	0.068	1.051	0.678
D_r = 40%	0.050	0.070	1.983	0.942
D_r = 65%	0.048	0.068	3.80	1.375
D_r = 90%	0.041	0.058	5.456	1.720

5.3. Comparison of Experimental and Theoretical Results

In this Chapter, the calculated theoretical results of single-model composite piles are compared to model load tests. All comparative results related to experimental modeling were already presented and discussed in Chapter Five, subsection (5.1.2.). The comparison is done by plotting both the theoretical and experimental results in one graph for each relative density, as well as the comparison is also presented in Tables.

5.3.1. Piles Base Capacity

The comparison of the theoretical and experimental results for the piles base capacity is given both in (Figure 5.9.) and in (Table 5.10.). However, pile base capacity was estimated based on Terzaghi (1943), Meyerhof (1963) and Hansen (1970). But due to the

significant difference between the experimental results and those of Meyerhof (1963) , the comparison graph (Figure 5.9.) only included experimental results with Terzaghi (1943) and Hansen (1970).

Note: All results in the comparative (Figure 5.9.) and (Table 5.10.) related to the experimental included the detachable shaft weight.

From the comparative (Figure 5.9.) and (Table 5.10.), it can be seen that the results of the Meyerhof method are out of the discussion, while Hansen method provides very conservative values. However, the Terzaghi (1943) method is well known for providing conservative values, but in this study, the Terzaghi method given values very close to the experimental results of the other three. Although at D_r = 90%, Terzaghi method provided higher value, while in the other three D_r = 10, D_r = 40%, and D_r = 65%, the lower values were found. These differences that were found in all the methods are due to the difference in the parameters taken into account by them in the estimation of the value of Nγ.

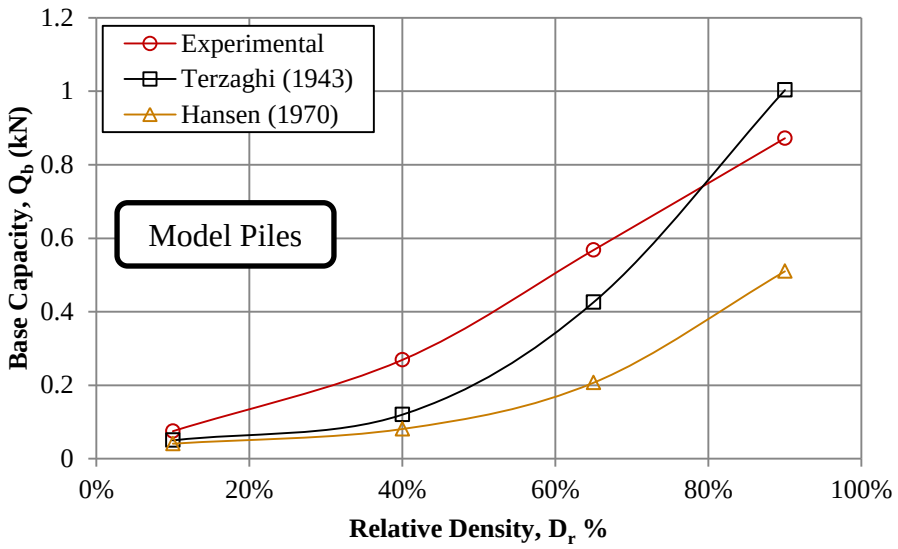

Figure 5.9. Comparison between theoretical and experimental base capacity (Q_b, kN) of single-model composite piles.

5.3.2. Piles Point Capacity

However, as explained before in this Chapter, subsection (5.3.1.), Terzaghi (1943), Meyerhof (1976), Coyle and Castello (1981), Janbu (1976), Hansen (1970) were used to estimate piles point capacity or piles end-bearing capacity. But due to the big difference, the comparison graphs (Figure 5.10. and 5.11.) only included experimental results with

Terzaghi (1943), Coyle and Castello (1981), and Janbu (1976), the other two are excluded. The comparisons of the theoretical and experimental results for the piles point capacity are given both in (Figure 5.10. and 5.11.) and (Table 5.11. and 5.12.).

Table 5.10. Comparison between theoretical and experimental base capacity (Q_b, kN) of single-model composite piles.

FRP & PVC Piles	Experimental, (Q_b, kN)	Terzaghi (1943)	Difference	Meyerhof (1963)	Difference	Hansen (1970)	Difference
D_r = 10%	0.075	0.05	-33%	0.39	+420%	0.041	-45%
D_r = 40%	0.269	0.12	-55%	0.913	+239%	0.081	-70%
D_r = 65%	0.568	0.426	-25%	3.152	+455%	0.207	-64%
D_r = 90%	0.872	1.003	+15%	10.749	+1133%	0.510	-42%

Note: The experimental results of the piles point capacity in the comparative (Figure 5.10. and 5.11.) and (Table 5.11. and 5.12.) were determined by subtracting the experimental pile shaft capacity from the experimental ultimate bearing capacity. In addition, all results in the comparative (Figure 5.10. and 5.11.) and (Table 5.11. and 5.12.) related to the experimental included the detachable shaft weight.

From the comparative (Figure 5.10. and 5.11.) and (Table 5.11. and 5.12.) it can been that there is a big difference between the results of Terzaghi and Experimental for D_r = 10% and 40%, the differences being negligible at D_r = 65% and 90%. In addition, the Coyle and Castello method was given higher results in the case where D_r = 10% and 40%, while it provided lower values where D_r = 65% and 90%. In Janbu method where D_r = 10%, higher values were obtained, while it provided roughly the same values at D_r = 90%, and provided lower values where D_r = 40 and 65%, these behaviors were not observed in others. As already explained, the methods of Meyerhof and Hansen provided very different results. Finally, in Janbu method, it can be concluded that if the surface angle (η) of the soil is chosen more precisely, the nearest value can be found for a case like this study. But because it is not easy to estimate the surface angle (η) accurately that really exist. So it can be concluded that the Terzaghi method provided the closest value for such a case, as in this study, compared to the others.

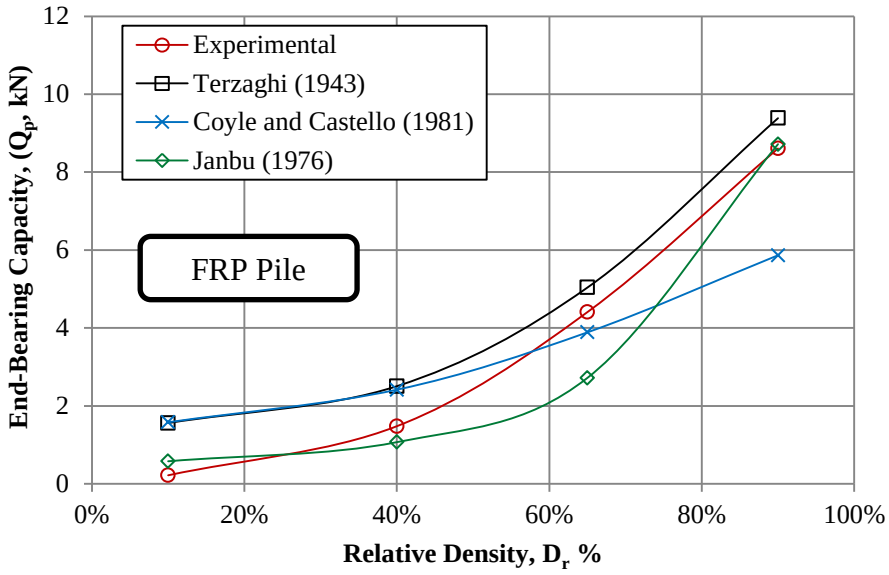

Figure 5.10. Comparison between theoretical and experimental point capacity (Q_p, kN) of single-model FRP composite pile.

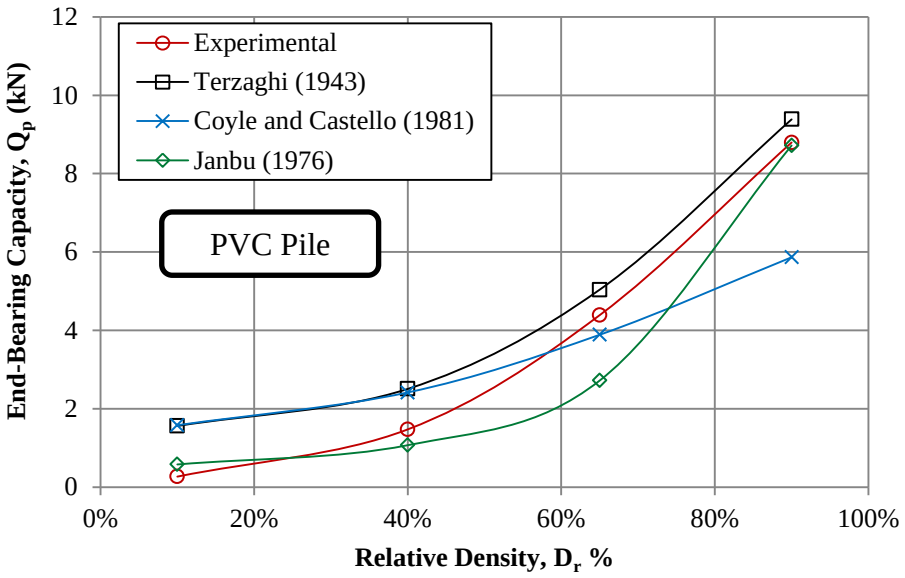

Figure 5.11. Comparison between theoretical and experimental point capacity (Q_p, kN) of single-model PVC composite pile.

5.3.3. Piles Shaft Capacity

In this study, in order to estimate the pile shaft capacity theoretically, several considerations of coefficient of lateral earth pressure (K) were considered. The first is the Coyle and Castello' K, and the others are K_o, $1.4K_o$ and K_p, and using the interface friction angle (δ) values were estimated from the interface shear box test.

Table 5.11. Comparison between theoretical and experimental point capacity (Q_p, kN) of single-model FRP composite pile.

FRP Pile	Experimental	Terzaghi (1943)	Difference %	Meyerhof (1976)	Difference %	Coyle and Castello (1981)	Difference %	Janbu (1976)	Difference %	Hansen (1970)	Difference %
D_r = 10%	0.219	1.56	+612	6.023	+2650	1.58	+621	0.579	+164	2.339	+968
D_r = 40%	1.479	2.506	+69	12.483	+744	2.416	+63	1.107	-28	4.042	+173
D_r = 65%	4.408	5.038	+14	26.735	+507	3.888	-12	2.719	-38	8.779	+99
D_r = 90%	8.608	9.385	+9	40.269	+368	5.866	-32	8.718	+1	18.748	+118

Table 5.12. Comparison between theoretical and experimental point capacity (Q_p, kN) of single-model PVC composite pile.

PVC Pile	Experimental	Terzaghi (1943)	Difference %	Meyerhof (1976)	Difference %	Coyle and Castello (1981)	Difference %	Janbu (1976)	Difference %	Hansen (1970)	Difference %
D_r = 10%	0.268	1.56	+482	6.023	+2147	1.58	+490	0.579	+116	2.339	+773
D_r = 40%	1.473	2.506	+70	12.483	+747	2.416	+64	1.107	-27	4.042	+174
D_r = 65%	4.388	5.038	+15	26.735	+509	3.888	-11	2.719	-38	8.779	+100
D_r = 90%	8.795	9.385	+7	40.269	+358	5.866	-33	8.718	-1	18.748	+113

5.3.3.1. Burland (1973)

In the Burland method, the estimated (δ) values from the interface shear box test were used, as well as the Coyle and Castello's K, K_o, $1.4K_o$ and K_p, were included in the calculation. The theoretical calculated results of pile shaft capacity for the different considerations of (K) versus measured values of pile shaft capacity are shown in (Figure 5.12. and 5.13.), and are given in (Table 5.13. and 5.14.).

Note: due to the big difference, the comparison graph (Figure 5.12 and 5.13) only included experimental results with Coyle and Castello's K (1981) and K_p the other two (K_o and 1.4 K_o) are excluded. In addition, the experimental results of the pile shaft capacity in the table (5.13. and 5.14.) are the net shaft friction capacity or net shaft capacity (i.e., total shaft friction capacity minus Styrofoam-Filter penetration resistance or filter system penetration resistance), as well as the weight of the detachable shaft were excluded.

Among all the results calculated with the different consideration of the (K) value. It can be concluded that there is no reliable result in each method, because of the complexity of the pile shaft behavior. This is attributed to presenting high levels of uncertainty in the estimation of pile shaft capacity, which depends on K and δ, and it is not easy to estimate these parameters accurately. However, K changes with the soil depth but several values of K have been presented by many researchers but it still remains controversial. In addition, the interface friction angle (δ) is measured using the interface shear box test, while its interface behavior and failure mechanism are quite different from those of the pile.

In general, if we use (δ) that measured using the interface shear box test as a constant with respect to the (K) values, it can be concluded that all the methods give very different values of pile shaft capacity, with the exception of the friction behavior of the Coyle and Castello's K, which have the same behavior as that observed in the model experiments, but with higher values. The behavior is that the pile shaft capacity increases with increasing internal friction angle or relative density.

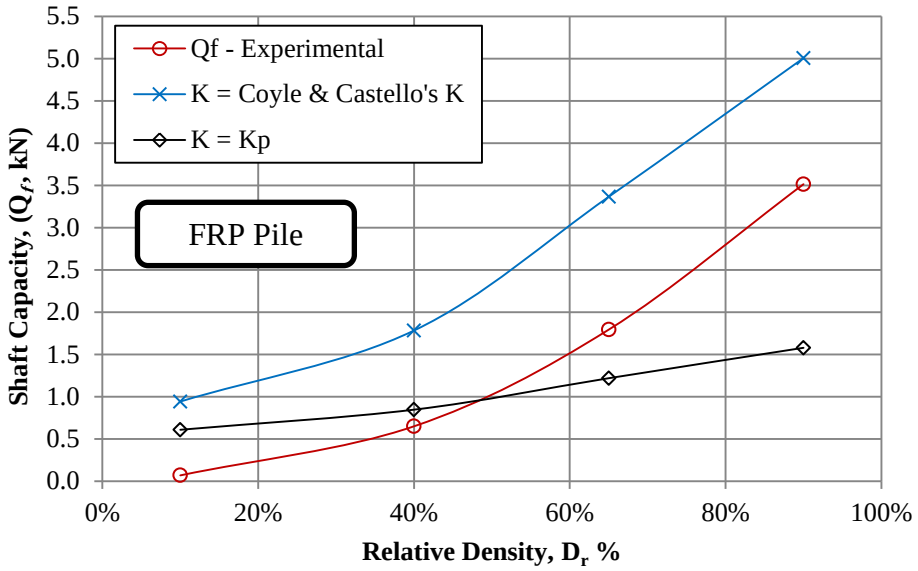

Figure 5.12. Comparison between theoretical and experimental shaft capacity (Q_f, kN) of single-model FRP composite pile.

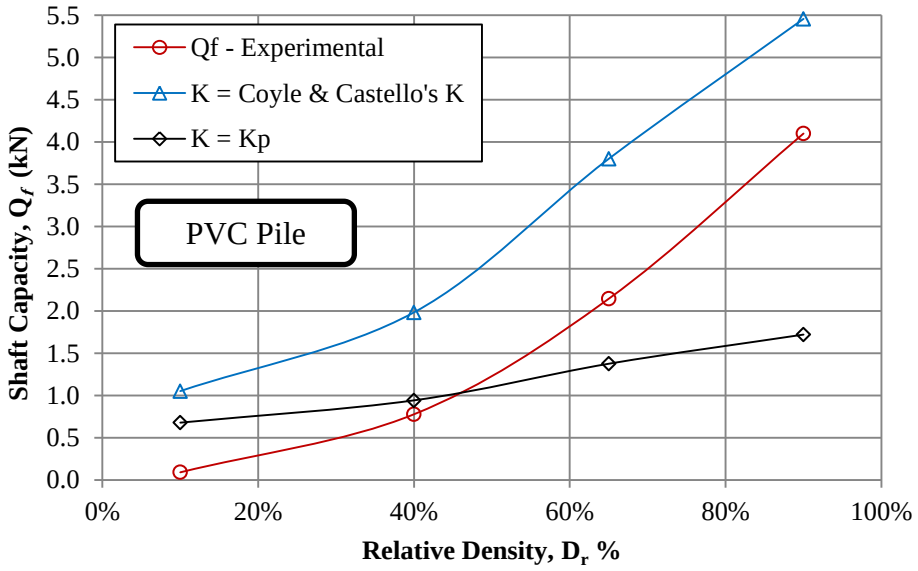

Figure 5.13. Comparison between theoretical and experimental shaft capacity (Q_f, kN) of single-model PVC composite pile.

Table 5.13. Comparison between theoretical and experimental shaft capacity (Q_f, kN) of single-model FRP composite pile.

FRP Pile	Q_f, Experimental	Q_f, K_o	Difference %	Q_f, 1.4 K_o	Difference %	Q_f, Coyle and Castello's K (1981)	Difference %	Q_f, K_p	Difference %
D_r = 10%	0.068	0.043	-37	0.061	-10	0.942	+1285	0.608	+794
D_r = 40%	0.649	0.045	-93	0.063	-90	1.782	+175	0.846	+30
D_r = 65%	1.793	0.043	-98	0.060	-97	3.365	+88	1.218	-32
D_r = 90%	3.514	0.038	-99	0.053	-99	5.006	+42	1.578	-55

Table 5.14. Comparison between theoretical and experimental shaft capacity (Q_f, kN) of single-model PVC composite pile.

PVC Pile	Q_f, Experimental	Q_f, K_o	Difference %	Q_f, 1.4 K_o	Difference %	Q_f, Coyle and Castello's K (1981)	Difference %	Q_f, K_p	Difference %
D_r = 10%	0.090	0.048	-47	0.068	-24	1.051	+1068	0.678	+653
D_r = 40%	0.777	0.050	-94	0.070	-91	1.983	+155	0.942	+21
D_r = 65%	2.144	0.048	-98	0.068	-97	3.800	+77	1.375	-36
D_r = 90%	4.099	0.041	-99	0.058	-99	5.456	+33	1.720	-58

5.4. Correlation of Piles Shaft Capacity

In general, there is no correlation between pile base and pile point capacity for such a case as in this study. In addition, there is also no reliable method for pile shaft capacity that gives values close to the experimental, with the exception of Coyle and Castello's K results, which provided higher values compared to the experimental, but with the same behavior as observed in model experiments where pile shaft capacity increases with increasing relative density or internal friction angle in a non-linear relationship. For that reason to find a correlation for pile shaft capacity. If the results of Coyle and Castello's K be multiplied by a factor, a close value can be reached. For example, in a case as under the same conditions of this study, if the results of this method be multiplied by a factor such that (Tanh D_r) and ($\mathrm{Sin}D_r \frac{180}{\pi}$) for FRP and PVC pile, respectively, an acceptable values can be obtained which is approximately equal to the measured values. The new values of pile shaft capacity obtained from the correlation between the Coyle and Castello's K with the experimental results are given in (Table 5.15. and 5.16.).

Table 5.15. Experimental and correlated shaft capacity results (Q_f, kN) of single-model FRP composite pile.

FRP Pile	Experimental	Coyle and Castello's K (1981)	Factor, Tanh D_r	New Values	Diffrence, %
D_r = 0.10	0.068	0.942	0.100	0.094	+38
D_r = 0.40	0.649	1.782	0.380	0.677	+4
D_r = 0.65	1.793	3.365	0.572	1.925	+7
D_r = 0.90	3.514	5.006	0.716	3.584	+2

Table 5.16. Experimental and correlated shaft capacity results (Q_f, kN) of single-model PVC composite pile.

PVC Pile	Experimental	Coyle and Castello's K (1981)	Factor, Sin $D_r \frac{180}{\pi}$	New Values	Diffrence, %
D_r = 0.10	0.090	1.051	0.100	0.105	+17
D_r = 0.40	0.777	1.983	0.390	0.773	-0.50
D_r = 0.65	2.144	3.800	0.605	2.300	+7
D_r = 0.90	4.099	5.456	0.783	4.272	+4

6. FINITE ELEMENT ANALYSIS

6.1. Introduction

While conventional pile design methods have been developed from empirical correlations, they still provide uncertain values of the pile bearing capacity. The finite element analysis developed recently has provided more reliable results for studying the reaction of the pile-soil interface under axial loading (Khelifi et al., 2011). However, pile bearing capacity can be more reliably estimated by performing field load tests, despite their efficiency, they need time, cost, experience, professional training and large equipment, so it is not desirable for economic reasons, especially for low budget projects. For these reasons, it has recently been recommended to determine the bearing capacity of piles using finite analysis methods.

Over the last decade, finite element packages have advanced considerably and their results have been reported to be more accurate and reliable (Mosher 1984, Lee and Poulos 1990, Hajiazizi et al., 2017). Common methods that have been developed among all analytical or numerical packages that are suitable for evaluating the pile behavior, as well as for incorporating the soil strain behavior are; (a) the finite element method, (b) the boundary element method and (c) the load transfer function method (t-z or p-y). The basic principles and its application of the finite element method to solve problems such as numerical analysis of pile behavior have been presented by a number of authors (Muqtadir and Desai 1986, Mabsout et al., 1995, Bransby and Springman 1996, Mohamedzein et al., 1999, Wakai et al., 1999; Comodromos et al., 2003; Wehnert and Vermeer 2004). In this study, the finite element analysis method–PLAXIS 3D is performed.

6.2. Plaxis 3D

PLAXIS 3D is a software coded on the basis of a three-dimensional finite element analysis. It is used to model and analyze geotechnical engineering structures. It is one of the most easily accessible programs on the market because of its input procedures and modeling steps that can be performed using graphical user interfaces (Yilmaz, 2010).

Recently, laboratory work and theoretical studies, as well as field load tests, have been studied by performing finite element analysis. In this Chapter, model experiments in terms of (p-y behavior) of two single-model composite piles at different relative densities

of model sand (i.e., D_r = 10%, D_r = 40%, D_r = 65%, D_r = 90%) were conducted in the laboratory and have already been presented and discussed in Chapter Four and Five, respectively, and are analyzed with PLAXIS 3D in this Chapter.

6.3. Finite Element Analysis of a Single Pile

Usually, in the finite element analysis of a single model pile, three major different methods are take into account such as (i) Linear Elastic (LE) model where surrounding soils and soils under the pile toe assumed to be linearly elastic, or a Complete Non-Linear (CNL) analysis such as (ii) Mohr-Coulomb (MC) model and (iii) Hardening Soil (HS) model, where the soil modeled totally based on the Hardening Soil (HS) or the Mohr Coulomb (MC) model, or sometimes an analysis from the combination based on (NL-LE) is performed, in this combination method the soil near the pile shaft (interface zone) is modeled using the HS model, and the other remaining area of the soils is modeled using either LE or MC material.

In this study, Linear Elastic (LE) model and Mohr-Coulomb failure criteria are used to perform finite element analysis for single-model composite piles and model sand, respectively. However, the model sand is in the dry state, the drained condition is considered for the Mohr-Coulomb failure criteria.

6.4. Boundary Condition

In the "PLAXIS 3D" software the boundary conditions of three-dimensional analysis are generated automatically or it can be modified and defined by the "Standard Fixities". The boundary conditions in the "PLAXIS 3D" software are in a similar logic to the plane strain conditions in the two-dimensional analysis (i.e., which allow vertical movement while limiting lateral movements).

In addition, in order to prevent any relative motion between the finite element nodes representing the structure and those representing the ground, all the model ground interfaces have been defined as being rigid. In this study, an elastoplastic law behavior obeying the Mohr-Coulomb failure criterion, as well as 15-node triangular elements, is considered to model the ground in the computer environment. The 15-node triangular elements in three-dimensional analysis such as PLAXIS 3D are shown in (Figure 6.1.).

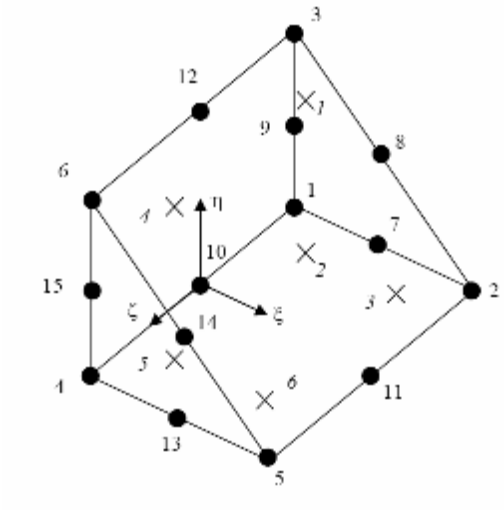

Nodes (●) and strain points (x)

Figure 6.1. 15-Node triangular elements in 3D analysis (Plaxis 3D Foundation Tutorial Manual, 2007).

6.5. The Mesh Generation

As in the two-dimensional analysis, the mesh is automatically generated by the standard PLAXIS 3D procedure, then refined for once globally, whereas this logic does not correspond in the same manner to the three-dimensional analysis (Kaltakci, 2009). In general, in the PLAXIS 3D,first, the two-dimensional mesh of the top view of the ground soil should be generated and then in the case of pile group it is refined for the cluster in which the raft is placed. After that by the standard procedure of the PLAXIS 3D the three-dimensional mesh is generated. A typical 2D and 3D generated mesh in PLAXIS 3D is shown in (Figure 6.2.).

6.6. The Parametric Study

In the current study, a total of 8 analyzes are conducted in the three-dimensional analyzes of PLAXIS 3D. In the parametric study, single-model composite piles of 50 cm and 5 cm in length and diameter, respectively, are taken into account. The typical configuration of the piles in the PLAXIS 3D environment after the mesh was generated and the pile was loaded for analysis is shown in (Figure 6.3.).

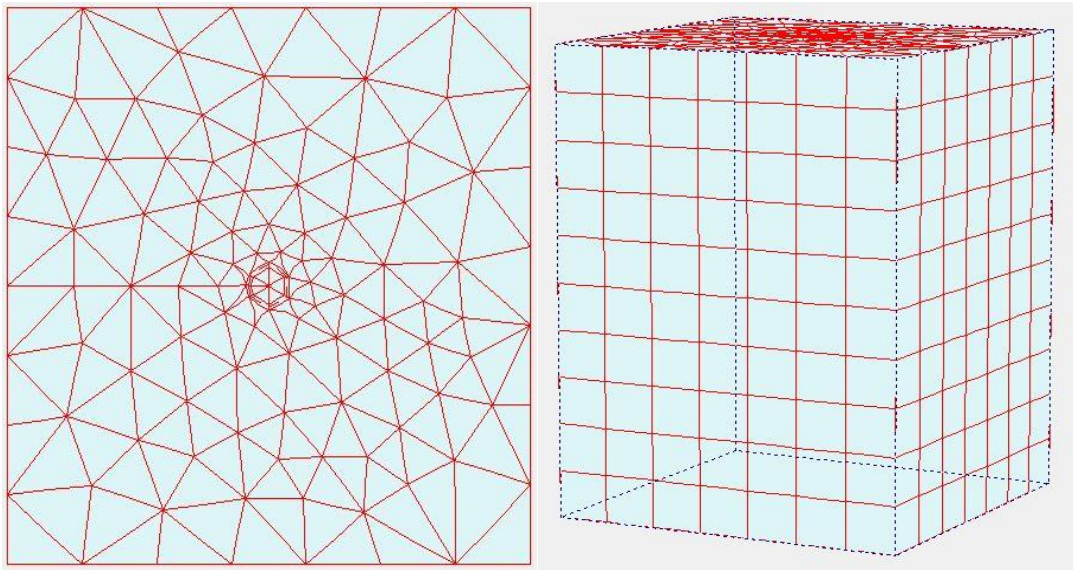

a b

Figure 6.2. a) Two-dimensional generated mesh and b) Three-dimensional generated mesh in PLAXIS 3D.

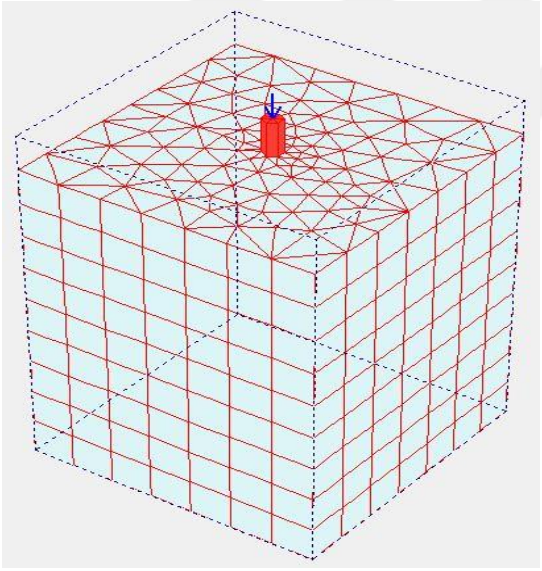

Figure 6.3. A single-model composite pile installed in PLAXIS 3D environment and loaded for analysis.

In this study, the angle of dilatancy of model sand, and modulus of elasticity and poisson's ratio of model composite piles calculated using the following equations;

$$\psi = \varphi - 30 \quad (6.1)$$

Where;

ψ = angle of dilatancy of model sand,

φ = internal friction angle of model sand,

$$E_{composite\ piles} = E_{concrete\ core} \times V_{concrete\ core} + E_{FRP\ or\ PVC\ shell} \times V_{FRP\ or\ PVC\ shell} \quad (6.2)$$

$$\nu_{composite\ piles} = \nu_{concrete\ core} \times V_{concrete\ core} + \nu_{FRP\ or\ PVC\ shell} \times V_{FRP\ or\ PVC\ shell} \quad (6.3)$$

where;

$E_{composite\ pile}$ = modulus of elasticity of composite pile,

$E_{concrete\ core}$ = modulus of elasticity of concrete core,

$V_{concrete\ core}$ = volumetric participation rate of concrete core,

$E_{shell\ material}$ = modulus of elasticity of shell material,

$V_{shell\ material}$ = volumetric participation rate of shell material,

$\nu_{composite\ pile}$ = poisson's ratio of composite pile,

$\nu_{concrete\ core}$ = poisson's ratio of concrete core,

$\nu_{shell\ material}$ = poisson's ratio of shell material.

All parameters of the model sand and single-model composite piles that are used in finite element analysis are given in the (Table 6.1. to 6.3.).

Note: The model sand used in this study is a pure sand which means it has zero cohesion (c), but because of the PLAXIS 3D conditions, we have given a small value of (c) to each relative density.

Table 6.1. The required parameter of the model sand in case of single-model FRP composite pile in PLAXIS 3D.

	Model Sand					
FRP pile	c (kN/m^2)	φ^o	ψ^o	E_s (kN/m^2)	ν	R_{int}
D_r = 10%	0.001	41	11	1000	0.20	0.64
D_r = 40%	0.100	44.3	14.3	6600	0.25	0.64
D_r = 65%	0.200	48.7	18.7	12750	0.30	0.64
D_r = 90%	0.200	52.4	22.4	16800	0.40	0.64

6.7. Finite Element Analysis Results

In the current study, the p-y behavior of two single-model composite piles at different relative densities of model sand (i.e., D_r = 10%, 40%, 65%, and 90%) is studied. In order to conduct the load-displacement behavior of single-model composite piles

numerically, a total of 8 finite element analyzes were performed with PLAXIS 3D. The ultimate bearing capacity of single-model composite piles that have already been measured in model experiments has used to analyze models piles with PLAXIS 3D, and their PLAXIS 3D results are given in (Table 6.4), and are shown in Figure (6.5. to 6.12.). The typical deformation of single-model composite piles is shown in (Figure 6.4.).

Table 6.2. The required parameter of the model sand in case of single-model PVC composite pile in PLAXIS 3D.

	Model Sand					
PVC pile	c (kN/m^2)	φ^o	ψ^o	E_s (kN/m^2)	ν	R_{int}
D_r = 10%	0.001	41	11	1000	0.20	0.67
D_r = 40%	0.100	44.3	14.3	6600	0.25	0.67
D_r = 65%	0.200	48.7	18.7	12750	0.30	0.67
D_r = 90%	0.200	52.4	22.4	16800	0.40	0.67

Note: The R_{int} in the (Table 6.2. and 6.3.) is used in PLAXIS 3D to simulate interface friction behavior.

Table 6.3. The required parameter of single-model composite piles in PLAXIS 3D.

	Single-model composite Piles	
	Es (kPa)	ν
FRP pile	20.3×10^6	0.21
PVC pile	13.7×10^6	0.24

The results of PLAXIS 3D finite element analysis (Figure 6.5. to 6.12.) show that the bearing capacity increases with increasing relative density in a semi-linear behavioral relationship, except in the case where D_r = 10%, with the very small contribution of the shaft capacity to the ultimate bearing capacity, especially where D_r = 40%, 65%, and 90%. However, at these relative densities, the model experiments have given the significant value of the pile shaft capacity. This is attributed to taking into account a very small contribution of the shaft capacity to the ultimate bearing capacity by PLAXIS 3D or the inappropriate use of PLAXIS 3D to find solutions for small model elements for such a case like in this study. In addition, in (Table 6.4.) and (Figure 6.13. and 6.14) a small difference is observed between pile settlement in experimental modeling and numerical analysis under certain conditions, which is attributed to the impossibility of controlling the relative densities of model sand when performing model experiments.

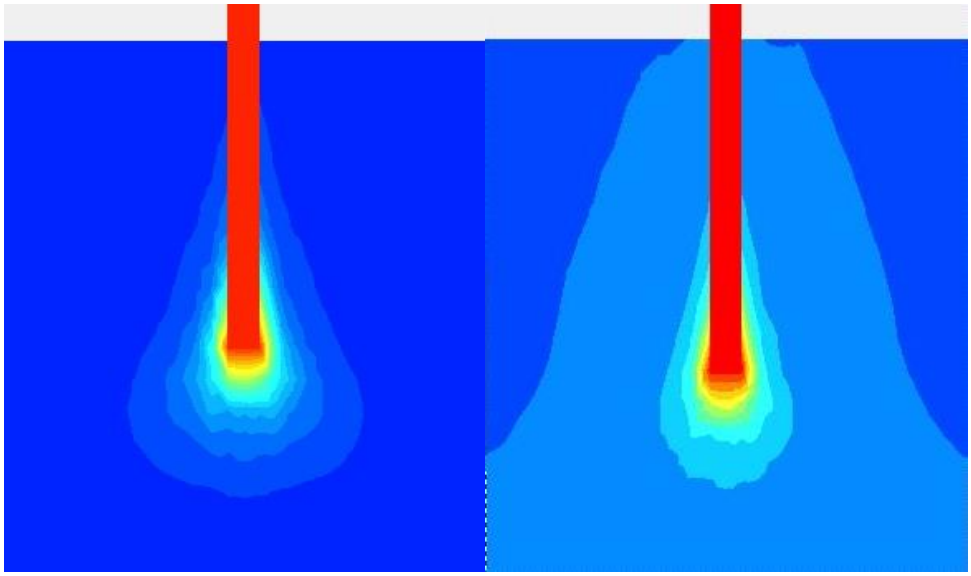

Figure 6.4. a) Total deformation shape, and b) vertical deformation shape of an analyzed pile in Plaxis 3D environment.

Note: The ultimate bearing capacity of single-model composite piles in (Table 6.4.) included the detachable shaft weight. In addition, all (mm and kN) are represented settlement at model failures and ultimate bearing capacity of single-model composite piles, respectively.

Table 6.4. Settlement behavior of single-model composite piles in Plaxis 3D at model failures of ultimate bearing capacity experiments.

	Model Sand							
	D_r = 10%		D_r = 40%		D_r = 65%		D_r = 90%	
Model Piles	mm	kN	mm	kN	mm	kN	mm	kN
FRP	4.15	0.287	7.89	2.128	9.38	6.201	10.09	12.122
PVC	5.04	0.358	8.28	2.250	9.68	6.532	9.95	12.894

The ultimate bearing capacity of single-model composite piles at different relative densities of model sand (i.e., D_r = 10%, D_r = 40%, D_r = 65%, and D_r = 90%) are shown in (Figure 6.5. to 6.12.) all graphs were redrawn in excel using PLAXIS data.

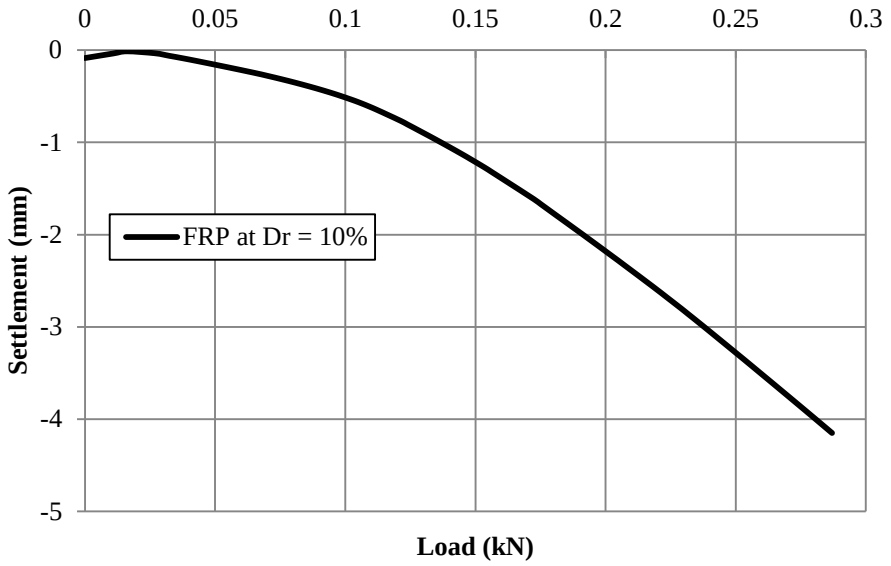

Figure 6.5. PLAXIS 3D analysis of single-model FRP composite pile at D_r = 10%.

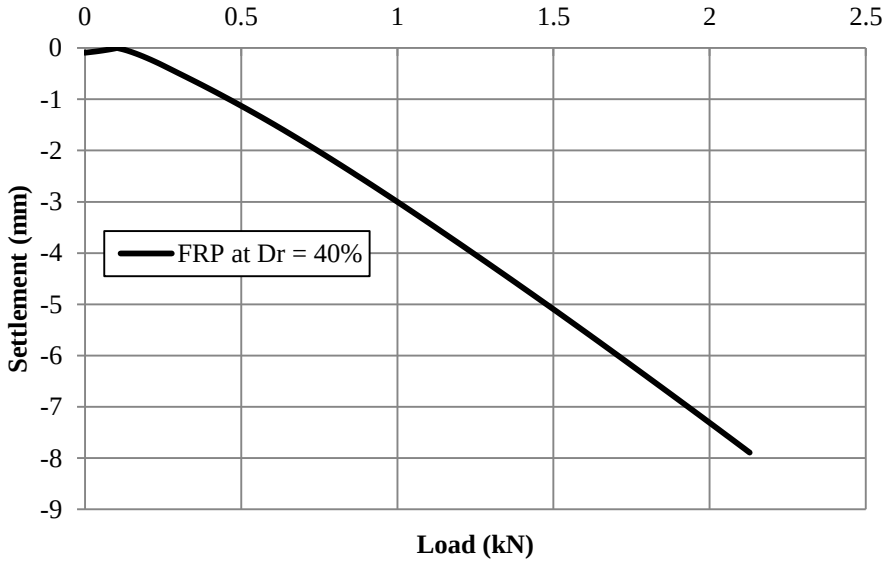

Figure 6.6. PLAXIS 3D analysis of single-model FRP composite pile at D_r = 40%.

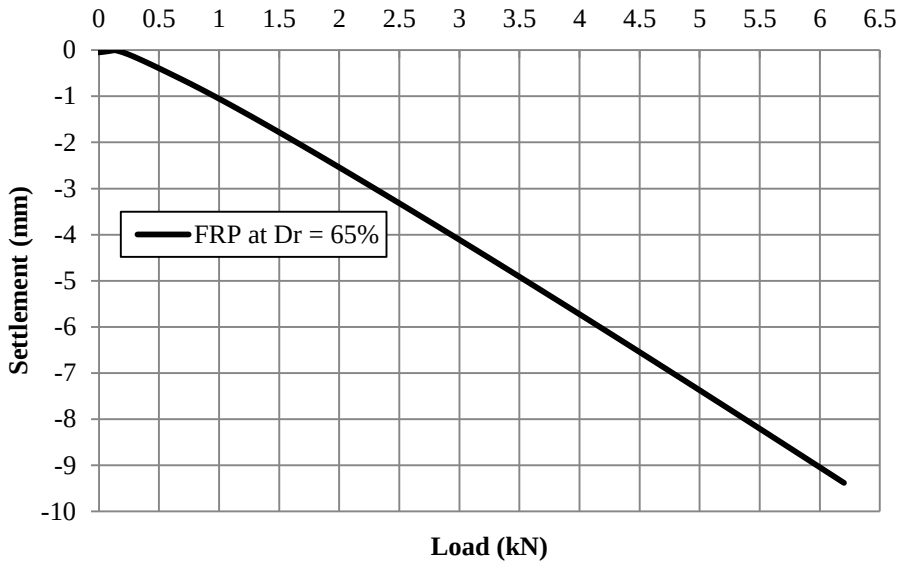

Figure 6.7. PLAXIS 3D analysis of single-model FRP composite pile at D_r = 65%.

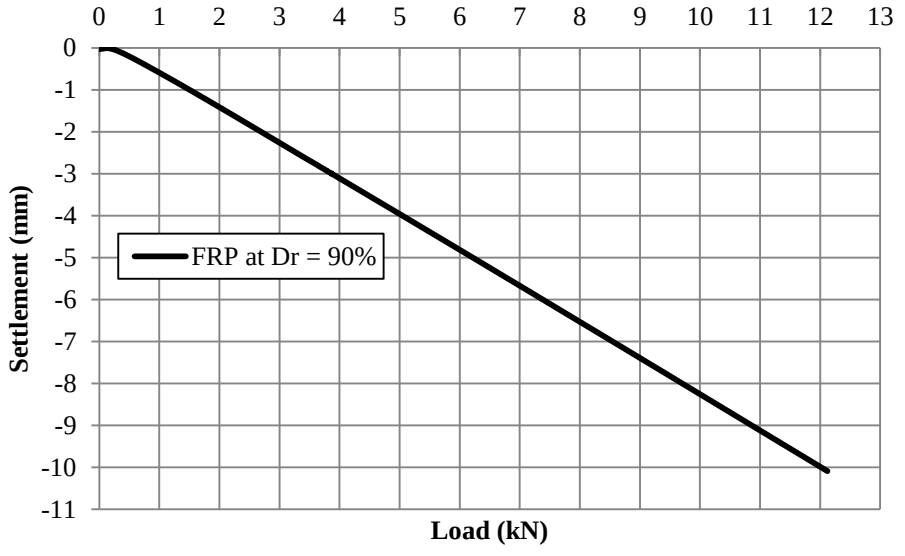

Figure 6.8. PLAXIS 3D analysis of single-model FRP composite pile at D_r = 90%.

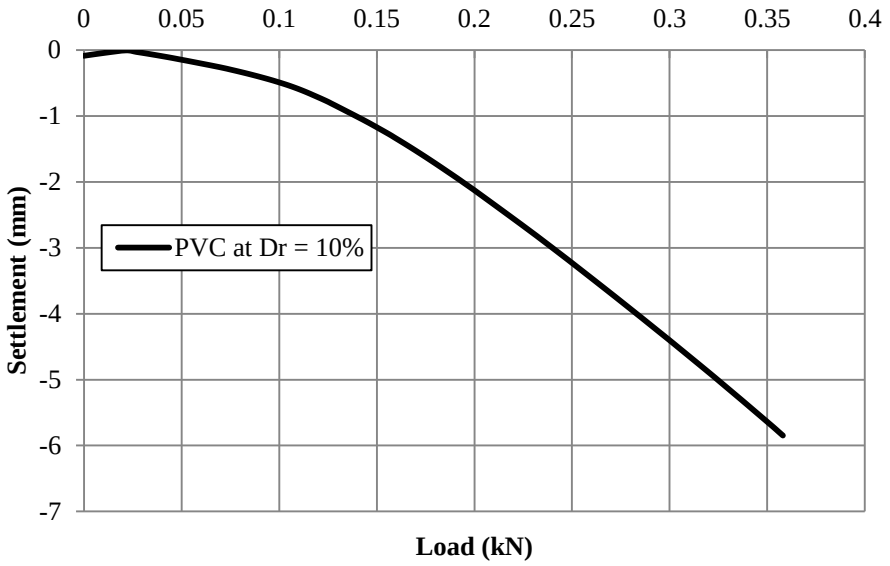

Figure 6.9. PLAXIS 3D analysis of single-model PVC composite pile at D_r = 10%.

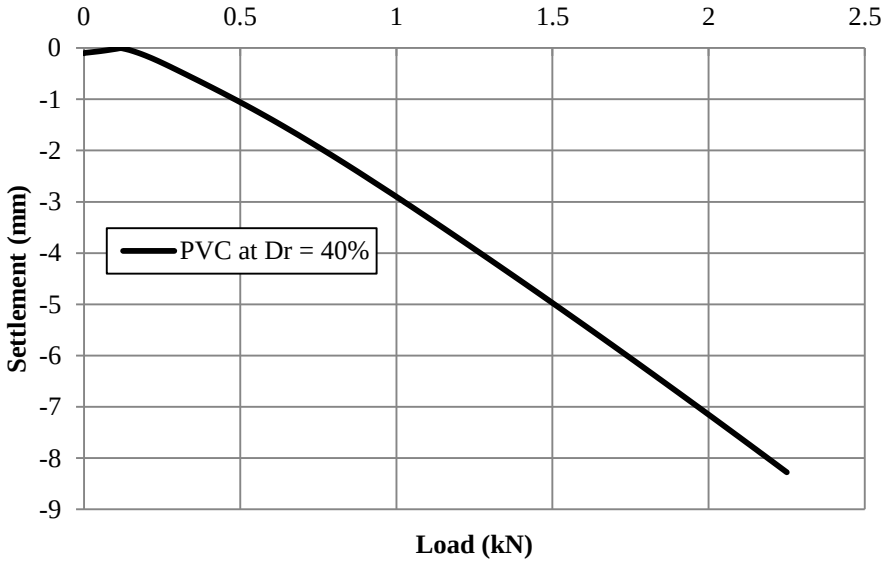

Figure 6.10. PLAXIS 3D analysis of single-model PVC composite pile at D_r = 40%.

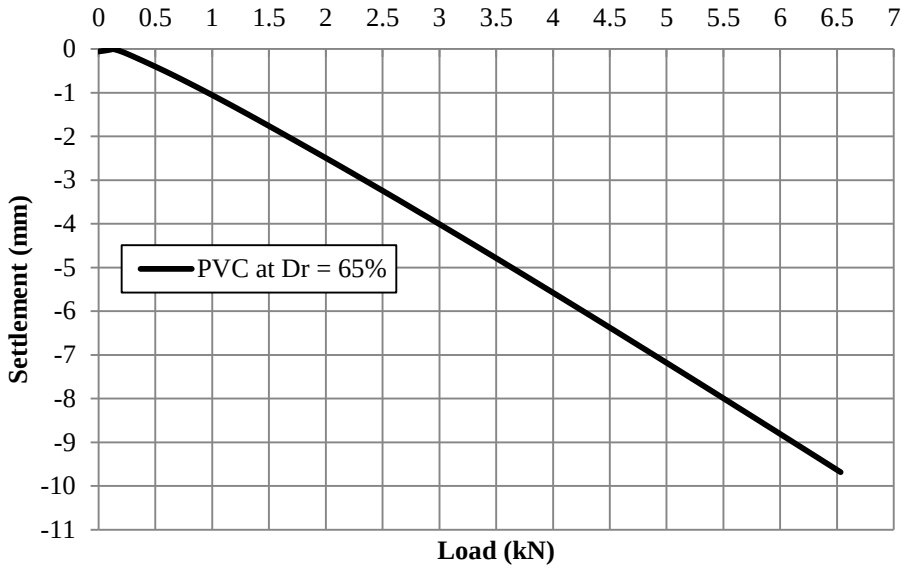

Figure 6.11. PLAXIS 3D analysis of single-model PVC composite pile at D_r = 65%.

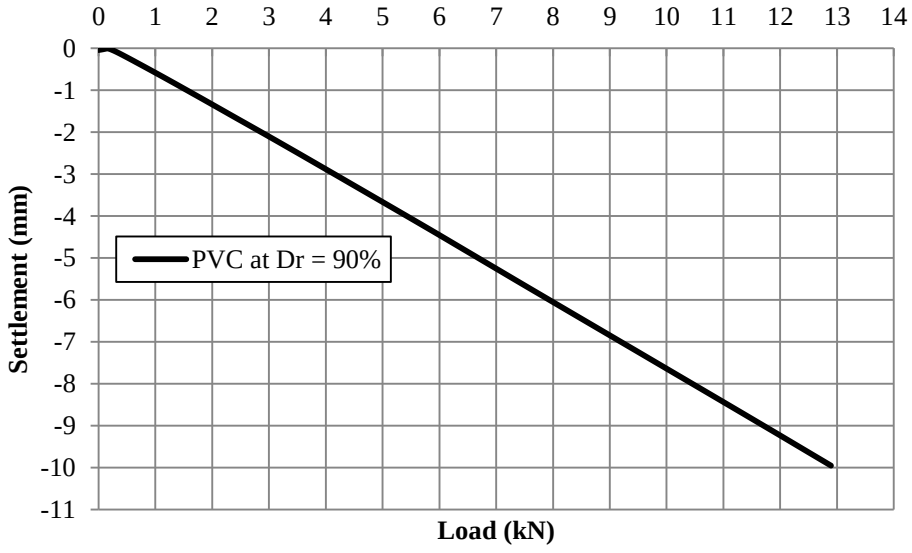

Figure 6.12. PLAXIS 3D analysis of single-model PVC composite pile at D_r = 90%.

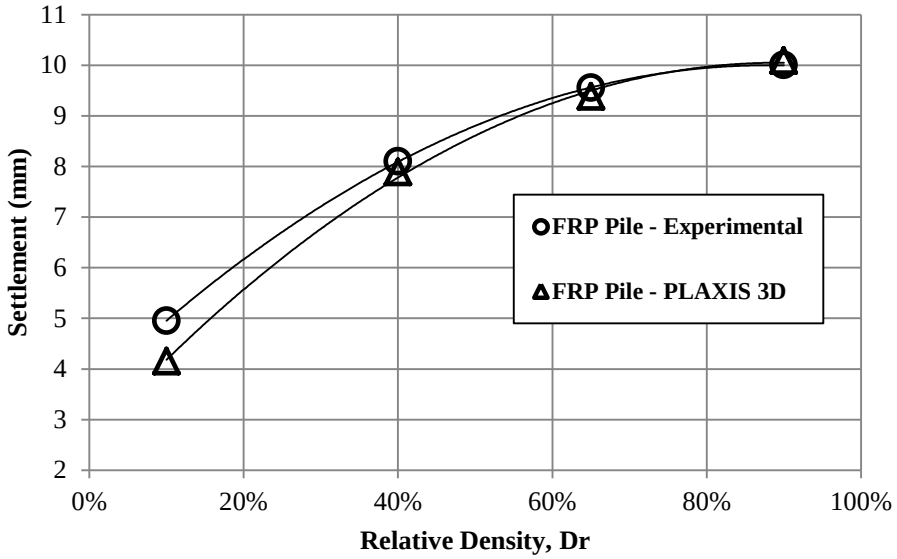

Figure 6.13. Settlement behavior of single-model FRP composite pile in model experiments and PLAXIS 3D.

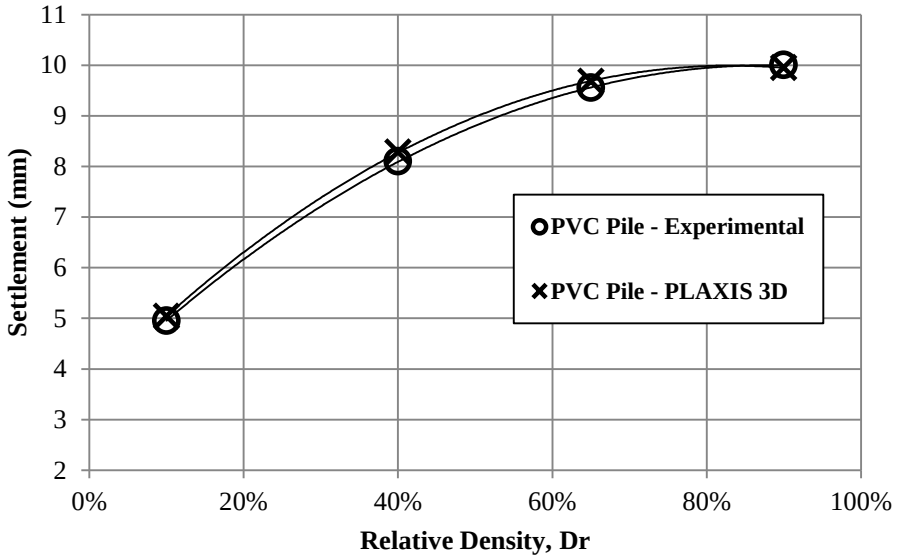

Figure 6.14. Settlement behavior of single-model PVC composite pile in model experiments and PLAXIS 3D.

7. CONCLUSIONS AND RECOMMENDATION

In this study, model experiments in terms of load-displacement behavior of two single-model composite piles (FRP and PVC concrete-filled pipe piles) at different relative densities (i.e., D_r = 10%, 40%, 65% and 90%) of the model sand were performed experimentally and numerically, as well as theoretical estimation using direct shear box test and interface shear box test. In addition, the interface shear box tests were also conducted to study the interface friction behavior of these single-model composite piles at different relative densities of model sand. The results of theoretical, experimental and numerical analysis can be concluded as below:

1. In the direct shear box test, the internal friction angle increases with the increase in relative density, but the hyperbolic curve of the internal friction angle of D_r = 10% to 40% has a different behavior that has been observed from D_r = 40% to 90%. Which is: attributed because of the normal load, as well as the high void ratio at low relative densities, leads to measuring the highest value that actually exists.

2. Although the interface friction angle increases with the increase of the relative density up to 65%, then it decreases or remains constant. Nevertheless, in model experiments, the interface friction angle increases with relative density and gets the highest value at higher densities. This is also attributed to the effect of the normal load compared to the void ratio and direction of applied load, which leads to measuring a high value of interface friction angle at low relative densities compared to a higher one. This behavior of interface friction angle confirms the fact that the interface shear box test has a working mechanism different from that of the piles.

3. The interface friction angles estimated from the back-calculation of the experimental results are very different from those of the interface shear box test. In a way, it cannot be neglected. The difference between the interface friction angles of the interface shear box test and experimental results is (+ 762%, + 24%, -24% and -42%) and (+ 615%, + 21%, -26% and -43%), for FRP and PVC piles, respectively.

4. The ratio (δ/φ) in the interface shear box test is (0.58, 0.59, 0.58 and 0.54) and (0.64, 0.65, 0.64 and 0.58) for FRP and PVC piles, respectively. Since this ratio in model experiments is (0.07, 0.48, 0.77 and 0.94) and (0.09, 0.53, 0.87 and 1.02) for piles in FRP and PVC, respectively. The ratio (δ/φ) in the model experiments emphasized that

the interface shear box test gives high values of interface friction angle at low relative densities as higher ones.

5. Pile base capacity increases with the increase of relative density in a non-linear relationship, but its settlement decreases with increase relative density. This is attributed to shear failure mode of sand, at low relative densities (i.e., D_r = 10%) because of presenting high level of void ratio the punching shear failure is occurred, and in the other three (D_r = 40, and D_r = 65% and D_r = 90%) because of decreasing in void ratio the local shear failure and general shear failure were occurred, respectively.

6. There is a significant difference between the theoretical and experimental pile base capacity, especially for low relative density (i.e., D_r = 10% and 40%). This is attributed to uncertainties in estimating the internal friction angle and Nγ.

7. In general, for pile point capacity, there is a considerable difference between experimental and theoretical results, especially for low relative densities. If we ignore these differences, it can be concluded that the Terzaghi bearing capacity method is the most reliable method for this case study.

8. There is no reliable method for determining the pile shaft capacity in a case as in this study, with the exception of the Coyle and Castello's K results, which have the same behavior as that observed in the model experiments, but it provided the higher values. If the results of the Coyle and Castello's K be multiplied by a factor such that (Tanh D_r) and ($\mathrm{Sin}D_r \frac{180}{\pi}$) for FRP and PVC pile, respectively, very close values are achieved.

9. The results obtained by finite element analysis in terms of (p-y behavior) confirm the fact that the axial behavior of the pile especially pile shaft behavior provides by theoretical solution still remains high levels of uncertainties. This is despite the strange behavior that was observed in finite element analysis at the high relative densities, where the load-displacement behavior (i.e., p-y) became linear at D_r = 40%, 65%, and 90%, whereas this behavior is in total contrast to the model experiments. However, finite element analysis has not yielded a good agreement in terms of load-displacement behavior as such a case as in this study, but the comparison of the numerical analysis results with the theoretical and experimental results, as well as, field tests is necessary to find better numerical solutions for pile bearing capacity.

10. However, single-model PVC composite pile has shown higher bearing capacity than single-model FRP composite pile, in particular, in shaft capacity, but because of the difference between their bearing capacity is not significant. Therefore, based on some

field works, experimental modeling, and a few knowledge in the database of FRP composite piles and depends on some institute or foundations, it can be said that the FRP composite piles are better than the PVC composite piles or Recycled Plastic Piles (RPPs). For example, the Federal Highway Administration (FHWA) in the United States of America has recommended that the FRP composite piling have a significant capacity as axial-bearing piles and have the potential to be an interesting option for conventional piling foundations (Juran and Komornik, 2006). In addition, due to the lack of sufficient studies on the structural behavior of reinforced RPPs, manufacturers often provide information on the performance of these piles (Pando et al., 2006). As a result, insufficient knowledge in the database of RPPs makes FRP piles better.

11. Finally, for the pile shaft behavior it can be concluded that, the hyperbolic behavior or the non-linear relations of the (p – y) behavior of the single-model composite piles conducted from the model experiments confirm the fact already observed in the result and discussions in Chapter Five. The fact is that the friction resistance behavior of the pile shaft is very different from the interface friction behavior conducted from the interface shear box test. This is why we have focused on other model and field research studies in this area to study this behavior in more detail. In addition, despite this fact, it has been observed during field load tests that the pile shaft capacity increases with the embedment length of the pile to a limit where (L_b/D) reaches its critical state $(L_b/D)_{cr}$ which is equal to 15 to 18D, while in this study, the initial (L_b/D) of the installed single-model composite piles is equal to 10, but the friction resistance of the single-model composite piles during loading experiments reached its maximum capacity approximately with an embedment ratio of 10.01, 10.16, 10.19 and 10.20 at relative density 10%, 40%, 65% and 90%, respectively, which is also emphasized for conducting considerable studies to study this behavior as well.

REFERENCES

Aksoy, H.S., Gör, M. and İnal, E., 2016. A new design chart for estimating friction angle between soil and pile materials, *Geomechanics and Engineering*, **10**(3), 315-324.

Al-Busoda, B.S. and Al-Rubaye, A.H., 2015. Bearing Capacity of Bored Pile Model Constructed in Gypseous Soil, *Journal of Engineering*, **21**(3), 109-128.

Almallah, A., El Naggar, H. and Sadeghian, P., 2018. Direct Shear Tests of Sandy Soils Interfaced with FRP Sheets, *In CSCE Annual Conference 2018, Fredericton, NB,* Canadian Society for Civil Engineering, 13-16 June, Canada, ST41 1-10.

Al-Mhaidib, A.I., 1999. Bearing capacity of a model pile in sand under different loading rates, *In The Ninth International Offshore and Polar Engineering Conference, International Society of Offshore and Polar Engineers*, 30 May-4 June, Brest, France.

Al-Mhaidib, A.I., 2001. Loading rate effect on piles in clay from laboratory model tests, *Journal of King Saud University-Engineering Sciences*, **13**(1), 39-54.

Al-Mhaidib, A.I., 2006. Influence of shearing rate on interfacial friction between sand and steel, *Engineering Journal of the University of Qatar*, **19**, 14-23.

Al-Mhaidib, A.I., 2006a. Experimental investigation of the behavior of pile groups in sand under different loading rates, Geotechnical & Geological Engineering, 24(4), 889.

Anonymous, 1999. Uncertainty principle (Pile predictions), *Ground Engineering Journal*, **32**(11), 32-34.

Ashford, S.A. and Jakrapiyanun, W., 2001. Drivability of glass FRP composite piling, *Journal of Composites for Construction*, **5**(1), 58-60.

ASTM D3080-72, 1989. Standard method for direct shear test of soils under consolidated drained conditions, *Annual Book of Standards*, Vol. 04.08, West Conshohoken, 376–378.

ASTM D422-63, 1989. Standard method for particle-size analysis of soils, *Annual Book of Standards*, Vol. 04.08, West Conshohoken, 86–92.

ASTM D4253-16, 2016. Standard Test Methods for Maximum Index Density and Unit Weight of Soils Using a Vibratory Table, *ASTM International*, West Conshohocken, PA, www.astm.org.

ASTM D5321/D5321M-14, 2014. Standard Test Method for Determining the Shear Strength of Soil-Geosynthetic and Geosynthetic-Geosynthetic Interfaces by Direct Shear, *ASTM International*, West Conshohocken, PA, www.astm.org.

ASTM D854-83, 1989. Standard test method for specific gravity of soils, *Annual Book of Standards*, Vol. 04.08, West Conshohoken, 162–164.

Axelsson, G. 1998. Long-term Increase in Shaft Capacity of Driven Piles in Sand, *Proceedings: fourth International Conference on Case Histories in Geotechnical Engineering, st. Louis, Missouri (Paper no. 125)*, 8-15 March, Royal Institute of Technology, Stockhohn, Sweden/Skanska Teknik AB, **57**.

Bagriacik, B. and Laman, M., 2011. Investigation of the Size Effect at Different Geometries on Stress Distribution of Sandy Soils, *International Balkans Conference on Challenges of Civil Engineering*, BCCCE, 19-21 May, EPOKA University, Tirana, ALBANIA.

Becque, J., Patnaik, A. K. and Rizkalla, S. H., 2003. Analytical models for concrete confined with FRP tubes, *Journal of Composites for Construction*, **7**(1), 31-38.

Bolton, M.D., Gui, M.W., Garnier, J., Corte, J.F., Bagge, G., Laue, J. and Renzi, R., 1999. Centrifuge cone penetration tests in sand, *Géotechnique*, **49**(4), 543-552.

Bowles, J.E., 1996. Foundation Analysis and Design, 5th Edition, *The McGraw-Hill Companies*, Inc., New York.

Bowles, L.E., 1996. *Foundation analysis and design*, McGraw-hill.

Bozorg-Haddad, A., Iskander, M. and Chen, Y., 2012. Compressive strength and creep of recycled HDPE used to manufacture polymeric piling, *Construction and Building Materials*, **26**(1), 505-515.

Bransby, M.F. and Springman, S.M., 1996. 3-D finite element modelling of pile groups adjacent to surcharge loads, *Computers and Geotechnics*, **19**, 301-324.

Brown, M. J., 2004. The rapid load testing of piles in fine grained soils, *PhD thesis*, University of Sheffield, England.

Chaudhuri, K.P.R. and Symons, M.V., 1983. Uplift resistance of model single piles, *In Geotechnical Practice in Offshore Engineering*, ASCE, 335-355.

Chow, F. C., Jardine, R. J., Nauroy, J. F. and Brucy, F., 1997. Time-related increases in the shaft capacities of driven piles in sand, *Geotechnique*, **47**(2), 353-361.

Chow, F., 1997. Fiona Chow asks is pile design progressing*?*, *Ground Engineering Journal*, **30**(10), 3.

Comodromos, E.M., Anagnostopoulos, C.T. and Georgiadis, M.K., 2003. Numerical assessment of axial pile group response based on load test, *Computers and Geotechnics*, **30**(6), 505-515.

Coyle, H.M. and Castello, R.R., 1981. New design correlations for piles in sand, *Journal of Geotechnical and Geoenvironmental Engineering*, ***107***(ASCE 16379), 965-986.

Das, B. M. (2015). Principles of foundation engineering, 8th edition, *Cengage learning*.

Das, B.M., 2010. Geotechnical engineering handbook, *J. Ross Publishing*.

Das, B.M., Seeley, G.R. and Pfeifle, T.W., 1977. Pullout resistance of rough rigid piles in granular soils, *Soils and Foundations*, **17**(3), 72-77.

Dijkstra, J., 2004. Influence of loading rate on pile capacity in unsaturated sand, Master's thesis, Faculty of Civil Engineering and Geosciences, TU Delft.

El Sawwaf, M., 2010. Experimental study of eccentrically loaded raft with connected and unconnected short piles, *Journal of geotechnical and geoenvironmental engineering*, **136**(10), 1394-1402.

Eslami, A. and Fellenius, B.H., 1997. Pile capacity by direct CPT and CPTu methods applied to 102 case histories, *Canadian Geotechnical Journal*, **34**(6), 886-904.

Fam, A. and Rizkalla, S. H., 2001a. Behavior of axially loaded concrete-filled circular FRP tubes, *ACI Structural journal*, **98**(3), 280-289.

Fam, A. Z. and Rizkalla, S. H., 2001b. Confinement model for axially loaded concrete confined by circular fiber-reinforced polymer tubes, *Structural Journal*, **98**(4), 451-461.

Fam, A. Z. Y. H., 2000. Concrete-filled fibre-reinforced polymer tubes for axial and flexural structural members, *PhD thesis*, University of Manitoba, Canada.

Fattah, M.Y., Al-Soudani, W.H. and Omar, M., 2016. Estimation of bearing capacity of open-ended model piles in sand, *Arabian Journal of Geosciences*, **9**(3), 242.

Fleming, K., Weltman, A., Randolph, M., Elson, K., 2008. Piling engineering, *Taylor & Francis Group*.

Fleming, W.G.K., Weltman, A.J., Randolph, M.F. and Elson, W.K., 1992. Piling Engineering, 2nd. Edition, *Blackie, Glasgow & London*.

Foray, P., Balachowski, L. and Colliat, J.L., 1998. Bearing capacity of model piles driven into dense overconsolidated sands,. *Canadian Geotechnical Journal*, **35**(2), 374-385.

Frost, J.D. and Han, J., 1999. Behavior of interfaces between fiber-reinforced polymers and sands, *Journal of geotechnical and geoenvironmental engineering*, **125**(8), 633-640.

Garcia, K., Hayes, M. D., Verghese, N. and Lesko, J. J., 1998. The effects of cyclic moisture aging on a glass/vinyl ester composite system, *Progress in Durability Analysis of Composite Systems*, Reifsnider & cardon (eds), Balkema, Rotterdam, 173.

Gathimba Naftary, K., Oyawa Walter, O. and Mang'uriu Geoffrey, N., 2014. Compressive strength characteristics of concrete-filled plastic tubes short columns, *Int J Sci Res (IJSR)*, **3**(9), 2168-2174.

Guades, E., Aravinthan, T., Islam, M. and Manalo, A., 2012. A review on the driving performance of FRP composite piles, *Composite Structures*, **94**(6), 1932-1942.

Gui, M.W. and Muhunthan, B., 2006. Bearing capacity of foundations on sand using the method of slip line, *Journal of Marine Science and Technology*, **14**(1), 1-14.

Hajiazizi, M., Bavali, M. and Fakhimi, A., 2017. Numerical and experimental study of the optimal location of concrete piles in a saturated sandy slope, *International Journal of Civil Engineering*, 1-9.

Han, J., Frost, J. and Brown, V., 2003. Design of fiber-reinforced polymer composite piles under vertical and lateral loads, *Transportation Research Record: Journal of the Transportation Research Board*, **1849**(1), 71-80.

Hanna, T. H. and Tan, R. H. S., 1973. The behavior of long piles under compressive loads in sand, *Canadian Geotechnical Journal*, **10**(3), 311-340.

Hansen, J.B., 1970. A revised and extended formula for bearing capacity.

Heinz, R., 1993. Plastic piling. *Civil Engineering*, **63**(4), 63.

Horeczko, G., 1995. Marine application of recycled plastics. *In Restructuring: America and Beyond*, ASCE, 834-837.

Igoe, D. J. P., Gavin, K. G. and O'Kelly, B. C., 2011. Shaft capacity of open-ended piles in sand, *Journal of Geotechnical and Geoenvironmental Engineering*, **137**(10), 903-913.

Iskander, M., 2002. Recent developments in FRP composite piling practice. *In Transportation Research Board Annual Meeting, Chicago, Paper* (No. 02-3589).

Iskander, M.G. and Hassan, M., 1998. State of the practice review in FRP composite piling, *Journal of Composites for Construction*, **2**(3), 116-120.

Iskander, M.G. and Hassan, M., 2001. Accelerated degradation of recycled plastic piling in aggressive soils, *Journal of Composites for Construction*, **5**(3), 179-187.

Iskander, M.G. and Stachula, A., 2002. Wave equation analyses of fiber-reinforced polymer composite piling, *Journal of Composites for Construction*, **6**(2), 88-96.

Iskander, M.G., Hanna, S. and Stachula, A., 2001. Driveability of FRP composite piling, *Journal of Geotechnical and Geoenvironmental Engineering*, **127**(2), 169-176.

Janbu, N., 1976. Static bearing capacity of friction piles, *In Sechste Europaeische Konferenz Fuer Bodenmechanik Und Grundbau*, **1.2**, 479-488.

Juran, I. and Komornik, U., 2006. Behavior of fiber-reinforced polymer (frp) composite piles under vertical loads (No. FHWA-HRT-04-107).

Kahyaoğlu, M.R., Seçer, M. And Kayalar, A.Ş., 2012. Cam Elyaf Takviyeli Plastik Profilli Pasif Kazık Grup Davranışının Deneysel Olarak İncelenmesi, *Teknik Dergi*, **23**(112).

Kaltakci, V., 2009. A Comparison of Two – Dimensional and Three – Dimensional Finite Element Analysis for Settlement Behavior of Piled Raft Foundations, Master Thesis, Middle East Technical University, Ankara, Turkey.

Kerisel, J., 1964. Deep foundations basic experimental facts, *In Proceedings of a Conference on Deep Foundations*, Mexico City, 5-44.

Khelifi, Z., Berga, A. and Terfaya, N., 2011. Modeling the Behavior of Axially and Laterally Loaded Pile with a Contact Model, *Electronic Journal of Geotechnical Engineering (EJGE)*, **16**.

Kraft Jr, L. M., 1991. Performance of axially loaded pipe piles in sand, *Journal of Geotechnical Engineering*, **117**(2), 272-296.

Lampo, R., 1999. Standards boost an industry, *ASTM standardization news*, **27**(7), 22-26.

Lampo, R., Nosker, T., Barno, D., Busel, J., Maher, A., Dutta, P. and Odello, R., 1998. Development and demonstration of FRP composite fender, loadbearing, and sheet piling systems, *USACERL TR-98/123*, U.S. Army Corps of Engineers.

Lee, C.Y. and Poulos, H.G., 1990. Axial response analysis of piles in vertically and horizontally non-homogeneous soils, *Computers and Geotechnics*, **9**(3), 133-148.

Leong, W.K., Yusoff, N.A., Abd Aziz, A.N. and Abu Talib, Z., 2015. Theoretical and Actual Bearing Capacity of Driven Piles Using Model Piles in Sand, *Applied Mechanics and Materials*, **773-774**, 1453-1459.

Loehr, J., Bowders, J., Owen, J., Sommers, L. and Liew, W., 2000. Slope stabilization with recycled plastic pins, *Transportation Research Record: Journal of the Transportation Research Board*, (1714), 1-8.

Lopez-Anido, R., Michael, A.P., Goodell, B. and Sandford, T.C., 2004. Assessment of wood pile deterioration due to marine organisms, *Journal of waterway, port, coastal, and ocean engineering*, **130**(2), 70-76.

Mabsout, M.E., Reese, L.C. and Tassoulas, J.L., 1995. Study of pile driving by finite-element method, *Journal of geotechnical engineering*, **121**(7), 535-543.

Manandhar, S. and Yasufuku, N., 2012. Analytical model for the end-bearing capacity of tapered piles using cavity expansion theory, *Advances in Civil Engineering*.

Manandhar, S. and Yasufuku, N., 2013. Vertical bearing capacity of tapered piles in sands using cavity expansion theory, *Soils and Foundations*, **53**(6), 853-867.

Mayerhof, G.G., 1976. Bearing capacity and settlement of pile foundations, *Journal of Geotechnical and Geoenvironmental Engineering*, ASCE 11962, **102(**GT3**)**, 197-228.

Mayoral, J.M., Pestana, J.M., and Seed, R.B., 2005. Determination of Multidirectional p-y Curves for Soft Clays, *Geotechnical Testing Journal*, **28**(3), 253-263.

Meyerhof, G. G., 1959. Compaction of sands and bearing capacity of piles, *Journal of the Soil Mechanics and Foundations Division*, **85**(6), 1-30.

Meyerhof, G.G., 1948. An investigation of the bearing capacity of shallow footings on dry sand, *In Proc. 2nd ICSMFE*, **1**, 238-243.

Meyerhof, G.G., 1951. The ultimate bearing capacity of foudations, *Geotechnique*, **2**(4), 301-332.

Meyerhof, G.G., 1961. Compaction of Sands and Bearing Capacities of Piles, *Transactions, American Society of Civil Engineers*, **126**, 1292 – 1323.

Meyerhof, G.G., 1963. Some recent research on the bearing capacity of foundations, *Canadian Geotechnical Journal*, **1**(1), 16-26.

Mirmiran, A., Shahawy, M. and Beitleman, T., 2001. Slenderness limit for hybrid FRP-concrete columns, *Journal of Composites for Construction*, **5**(1), 26-34.

Mirmiran, A., Shahawy, M. and Samaan, M., 1999. Strength and ductility of hybrid FRP-concrete beam-columns, *Journal of structural Engineering*, **125**(10), 1085-1093.

Mirmiran, A., Shao, Y. and Shahawy, M., 2002. Analysis and field tests on the performance of composite tubes under pile driving impact. *Composite Structures*, **55**(2), 127-135.

Mitchell, J. K. and Solymar, Z. V., 1984. Time-dependent strength gain in freshly deposited or densified sand, *Journal of Geotechnical Engineering*, **110**(11), 1559-1576.

Miura, N., 1983. Point resistance of piles in sand, *Technology reports of the Yamaguchi University*, **3**(2), 129-139.

Mohamedzein, Y.E., Mohamed, M.G. and El Sharief, A.M., 1999. Finite element analysis of short piles in expansive soils, *Computers and Geotechnics*, **24**(3), 231-243.

Moran, D. A. and Pantelides, C. P., 2002. Variable strain ductility ratio for fiber-reinforced polymer-confined concrete, *Journal of Composites for Construction*, **6**(4), 224-232.

Mosher, R.L., 1984. Load-Transfer Criteria for Numerical Analysis of Axially Loaded Piles in Sand, *Part 1. Load-Transfer Criteria* (No. WES-TR-K-84-1), ARMY ENGINEER WATERWAYS EXPERIMENT STATION VICKSBURG MS.

Muqtadir, A. and Desai, C.S., 1986. Three-dimensional analysis of a pile-group foundation, *International journal for numerical and analytical methods in geomechanics*, **10**(1), 41-58.

Nanda, S. and Patra, N.R., 2011. Shaft resistance of piles in normally consolidating marine clay subjected to compressive and uplift load, *In Geo-Frontiers Congress2011: Advances in Geotechnical Engineering,* Dallas, Texas, 13-16 March, United States, 263-272.

Ohno, S., 1999. Bearing capacity of piles in sands with different crushabilities under various stress conditions, *In Proc. of the 11th Asian Regional Conf. on SMGE,* Seoul, **1**, 249-252.

Olson, R.E., 2002. Axial Load Capacity of Driven Piles, *Proceedings, 50th Annual Geotechnical Engineering Conference,* University of Minnesota, Saint Paul, Minnesota, United States, 161-178

O'rourke, T.D., Druschel, S.J. and Netravali, A.N., 1990. Shear strength characteristics of sand-polymer interfaces, *Journal of geotechnical engineering*, **116**(3), 451-469.

Pando, M., Lesko, J., Fam, A. and Rizkalla, S., 2002b. Durability of concrete-filled tubular FRP piles, *In The 3rd Int. Conf. on Composites in Infrastructure, ICCI* , **2**, 10-12.

Pando, M.A., 2003. A laboratory and field study of composite piles for bridge substructures, *PhD thesis,* Virginia Tech, United States.

Pando, M.A., Ealy, C.D., Filz, G.M., Lesko, J.J. and Hoppe, E.J., 2006. A laboratory and field study of composite piles for bridge substructures (No. FHWA-HRT-04-043), United States, *Federal Highway Administration, Office of Infrastructure Research and Development.*

Pando, M.A., Filz, G.M., Dove, J.E. and Hoppe, E.J., 2002a. Interface shear tests on FRP composite piles, *In Deep Foundations 2002: An International Perspective on Theory, Design, Construction, and Performance,* 14-16 February, Orlando, Florida, United States, 1486-1500.

Potyondy, J.G., 1961. Skin friction between various soils and construction materials. *Geotechnique,* 11(4), 339-353.

Poulos, H. G., 1989. Pile behavior-theory and application, *Geotechnique*, **39**(3), 365-415.

Prandtl, L., 1920. Über die härte plastischer körper. *Nachrichten von der Gesellschaft der Wissenschaften zu Göttingen, Mathematisch-Physikalische Klasse, 1920,* 74-85.

Randolph, M. F., 2003. Science and empiricism in pile foundation design, *Géotechnique*, **53**(10), 847-876.

Randolph, M. F., Dolwin, R. and Beck, R., 1994. Design of driven piles in sand, *Géotechnique*, **44**(3), 427-448.

Rausche, F., Goble, G.G. and Likins Jr, G.E., 1985. Dynamic determination of pile capacity, *Journal of Geotechnical Engineering*, **111**(3), 367-383.

Reissner, H., 1924. Zum Erddruckproblem, *In Proceedings of the 1st International Congress of Applied Mechanics, Delft*, 295-311.

Rinne, N.F., 1989. Evaluation of interface friction between cohesionless soil and common construction materials, Master Thesis, University of British Columbia, Vancouver, Canada.

Roberts, L.A. and Brandner, E., 2010. Support of Structures in Expansive Shale Using Recycled Plastic Piles, *DFI Journal - The Journal of the Deep Foundations Institute*, **4**(1), 45-58.

Robinsky, E.I. and Morrison, C.F., 1964. Sand displacement and compaction around model friction piles, *Canadian Geotechnical Journal*, **1**(2), 81-93.

Robinson, B. and Iskander, M., 2008. Static and dynamic load tests on driven polymeric piles, *In GeoCongress 2008: Geosustainability and Geohazard Mitigation*, New Orleans, Louisiana, 9-12 March, United States, 939-946.

Sadrekarimi, J., Gouhari, M.B. and Roohimehr, A., 2009. Surface roughness effects on the bearing capacity of piles in dry sand, *The Electronic Journal of Geotechnical Engineering*, **14, Bund. A**.

Sakr, M., El Naggar, M.H. and Nehdi, M., 2005. Interface characteristics and laboratory constructability tests of novel fiber-reinforced polymer/concrete piles, *Journal of Composites for Construction*, **9**(3), 274-283.

Sakr, M., Naggar, M. H. E. and Nehdi, M., 2004. Novel toe driving for thin-walled piles and performance of fiberglass-reinforced polymer (FRP) pile segments, *Canadian geotechnical journal*, **41**(2), 313-325.

Samaan, M., Mirmiran, A. and Shahawy, M., 1998. Model of concrete confined by fiber composites, *Journal of structural engineering*, **124**(9), 1025-1031.

Schmertmann, J. H., 1991. The mechanical aging of soils, *Journal of Geotechnical Engineering*, **117**(9), 1288-1330.

Shaia, H., 2013. Behaviour of Fibre Reinforced Polymer Composite Piles: Experimental and Numerical Study, Doctoral Dissertation, The University of Manchester, Manchester, United Kingdom.

Shin, E.C., Das, B.M., Puri, V.K., Yen, S.C. and Cook, E.E., 1993. Ultimate uplift capacity of model rigid metal piles in clay, *Geotechnical & Geological Engineering*, **11**(3), 203-215.

Shooshpasha, I., Hasanzadeh, A., and Taghavi, A., 2013. Prediction of the axial bearing capacity of piles by SPT-based and numerical design methods, *International Journal of GEOMATE*, **4**(2), 560-564.

Springer, G. S., Sanders, B. A. and Tung, R. W., 1980. Environmental effects on glass fiber reinforced polyester and vinylester composites, *Journal of Composite Materials*, **14**(3), 213-232.

Tan, R. H. S. and Hanna, T. H., 1974. Long piles under tensile loads in sand, *Geotech. Engrg*, **5**(2), 109-124.

Taylan, Z.N., 2013. Experimental and numerical modeling studies for interpreting and estimating the δ behavior of single piles in unsaturated soils, *PhD thesis,* Istanbul Technical University, Istanbul, Turkey.

Terzaghi, K. and Peck, R., 1967. Soil Mechanics in Engineering Practice, 2nd Edition, John Wiley, New York, United States.

Terzaghi, K. and Peck, R.B., 1948. Soil Mechanics in Engineering Practice, *John Wiley and Sons, New York, NY,* United States.

Terzaghi, K., 1943. Theoretical soil mechanics, *John Wiley and Sons, New York, Inc.; London, Chapman and Hall, Limited*.

Terzi, N.U., Kiliç, H. and Gültekin, S., 2009. Yanal yüklü bir model kaziğin kum ortamindaki davranişinin deneysel ve nümerik yöntemlerle incelenmesi, *Pamukkale Üniversitesi Mühendislik Bilimleri Dergisi*, **15**(1), 119-127.

Tetra Tech, 1999. Plastic Pier Piling Evaluation Report, *Reprt Prepared for Navy Region Southwest, Navy Environmental Leadership Program*, Tetra Tech EM, Inc, 591 Camino De La Reina, #640, San Diego, CA 92108, Contract no. N62474-94-D-7609, United States.

Ukritchon, B., Whittle, A.J. and Klangvijit, C., 2003. Calculations of bearing capacity factor Nγ using numerical limit analyses, *Journal of Geotechnical and Geoenvironmental Engineering*, **129**(5), 468-474.

URL-1, www.plasticpiling.co.uk Plastic Pilings, Inc. 2001.

URL-2, http://www.seaward.co.uk/SEAPILE.html Seaward International. 2001.

Vesic, A. S., 1970. Tests on Instrumented Piles, Ogeechee River Site, *Journal of the Soil Mechanics and Foundations Division,* **96**(2), 561-584.

Vesic, A.S. 1964. Investigations of bearing capacity of piles in sand, *In Proc. North American Conf. on Deep Found., Mexican Society of Soil Mechanics*, **1**, 197-224.

Vesic, A.S., 1963. Bearing capacity of deep foundation in sand, *Highway Research Record, National Academy of Sciences, National Research Council*, (39), 112-153.

Vesic, A.S., 1973. Analysis of ultimate loads of shallow foundations, *Journal of Soil Mechanics & Foundations Div.*, **99**(sm1), 45-73.

Wakai, A., Gose, S. and Ugai, K., 1999. 3-D elasto-plastic finite element analyses of pile foundations subjected to lateral loading, *Soils and Foundations*, **39**(1), 97-111.

Wehnert, M. and Vermeer, P.A., 2004. Numerical analyses of load tests on bored piles, *Numerical methods in geomechanics–NUMOG 9th,* 20-25 August 2004, Ottawa, Canada., 505-511.

Wheeler, P., 2000. Behavior problems (Design and reality), *Ground Engineering Journal, European Foundations Supplement,* 24-25.

Yasufuku, N. and Hyde, A.F.L., 1995. Pile end-bearing capacity in crushable sands, *Geotechnique*, **45**(4), 663-676.

Yilmaz, B., 2010. An analytical and experimental study on piled raft foundations, Master thesis, Middle East Technical University, Ankara, Turkey.

Zyka, K. and Mohajerani, A., 2016. Composite piles: A review, *Construction and Building Materials*, **107**, 394-410.

APPENDIX

APPENDIX-1 (Experimental Time-Load and Time-Displacement Behaviors of Single-Model FRP Composite Pile in the Ultimate Bearing Capacity Model Experiments)

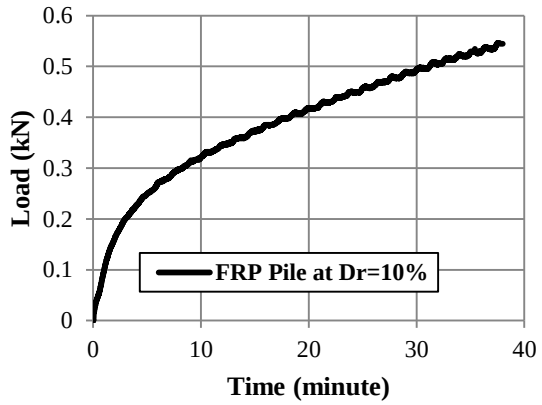

a) Time-Load Behavior

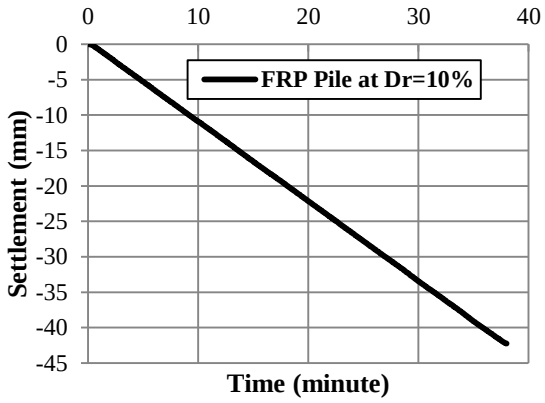

b) Time-Settlement Behavior

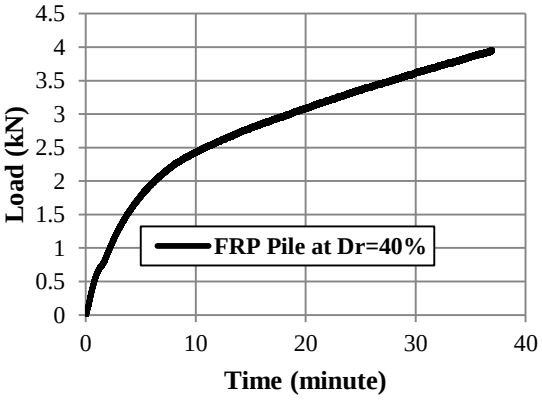

c) Time-Load Behavior

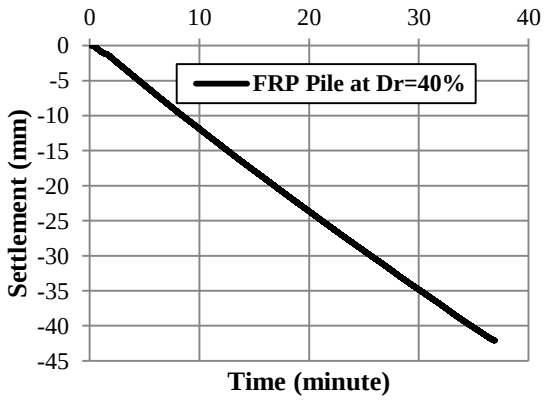

d) Time-Settlement Behavior

Figure A.1. a), c), e), g); Time-Load Behavior, and b), d), f), h); Time-Settlement Behavior of single-model composite FRP pile in the ultimate bearing capacity model experiments at (D_r = 10%, 40%, 65% and 90%), respectively.

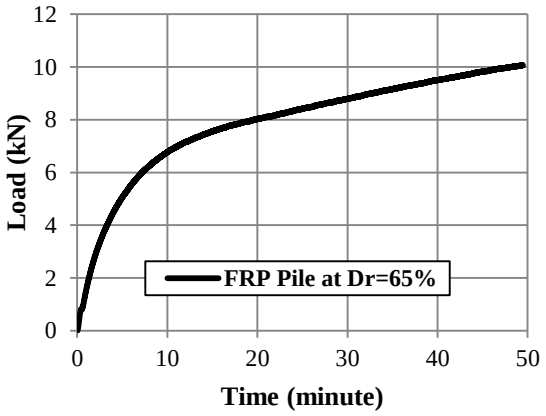

e) Time-Load Behavior

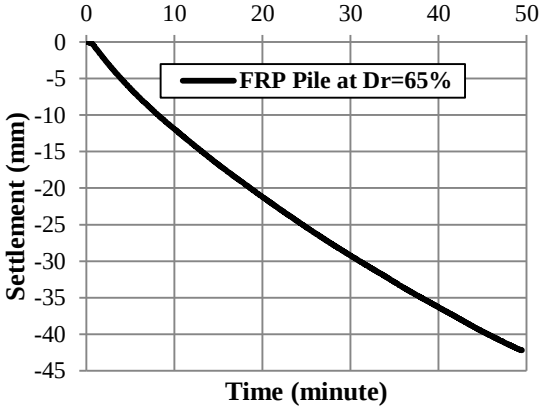

f) Time-Settlement Behavior

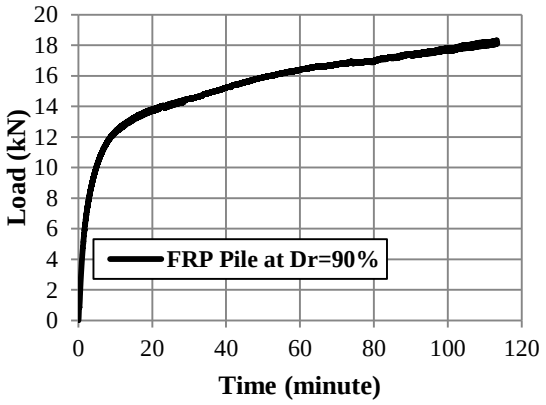

g) Time-Load Behavior

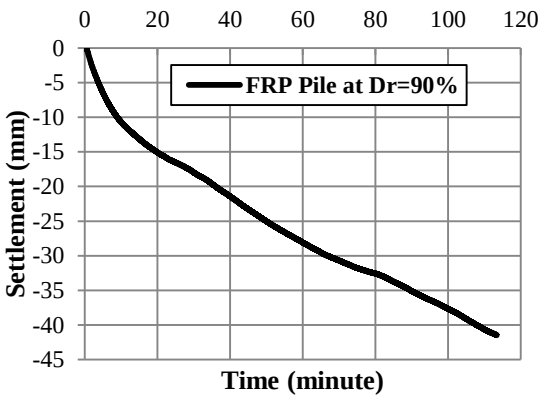

h) Time-Settlement Behavior

Figure A.1. (continue)

APPENDIX-2 (Experimental Time-Load and Time-Displacement Behaviors of Single-Model PVC Composite Pile in the Ultimate Bearing Capacity Model Experiments)

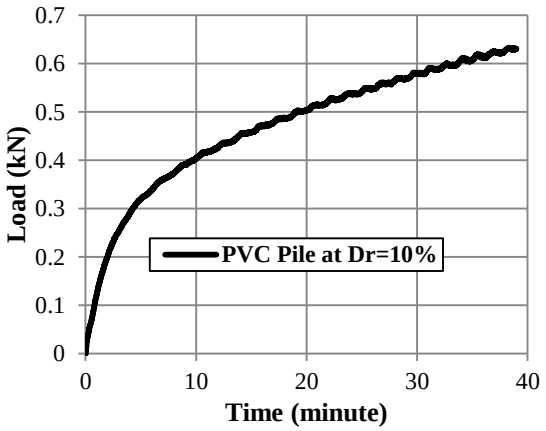

a) Time-Load Behavior

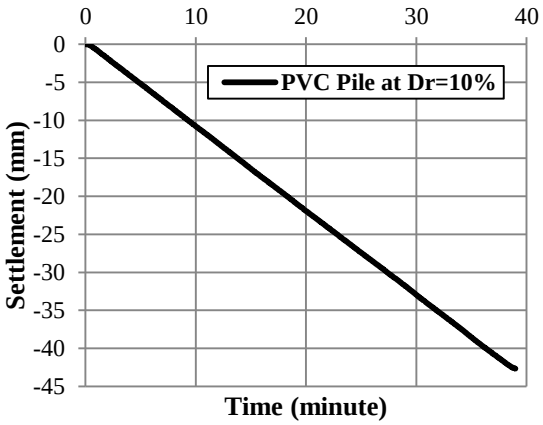

b) Time-Settlement Behavior

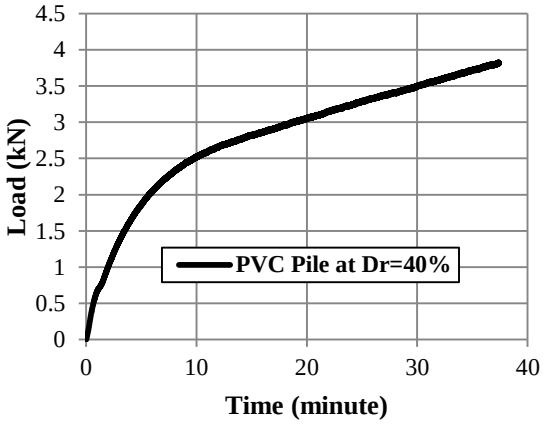

c) Time-Load Behavior

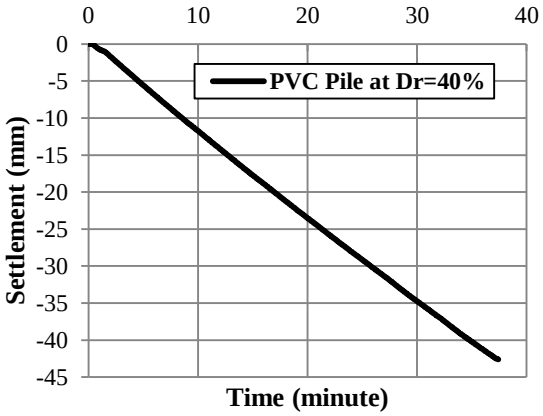

d) Time-Settlement Behavior

Figure A.2. a), c), e), g); Time-Load Behavior, and b), d), f), h); Time-Settlement Behavior of single-model PVC composite pile in the ultimate bearing capacity model experiments at (D_r = 10%, 40%, 65% and 90%), respectively.

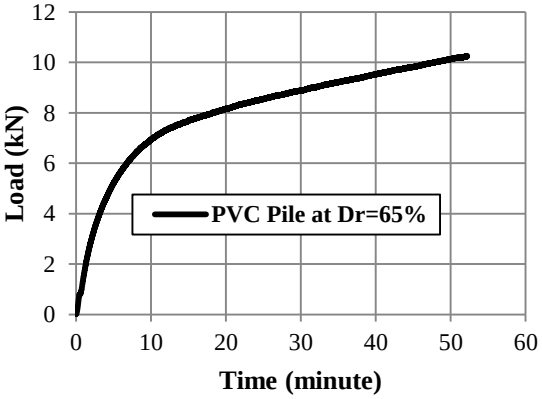

e) Time-Load Behavior

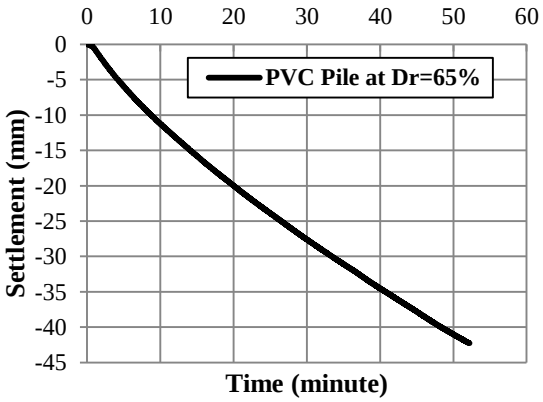

f) Time-Settlement Behavior

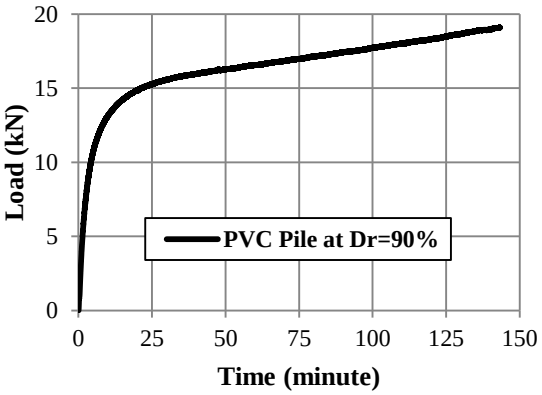

g) Time-Load Behavior

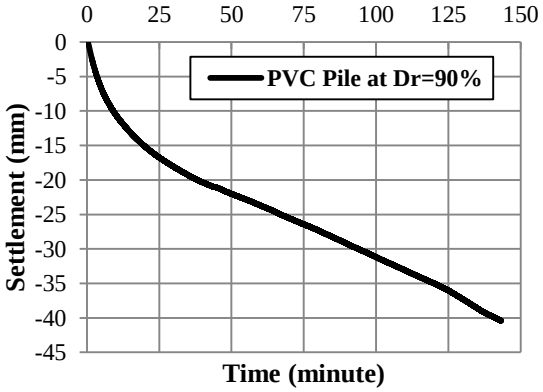

h) Time-Settlement Behavior

Figure A.2. (continue)

APPENDIX-3 (Experimental Time-Load and Time-Displacement Behaviors of Single-Model Composite Piles in the Base Capacity Model Experiments)

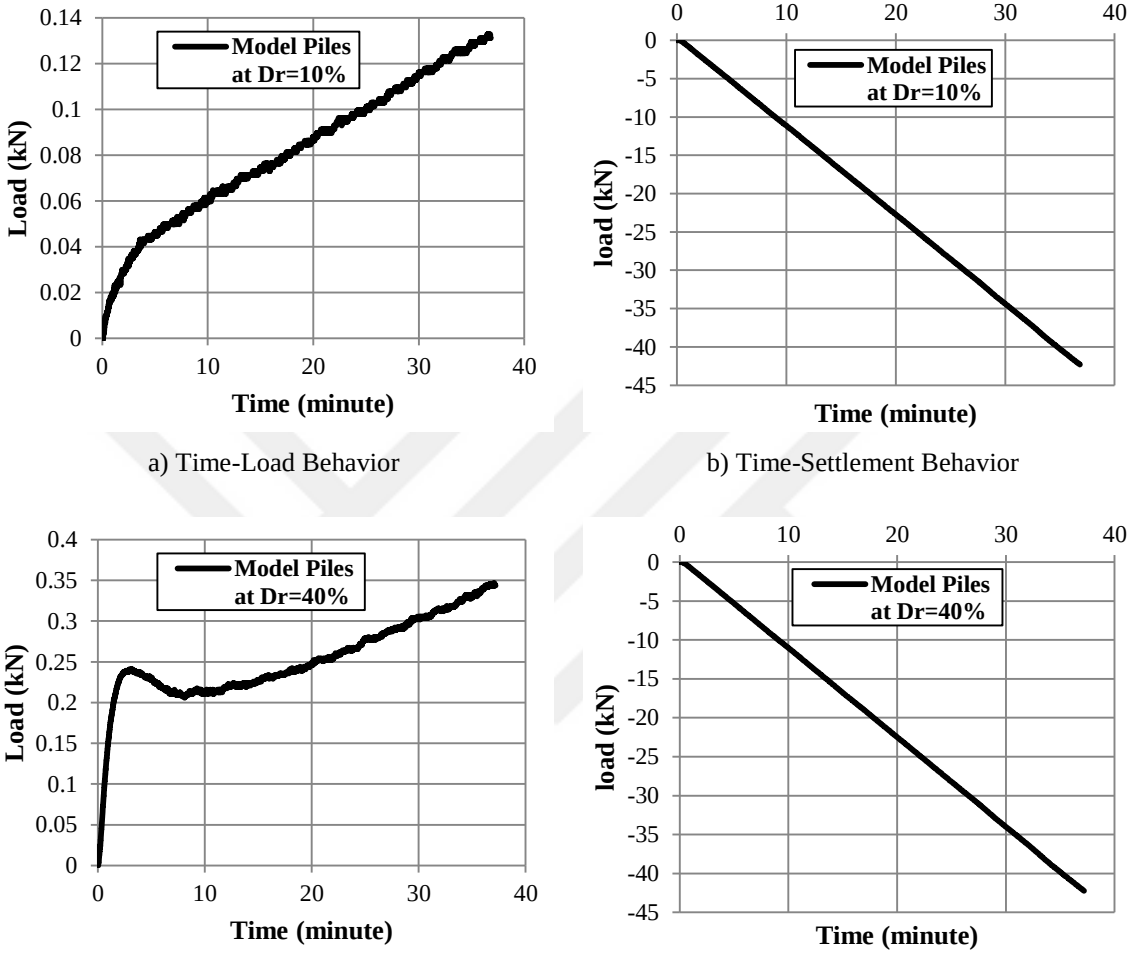

a) Time-Load Behavior

b) Time-Settlement Behavior

c) Time-Load Behavior

d) Time-Settlement Behavior

Figure A.3. a), c), e), g); Time-Load Behavior, and b), d), f), h); Time-Settlement Behavior of single-model composite piles in the base capacity model experiments at (D_r = 10%, 40%, 65% and 90%), respectively.

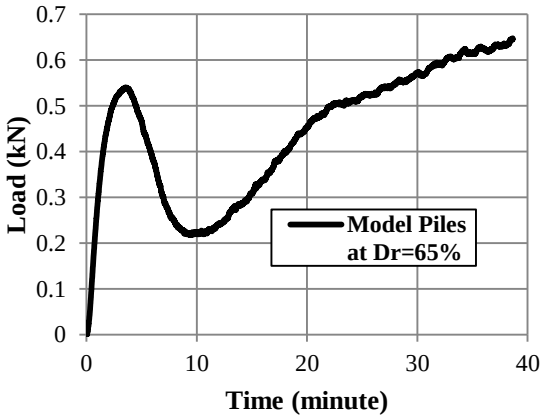

e) Time-Load Behavior

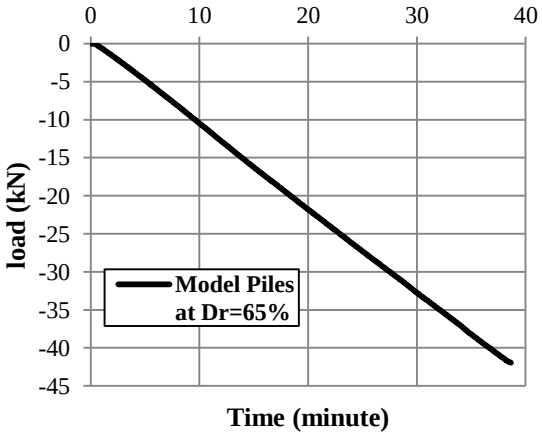

f) Time-Settlement Behavior

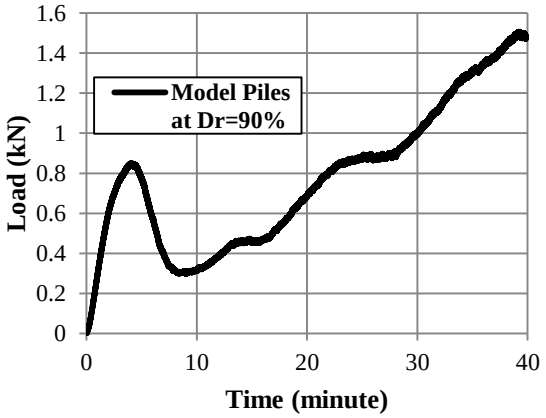

g) Time-Load Behavior

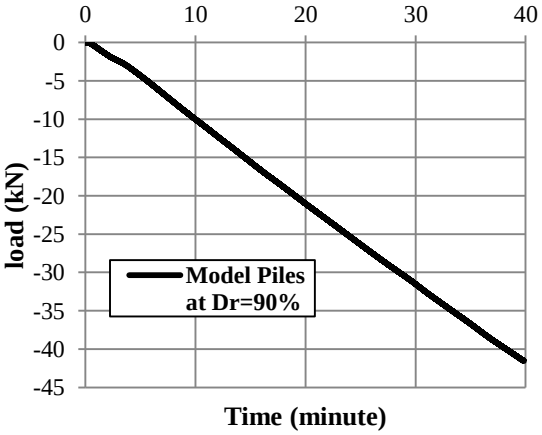

h) Time-Settlement Behavior

Figure A.3. (continue)

APPENDIX-4 (Experimental Time-Load and Time-Displacement Behaviors, and Load-Displacement Behavior of Styrofoam-Filter Penetration Resistance of Single-Model FRP Composite Pile in the Shaft Capacity Model Experiments)

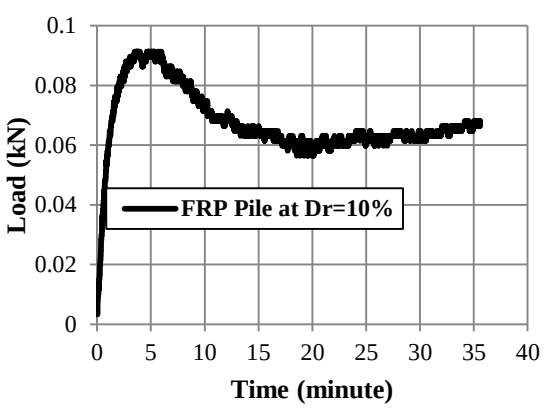

a) Time-Load Behavior

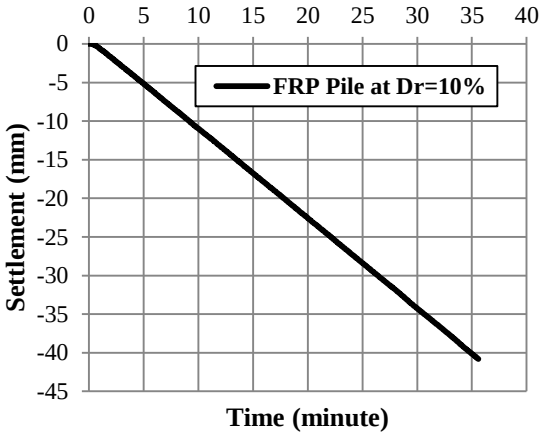

b) Time-Settlement Behavior

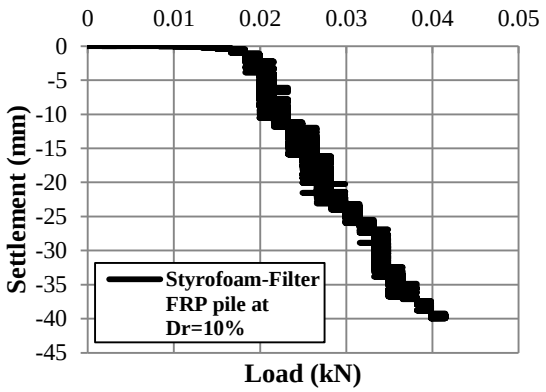

c) Load-Displacement Behavior

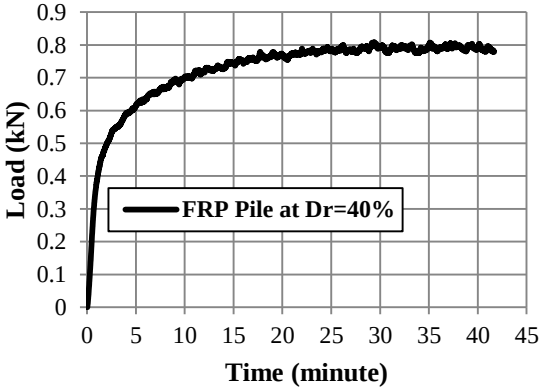

d) Time-Load Behavior

Figure A.4. a), d), g), j); Time-Load Behavior, and b), e), h), k); Time-Settlement Behavior, and c), f), i), l); Load-Displacement Behavior of Styrofoam-Filter Penetration Resistance of single-model FRP composite pile in the shaft capacity model experiments at (D_r = 10%, 40%, 65% and 90%), respectively.

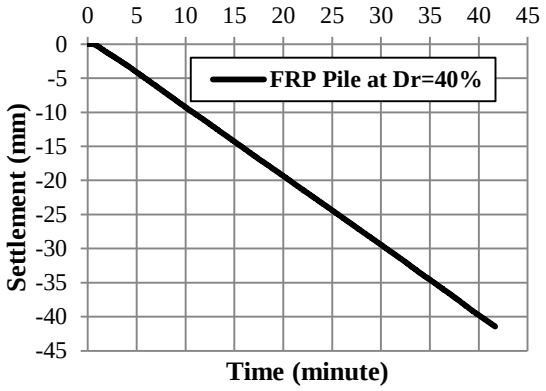

e) Time-Settlement Behavior

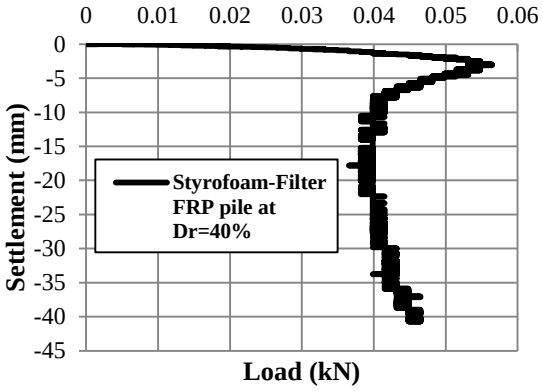

f) Load-Displacement Behavior

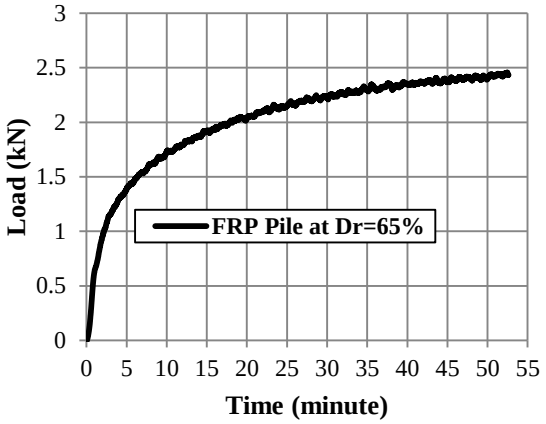

g) Time-Load Behavior

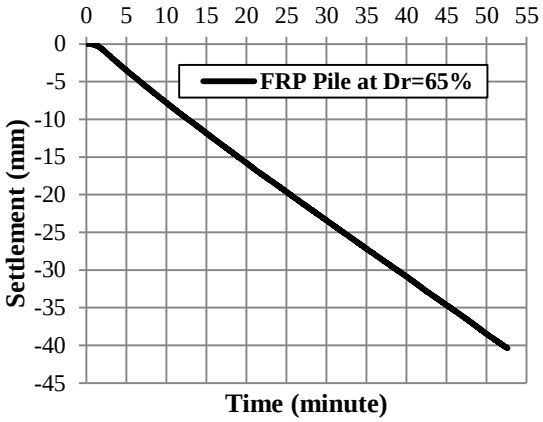

h) Time-Settlement Behavior

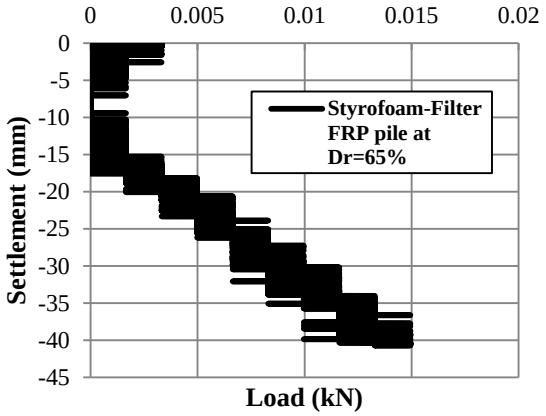

i) Load-Displacement Behavior

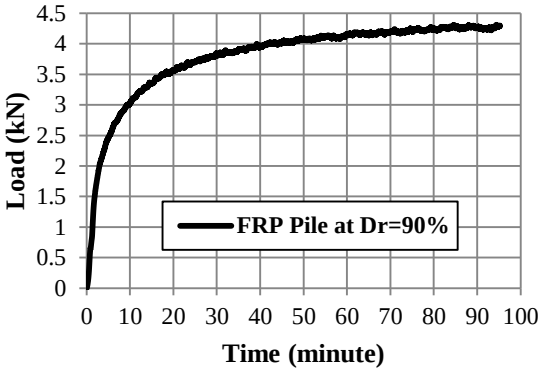

j) Time-Load Behavior

Figure A.4. (continue)

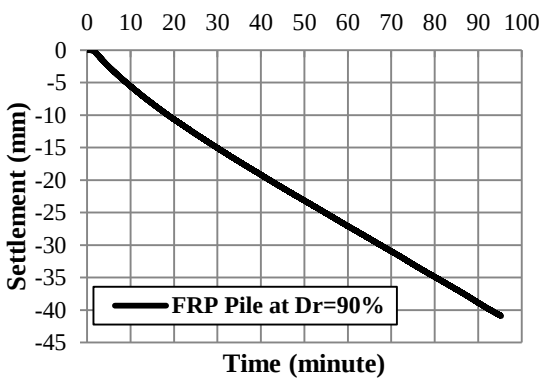

k) Time-Settlement Behavior

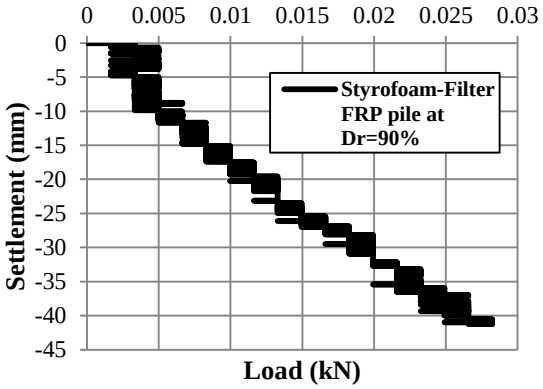

l) Load-Displacement Behavior

Figure A.4. (continue)

APPENDIX-5 (Experimental Time-Load and Time-Displacement Behaviors, and Load-Displacement Behavior of Styrofoam-Filter Penetration Resistance of Single-Model PVC Composite Pile in the Shaft Capacity Model Experiments)

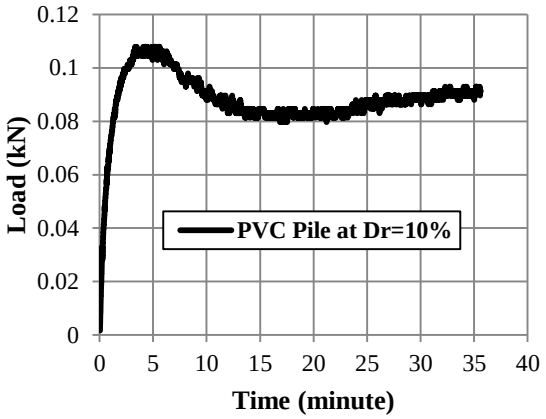

a) Time-Load Behavior

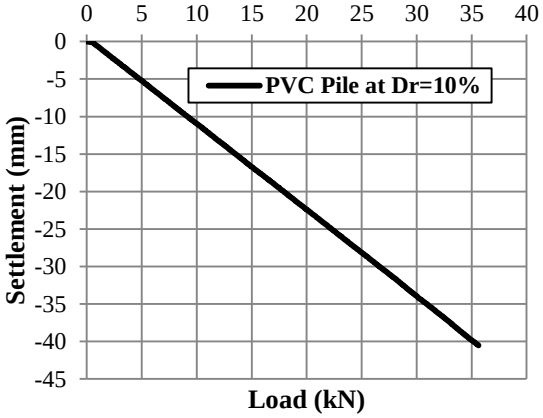

b) Time-Settlement Behavior

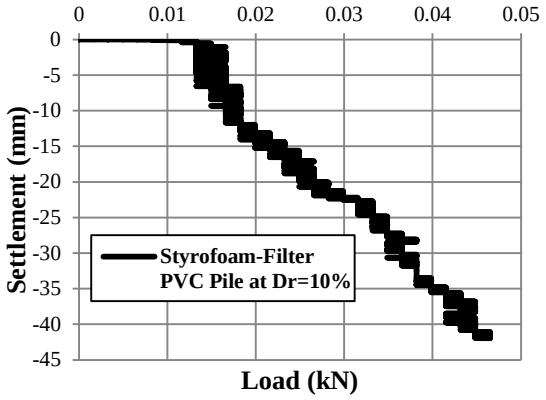

c) Load-Displacement Behavior

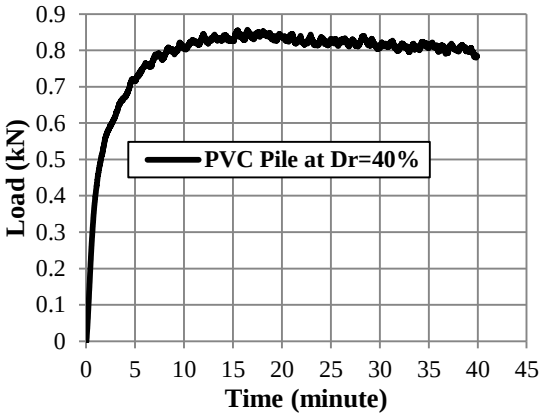

d) Time-Load Behavior

Figure A.5. a), d), g), j); Time-Load Behavior, and b), e), h), k); Time-Settlement Behavior, and c), f), i), l); Load-Displacement Behavior of Styrofoam-Filter Penetration Resistance of single-model PVC composite pile in the shaft capacity model experiments at (D_r = 10%, 40%, 65% and 90%), respectively.

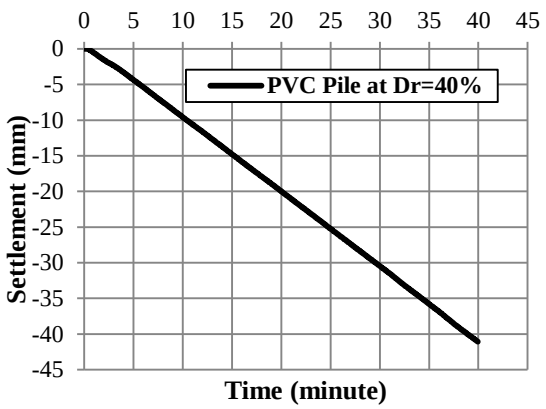

e) Time-Settlement Behavior

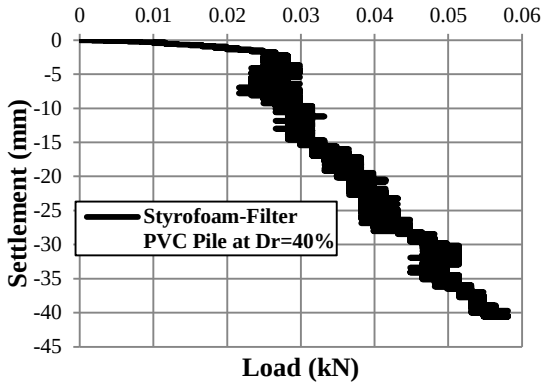

f) Load-Displacement Behavior

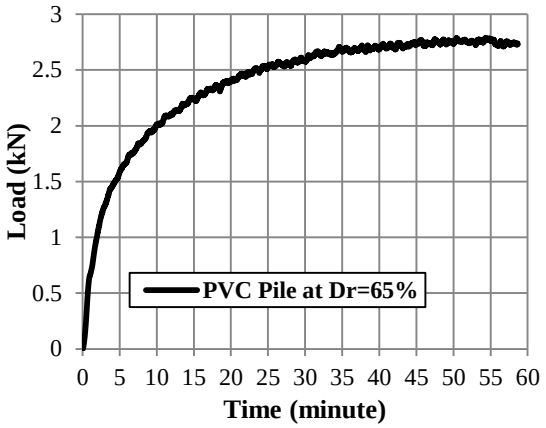

g) Time-Load Behavior

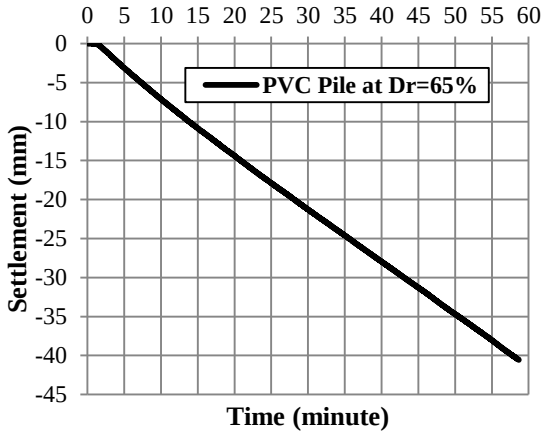

h) Time-Settlement Behavior

Figure A.5. (continue)

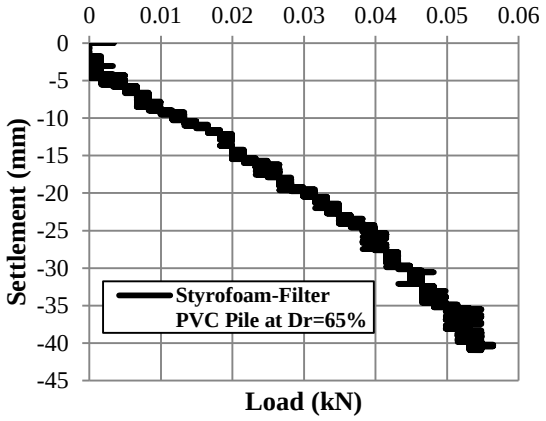

i) Load-Displacement Behavior

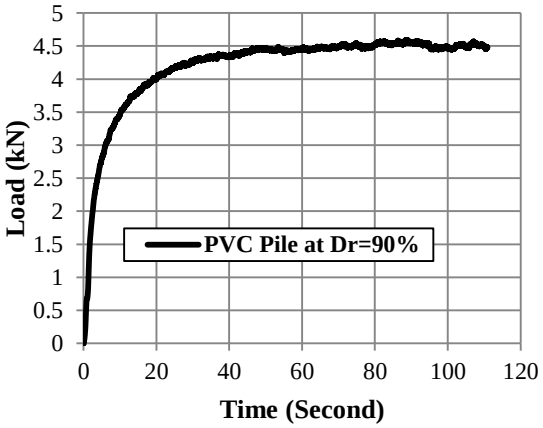

j) Time-Load Behavior

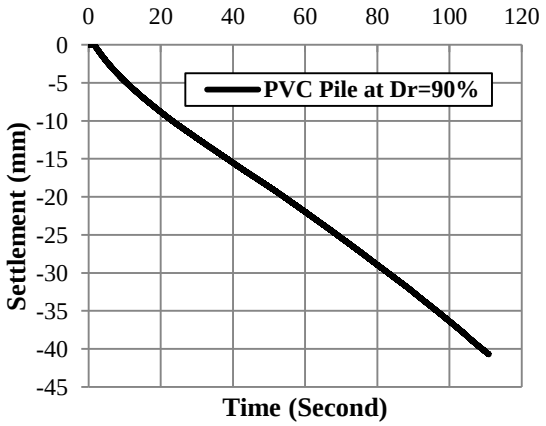

k) Time-Settlement Behavior

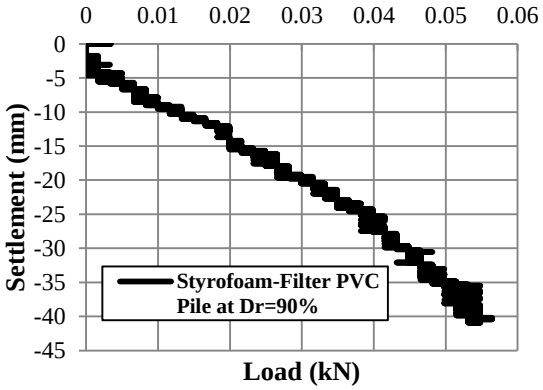

l) Load-Displacement Behavior

Figure A.5. (continue)

CURRICULUM VITAE

Omer Muhammad Edan
Civil Engineer

Personal Details:

Name: Omer Muhammad Edan
Nationality: Iraqi
Date of birth: 14-10-1986
Gender: Male
Address: Chwarqurna twon/Ranya city/Sulaimani province, Iraq
Phone: +964 (0)770 247 6701
E-mail: omer.edan@gmail.com

Skills

Languages: Mother Language (Kurdish); Intermediate (English); Fair (Arabic), Fair (Turkish).

Software: MS Office Word, Excel, Power Point, AutoCAD, Autodesk Autocad Civil 3D (medium), CSI Etabs (medium), Staad Pro. (medium) ,Plaxis 3D (medium).

Instrument: Advance use of Level and Theodolite.